UNIVERSITY OF CRETE

SCHOOL OF MEDICINE

DEPARTMENT OF MEDICAL IMAGING

HEAD: PROF. APOSTOLOS KARANTANAS

PhD THESIS

EVALUATION OF PERCUTANEOUS TRANSLUMINAL ANGIOPLASTY OUTCOME IN PATIENTS WITH PERIPHERAL ARTERIAL DISEASE USING MODERN MEDICAL IMAGING TECHNIQUES (CT AND MR PERFUSION)

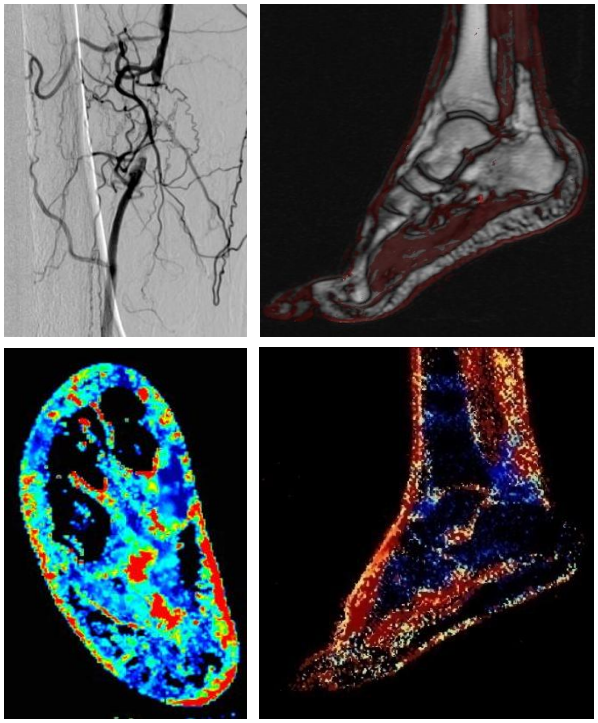

Supervisor: Dimitrios Tsetis MD, PhD, EBIR, FCIRSE

Professor of General Radiology/Interventional Radiology

Nikolaos Galanakis MD

Radiologist

Department of Medical Imaging

University Hospital of Heraklion

Heraklion 2020

ΠΑΝΕΠΙΣΤΗΜΙΟ ΚΡΗΤΗΣ

ΙΑΤΡΙΚΗ ΣΧΟΛΗ

ΕΡΓΑΣΤΗΡΙΟ ΙΑΤΡΙΚΗΣ ΑΠΕΙΚΟΝΙΣΗΣ

ΔΙΕΥΘΥΝΤΗΣ: ΚΑΘ. ΑΠΟΣΤΟΛΟΣ ΚΑΡΑΝΤΑΝΑΣ

ΔΙΔΑΚΤΟΡΙΚΗ ΔΙΑΤΡΙΒΗ

ΕΚΤΙΜΗΣΗ ΑΠΟΤΕΛΕΣΜΑΤΩΝ ΔΙΑΔΕΡΜΙΚΗΣ ΑΓΓΕΙΟΠΛΑΣΤΙΚΗΣ ΣΕ ΠΕΡΙΦΕΡΙΚΗ ΑΡΤΗΡΙΑΚΗ ΝΟΣΟ ΜΕ ΣΥΓΧΡΟΝΕΣ ΤΕΧΝΙΚΕΣ ΙΑΤΡΙΚΗΣ ΑΠΕΙΚΟΝΙΣΗΣ

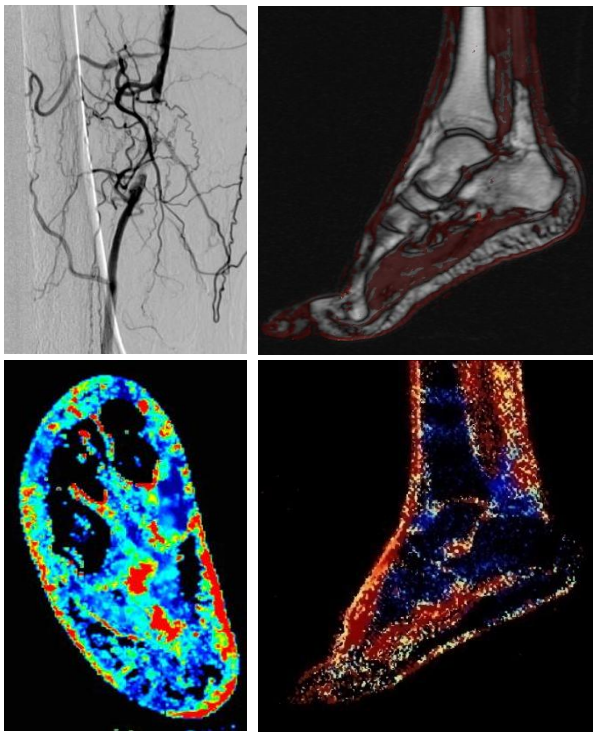

Επιβλέπων: Δημήτριος Τσέτης MD, PhD, EBIR, FCIRSE

Καθηγητής Γενικής/Επεμβατικής Ακτινολογίας

Νικόλαος Γαλανάκης MD

Ακτινολόγος

Εργαστήριο Ιατρικής Απεικόνισης

Πανεπιστημιακό Γενικό Νοσοκομείο Ηρακλείου

Ηράκλειο 2020

Στους γονείς οφείλομεν το ζην, στους δε διδασκάλους το ευ ζην

Μέγας Αλέξανδρος

Στους γονείς μου Γιάννη και Φρόσω...

Στους δασκάλους μου....

Επιβλέπων

Δημήτριος Τσέτης

Καθηγητής Γενικής/Επεμβατικής Ακτινολογίας

Συνεπιβλέποντες

Θωμάς Μαρής

Καθηγητής Ιατρικής Φυσικής

Χρήστος Ιωάννου

Αναπλ. Καθηγητής Αγγειοχειρουργικής

Επταμελής εξεταστική επιτροπή

Δημήτριος Τσέτης

Καθηγητής Γενικής/Επεμβατικής Ακτινολογίας

Θωμάς Μαρής

Καθηγητής Ιατρικής Φυσικής

Χρήστος Ιωάννου

Αναπλ. Καθηγητής Αγγειοχειρουργικής

Απόστολος Καραντάνας

Καθηγητής Ακτινολογίας

Γεώργιος Κοχιαδάκης

Καθηγητής Καρδιολογίας

Κωνσταντίνος Περισυνάκης

Καθηγητής Ιατρικής Φυσικής

Νικόλαος Κοντοπόδης

Επίκουρος Καθηγητής Αγγειοχειρουργικής

ΕΥΧΑΡΙΣΤΙΕΣ

Ο νομπελίστας Βιοχημικός Albert Szent-Gyorgyi είχε πει ότι έρευνα είναι να βλέπεις ότι και πολλοί άλλοι έχουν δει, αλλά να σκεφτείς αυτό που κανείς άλλος δεν έχει σκεφτεί. Ο δρόμος όμως της επιστημονικής αναζήτησης δεν είναι μοναχικός. Άνθρωποι από διαφορετικά επιστημονικά πεδία συνεργάζονται και συνεισφέρουν για ένα κοινό στόχο, την αναζήτηση της γνώσης και της αλήθειας.

Στα πλαίσια της παρούσας διδακτορικής διατριβής, συνέβαλαν με διαφορετικό τρόπο πολλοί και διαφορετικοί άνθρωποι.

Πρώτα από όλα, ευχαριστώ θερμά, τον εμπνευστή της συγκεκριμένης ιδέας, επιβλέποντα της Διδακτορικής Διατριβής και μέντορα μου στον τομέα της επεμβατικής ακτινολογίας, Καθηγητή Δημήτριο Τσέτη. Ο ρόλος του υπήρξε καθοριστικός σε όλη τη διάρκεια της επιστημονικής μου πορείας, τόσο μεταδίδοντας μου γνώσεις και εμπειρίες στο χώρο της επεμβατικής ακτινολογίας όσο και εμπνέοντας με θέληση για έρευνα και εξέλιξη σε αυτό τον απαιτητικό τομέα.

Θα ήθελα επίσης να ευχαριστήσω τον συνεπεπιβλέποντα της ΔΔ, Καθηγητή Ιατρικής Φυσικής Θωμά Μαρή, ο οποίος υλοποίησε την ιδέα της τεχνικής αιματικής διήθησης με Μαγνητικό Τομογράφο. Ακόμη τον ευχαριστώ για ένα ακόμη λόγο, με έκανε να "αγαπήσω" ξανά την Φυσική και να κατανοήσω πόσο στενά συνδεδεμένη και αλληλεξαρτώμενη είναι με την ακτινολογία.

Ακόμη θα ήθελα να ευχαριστήσω, τον έτερο συνεπεπιβλέποντα της ΔΔ, Καθηγητή Αγγειοχειρουργικής Χρήστο Ιωάννου, για την εμπιστοσύνη που μου έδειξε και το άριστο κλίμα συνεργασίας καθ' όλη τη διάρκεια της ΔΔ μεταξύ της μονάδας επεμβατικής ακτινολογίας και της αγγειοχειρουργικής κλινικής.

Επιπροσθέτως, θα ήθελα να ευχαριστήσω τον Καθηγητή Ακτινολογίας και διευθυντή του Εργαστηρίου Ιατρικής Απεικόνισης κ. Αποστόλο Καραντάνα, για τη συμβολή του στην επιστημονική μου

κατάρτιση κατά τη διάρκεια της ειδικότητας μου αλλά και τις δυνατότητες που μου προσέφερε για να υλοποιηθεί η παρούσα ΔΔ.

Ιδιαίτερες ευχαριστίες στον επίκουρο καθηγητή Αγγειοχειρουργικής Νικόλαο Κοντοπόδη για την καθοριστική συνεισφορά του στην παρακολούθηση των ασθενών αλλά και την ουσιαστική συνεργασία και βοήθεια που μου προσέφερε όλα αυτά τα χρόνια.

Θα ήθελα επίσης να ευχαριστήσω τον Καθηγητή Επεμβατικής Ακτινολογίας Αδάμ Χατζηδάκη, τον Καθηγητή Ιατρικής Φυσικής Κωνσταντίνο Περισυνάκη, τον Ακτινοφυσικό Αντώνη Παπαδάκη και τον τεχνολόγο-ακτινολόγο Νικόλαο Κοσιδεκάκη για τη συμβολή τους στην υλοποίηση και εφαρμογή του πρωτοκόλλου αιματικής διήθησης με υπολογιστικό τομογράφο.

Ακόμη θα ήθελα να ευχαριστήσω τον μεταδιδακτορικό ερευνητή στο ΙΤΕ και διδάκτωρ Ιατρικής Γιώργο Ιωαννίδη για τη συμβολή του στην συσχέτιση μεταξύ των διαφορετικών τεχνικών αιματικής διήθησης με τη χρήση Μαγνητικής Τομογραφίας καθώς και τον ηλεκτρολόγο μηχανολόγο και διδάκτωρ Ιατρικής Γιώργο Καλαιτζάκη για τη συνεισφορά του στην ανάλυση των δεδομένων αιματικής διήθησης με τη χρήση Μαγνητικής Τομογραφίας.

Όλα αυτά βέβαια δε ήταν εφικτά χωρίς την συμβολή του προσωπικού της μονάδας επεμβατικής ακτινολογίας του ΠΑΓΝΗ στην αντιμετώπιση της περιφερικής αρτηριακής νόσου των ασθενών και συγκεκριμένα των ιατρών Ηλία Κεχαγία και Νέλλυ Χόλτσεβα, των νοσηλευτών Αγγέλα Πουλή, Μανώλη Χαρωνιτάκη, Νεκτάριο Κυπράκη, Λευτέρη Μπλαζάκη, των τεχνολόγων Νίκο Φιλλιπάκη και Ροδούλα Μπιμπάκη αλλά και των γιατρών και νοσηλευτών της αγγειοχειρουργικής κλινικής.

Κλείνοντας, θα ήθελα να αφιερώσω την ΔΔ στους ανθρώπους που με στήριξαν και με στηρίζουν όλα αυτά τα χρόνια και στέκονται στο πλευρό μου σε όλη τη διάρκεια των σπουδών και της επιστημονικής μου σταδιοδρομίας, στους γονείς μου, Γιάννη και Φρόσω.

Index of contents

Abreviations

ABI: Anke-brachial index

AIF: Arterial input function

AMI: Acute myocardial infarction

ASL: Arterial spin labeling

ATA: Anterior Tibial Artery

ATH: Adiabatic tissue homogeneity

AUC: Area under curve

BF: Blood flow

BOLD: Blood oxygenation level-dependent

BV: Blood volume

BTK: Bellow the knee

CA: Constrast agent

CAD: Coronary artery disease

CEUS: Contrast-enhanced ultrasound

CDUS: Color duplex ultrasound

CIA: Common Iliac Artery

CISS: Constructive Interference in Steady State

CLI: Critical limb ischemia

CT: Computed tomography

CTA: Computed tomography angiography

CTFP: Computed tomography foot perfusion examination

DCB: Drug-coated balloon

DCE-MRI: Dynamic contrast-enhanced magnetic resonance imaging

DLP: Dose-length product

DM: Diabetes Mellitus

DSA: Digital subtraction angiography

DWI: Diffusion weighted imaging

EES: Extravascular extracellular space

EIA: External Iliac Artery

ETM: Extended Tofts model

FA: Flip angle

FOV: Field of view

GCTT: Gamma capillary transit time model

GD: Gadolinium

HASTE: Half-Fourier Acquisition Single-shot Turbo spin Echo

HL: Hyperlipidemia

HT: Hypertension

IC: Intermittent claudication

ICC: Intra-class correlation coefficient

IRF: Impulse residue function

IVIM: Intra-Voxel Incoherent Motion

MRA: Magnetic resonance angiography

MRI: Magnetic resonance imaging

PA: Peroneal Artery

PAD: Peripheral arterial disease

POPA: Popliteal Artery

PS: Permeability surface

PTA: Percutaneous transluminal angioplasty

PWI: Perfusion weighted imaging

RER: Relative enhancement ratio

RMSE: Root mean squared error

ROI: Region of interest

SD: Standard deviation

SFA: Superficial Femoral Artery

SM: Smoking

SSM: steady state model

TE: Time of echo

TcPO2 : Transcutaneous oxygen partial pressure

TPT: Tibioperoneal trunk

VIBE: Volume Interpolated Breath hold Examination

Περίληψη

Εισαγωγή

Η Περιφερική Αρτηριακή Νόσος (ΠΑΝ) χαρακτηρίζει τη μειωμένη αιματική ροή στο άκρο ως αποτέλεσμα στένωσης ή απόφραξης των αρτηριών του κάτω μέλους στα πλαίσια αθηροσκληρυντικής νόσου. Ο επιπολασμός της νόσου υπολογίζεται σε 3-10% σε ενήλικες νεότερους των 70 ετών και έως 15-20% σε ενήλικες μεγαλύτερους των 70 ετών. Οι κύριοι παράγοντες κινδύνου για την ΠΑΝ είναι ο σακχαρώδης διαβήτης, η αρτηριακή υπέρταση, η υπερλιπιδαιμία, η στεφανιαία νόσος και το κάπνισμα. Το κύριο σύμπτωμα της νόσου αποτελεί η διαλείπουσα χωλότητα, ενώ σε πιο σοβαρές περιπτώσεις μπορεί να εμφανιστεί κρίσιμη ισχαιμία άκρου (ΚΙΑ), η οποία απαιτεί επαναγγείωση για την αποφυγή ακρωτηριασμού. Η ΚΙΑ αποτελεί το τελικό στάδιο της ΠΑΝ, όπου υπάρχει σημαντική μείωση στην αιμάτωση του άκρου και μπορεί να εκδηλωθεί με τη μορφή άλγους ηρεμίας, γάγγραινας ή έλκους κάτω μέλους. Οι τεχνικές επαναγγείωσης περιλαμβάνουν είτε ενδαγγειακές τεχνικές όπως η διαδερμική αγγειοπλαστική (PTA) με ή χωρίς τοποθέτηση stent είτε χειρουργικές τεχνικές όπως η χειρουργική αναστόμωση (by-pass). Η επιλογή της κατάλληλης θεραπείας βασίζεται στην κλινική κατάσταση του ασθενούς, στην σοβαρότητα της ισχαιμίας του άκρου και στην ανατομική κατανομή των αθηροσκληρυντικών αλλοιώσεων. Η αξιολόγηση της ΠΑΝ περιλαμβάνει τη λήψη ιατρικού ιστορικού, κλινική εξέταση, λειτουργικές δοκιμασίες όπως ο σφυροβραχιόνιος δείκτης και οι τμηματικές πιέσεις των άκρων και ανατομικές/ακτινολογικές εξετάσεις, όπως το έγχρωμο υπερηχογράφημα Doppler (CDUS), η υπολογιστική αγγειογραφία (CTA) και η μαγνητική αγγειογραφία (MRA). Οι παραπάνω μέθοδοι παρέχουν σημαντικές πληροφορίες σχετικά με την κατανομή των μακροαγγειακών αλλοιώσεων των άκρων (στενώσεις, αποφράξεις) αλλά όχι για την μικροαγγειακή αιματική διήθηση (perfusion) των άκρων. Μπορούν να χρησιμοποιηθούν στην κλινική πράξη για να εκτιμήσουν την έκταση της νόσου, να

σχεδιάσουν τη στρατηγική επαναγγείωσης και τέλος να εκτιμήσουν την βατότητα των αρτηριών μετά τη θεραπευτική αντιμετώπιση. Ωστόσο, δεν μπορούν να μετρήσουν την αιματική ροή (BF) στο άκρο ή να εκτιμήσουν την επίδραση των παράπλευρων αγγείων στην αιμάτωση του άκρου. Επιπλέον δε μπορούν να εκτιμήσουν τα αποτελέσματα των θεραπευτικών επεμβάσεων όσον αφορά την βελτίωση της αιμάτωσης.

Σκοπός

Οι στόχοι της παρούσας διδακτορικής διατριβής είναι:

- Η ανάδειξη της υποαίματωσης των κάτω άκρων σε ασθενείς με ΚΙΑ και η εκτίμηση των αποτελεσμάτων της PTA στην αντιμετώπιση της νόσου, με χρήση σύγχρονων τεχνικών ποσοτικής απεικόνισης όπως η τεχνική Αιματικής Διήθησης με Μαγνητικό Συντονισμό (MR Perfusion Imaging) και η τεχνική Αιματικής Διήθησης με Υπολογιστική Τομογραφία (CT Perfusion)
- Η σύγκριση των δυνατοτήτων διαφορετικών τεχνικών MR Perfusion στην μελέτη της αιμάτωσης των άκρων
- Η συσχέτιση των αποτελεσμάτων αιματικής διήθησης με την κλινική εικόνα και τις απεικονιστικές εξετάσεις των ασθενών μετά την PTA για τον καθορισμό της πιθανής προγνωστικής αξίας του MR/CT Perfusion.

Υλικά και μέθοδοι

Στις ερευνητικές μελέτες συμμετείχαν ασθενείς με ΚΙΑ (κατηγορίας Rutherford 4-6). Η ανατομική κατανομή των αθηροσκληρωτικών αλλοιώσεων και η κλινική κατάσταση του ασθενούς θα έπρεπε να τον καθιστούν κατάλληλο για ενδοαγγειακή αντιμετώπιση της ΚΙΑ. Οι ασθενείς που παρουσίασαν λιγότερο προχωρημένη ΠΑΝ ή οξεία ισχαιμία κάτω άκρου αποκλείονταν από τη μελέτη. Παρομοίως, αποκλείστηκαν ασθενείς που υποβλήθηκαν σε χειρουργική επαναγγείωση ή εκείνοι στους οποίους πραγματοποιήθηκε συντηρητική αντιμετώπιση ή ακρωτηριασμός.

Οι ασθενείς που πληρούσαν τα προαναφερθέντα κριτήρια υποβλήθηκαν σε εξέταση CT perfusion (CTFP) ή MR perfusion με πρωτόκολλο που απαιτούσε χορήγηση παραμαγνητικής ουσίας (DCE-MRI) και ακολουθίες μοριακής διάχυσης (DW-MRI) πριν και μετά την PTA. Όλοι οι ασθενείς που συμμετείχαν στην μελέτη εντάχθηκαν σε τακτικό πρόγραμμα παρακολούθησης με κλινική εξέταση στους 1, 3, 6 και 12 μήνες και CDUS σε συνδυασμό με κλινική εξέταση σε ετήσια βάση.

Οι εξετάσεις CT perfusion πραγματοποιήθηκαν σε υπολογιστικό τομογράφο 128 τομών (Revolution GSI, GE Healthcare, USA). Οι εικόνες ελήφθησαν μετά τη χορήγηση 40 ml ιωδιούχου μη ιονικού σκιαγραφικού ακολουθούμενου από 30 ml φυσιολογικού ορού με ρυθμό έγχυσης 4 ml/s. Οι εικόνες μεταφέρθηκαν σε ειδικό σταθμό εργασίας (AW server 3.2, GE Medical Systems) για περαιτέρω ανάλυση με κατάλληλο απεικονιστικό πρόγραμμα (CT-Perfusion-4D, GE Medical Systems). Στη συνέχεια δημιουργήθηκαν παραμετρικοί χάρτες αιματικής διήθησης για ποικίλες αιμοδυναμικές παραμέτρους όπως ο όγκος αίματος (blood volume [BV]), η ροή αίματος (blood flow [BF]) και η διαπερατότητα επιφανείας (permeability surface [PS]) μέσω αλγορίθμου αποσυγκέντρωσης και υπολογίστηκε η σχετική αλλαγή σε παραμέτρους perfusion πριν και μετά την ενδαγγειακή αντιμετώπιση. Παράλληλα, εξετάσεις από 6 ασθενείς αναλύθηκαν και από έναν δεύτερο παρατηρητή για τον προσδιορισμό της αναπαραγωγιμότητας μεταξύ παρατηρητών.

Οι εξετάσεις MR perfusion πραγματοποιηθήκαν σε μαγνητικό τομογράφο 1.5 Tesla (Vision/Sonata Hybrid system, Siemens, Erlangen, Germany) ενισχυμένο με ένα ισοδύναμο σύστημα διαβάθμισης 3 Tesla. Το πρωτόκολλο MR perfusion περιελάβανε:

- συμβατικές ακολουθίες T1w 3D GRE VIBE and T2/T1w 3D GRE CISS.
- ακολουθίες μοριακής διάχυσης Diffusion-weighted (DW) σε οβελιαίο επίπεδο χρησιμοποιώντας ακολουθίες υψηλής ανάλυσης HASTE (Half-Fourier Acquisition Single-shot Turbo spin Echo) με πολλαπλά b values (b = 0, 50, 100, 150, 200, 500, 800, 1000 s/mm^2).

- T1w 3D GRE VIBE ακολουθίες σε οβελιαίο επίπεδο με ποικίλες flip angles (FA = 5^{o},10^{o},15^{o},20^{o},25^{o},30^{o}) για τον αρχικό προσδιορισμό των παραμετρικών T1 χαρτών και T1w 3D GRE VIBE ακολουθίες perfusion που επαναλήφθηκαν για 10 λεπτά μετά την ενδοφλέβια χορήγηση παραμαγνητικής σκιαγραφικής ουσίας (0.1 mmol/kg).

Η ανάλυση των ακολουθιών αιματικής διήθησης μετά τη χορήγηση παραμαγνητικής ουσίας (DCE-MRI) πραγματοποιήθηκε χρησιμοποιώντας ένα εκτεταμένο μοντέλο Tofts και ποσοτικοί χάρτες για διάφορες αιμοδυναμικές παραμέτρους όπως η ροή αίματος (blood flow [BF]), το K^{trans} και K_{ep} δημιουργήθηκαν από τα παραμετρικά δεδομένα προσαρμοσμένα στο εκτεταμένο μοντέλο Tofts, χρησιμοποιώντας μια πληθυσμιακή λειτουργία αρτηριακής εισόδου (AIF).

Όσον αφορά τη σύγκριση μεταξύ των διαφορετικών τεχνικών MR perfusion (με χρήση ή μη παραμαγνητικής ουσίας) ενσωματώθηκαν γραμμικοί και μη γραμμικοί αλγόριθμοι για τον ποσοτικό προσδιορισμό των παραμέτρων μέσω μιας ποικιλίας μοντέλων, ικανών να εξαγάγουν πληροφορίες από κάθε τεχνική απεικόνισης. Όλοι οι αριθμητικοί υπολογισμοί πραγματοποιήθηκαν σε σύστημα Python 3.5 και περιλαμβάναν: Intra voxel incoherent motion μοντέλο για τις ακολουθίες διάχυσης και μοντέλο Patlak, εκτεταμένο μοντέλο Tofts και μοντέλο Gamma Capillary Transit time (GCTT) για τις ακολουθίες DCE-MRI.

Οι ακολουθίες μοριακής διάχυσης (DW-MRI) αναλύθηκαν επίσης σε ειδικό λογισμικό (QMRI Utilities-X) και δημιουργήθηκαν έγχρωμοι παραμετρικοί χάρτες του συντελεστή διάχυσης ιστού (D) και της εξαρτώμενης από τη ροή ψευδοδιάχυσης στο δίκτυο των τριχοειδών αγγείων (D*). Οι παραμετρικοί αυτοί χάρτες μεταφέρθηκαν και αναλύθηκαν από εμπορικά διαθέσιμο λογισμικό (nordicICE v4.0, NNL, Bergen, Norway).

Αποτελέσματα

Όσον αφορά τις εξετάσεις CTFP, 22 ασθενείς συμμετείχαν στη μελέτη. Η επαναγγείωση επιτεύχθηκε σε 19 ασθενείς, ενώ η αξιολόγηση του CTFP δεν ήταν εφικτή σε 5 εξετάσεις και ένας ασθενής πέθανε πριν από την μετεπεμβατική εξέταση. Συνολικά, 13 ασθενείς (10 άνδρες, 3 γυναίκες) συμπεριλήφθηκαν στην ανάλυση. Η μέση ηλικία ήταν 72 έτη (εύρος 51-84 έτη). Σύμφωνα με την ταξινόμηση της ΠΑΝ κατά Rutherford, ένας ασθενής κατατάχθηκε στην κατηγορία 4, οκτώ ασθενείς στην κατηγορία 5 και τέσσερις ασθενείς στην κατηγορία 6. Η επαναγγείωση ήταν τεχνικά επιτυχής σε όλους τους ασθενείς και ο μέσος σφυροβραχιόνιος δείκτης αυξήθηκε από 0,36 ± 0,16 σε 0,75 ± 0,22. Μετά την επαναγγείωση, ο δείκτης BV αυξήθηκε από 1,55 mL / 100 g ± 0,83 σε 4,51 mL / 100 g ± 1,53, ο δείκτης BF αυξήθηκε από 16,28 mL / 100 g / min ± 4,97 σε 31,49 mL / 100 g / min ± 6,86 και ο δείκτης PS αυξήθηκε από 3,1 mL / min / 100 g ± 1,95 σε 8,67 mL / min / 100 g ± 3,85 (P <0,05). Η αύξηση των παραμέτρων διάχυσης ήταν μεγαλύτερη στο δέρμα σε σύγκριση με περιοχές μυϊκού ιστού (p = 0,0016 για BV, p = 0,0333 για BF και p = 0,0027 για PS). Επιπλέον, οι ασθενείς με φτωχή ανταπόκριση στην επαναγγείωση, οι οποίοι τελικά υποβλήθηκαν σε ακρωτηριασμό παρουσίασαν χαμηλότερες τιμές παραμέτρων perfusion μετά την PTA σε σχέση με τους ασθενείς με σημαντική κλινική βελτίωση (P <.05). Όλες οι μετρήσεις έδειξαν πολύ καλή επαναληψιμότητα μεταξύ των παρατηρητών και οι συντελεστές ενδοταξικής συσχέτισης ήταν 0,91 για το BV, 0,94 για το BF και 0,95 για το PS. Η μέση δόση-μήκους σάρωσης του CTFP ήταν 1430,4 mGy * cm και η μέση δραστική δόση ήταν 0,29 mSv.

Όσον αφορά το πρωτόκολλο DCE-MRI, 16 ασθενείς συμμετείχαν στη μελέτη. Η επαναγγείωση επιτεύχθηκε σε 13 ασθενείς, ενώ ένας ασθενής απεβίωσε και ένας άλλος υπέστη ακρωτηριασμό πριν από την μετεπεμβατική εξέταση DCE-MRI. Η ανάλυση επίσης δεν ήταν εφικτή σε μία περίπτωση. Συνολικά, 10 ασθενείς (6 άνδρες, 4 γυναίκες) με μέση ηλικία τα 68 έτη (εύρος 58-79 έτη) συμπεριλήφθηκαν στην τελική ανάλυση. Σύμφωνα με την ταξινόμηση της ΠΑΝ, κατά Rutherford, δύο ασθενείς κατατάχθηκαν

στην κατηγορία 4, έξι ασθενείς στην κατηγορία 5 και δύο ασθενείς στην κατηγορία 6. Η επαναγγείωση ήταν τεχνικά επιτυχής σε όλους τους ασθενείς και ο μέσος σφυροβραχιόνιος δείκτης (ABI) αυξήθηκε από 0,37 ± 0,18 σε 0,76 ± 0,23, p <0,05. Μετά την PTA, ο δείκτης BF αυξήθηκε από 6.232 ± 2.867–9.867 ± 2.965 mL / min / 100 g, ο δείκτης K^{trans} αυξήθηκε από 0.060 ± 0.022 σε 0.107 ± 0.041 min^{-1} και ο δείκτης K_{ep} αυξήθηκε από 0.103 ± 0.024 σε 0.148 ± 0.024 min^{-1}, p <0,05. Όλες οι μετρήσεις έδειξαν πολύ καλή αξιοπιστία μεταξύ των παρατηρητών με συντελεστή ενδοταξικής συσχέτισης > 0,85 για όλες τις παραμέτρους perfusion.

Όσον αφορά τη σύγκριση μεταξύ των παραμέτρων διάχυσης και αιματικής διήθησης, η ανάλυση συσχέτισης voxel με voxel δεν έδειξε σημαντική συσχέτιση με βάση τη συσχέτιση κατά Pearson. Όταν εφαρμόστηκε ένα φίλτρο Gaussian στους παραμετρικούς χάρτες, επιτεύχθηκε ένας καλός συσχετισμός (> 0,5) μεταξύ των παραμέτρων διάχυσης και αιματικής διήθησης.

Τέλος, 8 ασθενείς (5 άντρες, 3 γυναίκες) με διάμεση ηλικία τα 69 έτη (εύρος 56-79 έτη) υποβλήθηκαν σε εξετάσεις μοριακής διάχυσης (DW-MRI) πριν και μετά την PTA. Σύμφωνα με την ταξινόμηση της ΠΑΝ κατά Rutherford, δύο ασθενείς κατατάχθηκαν στην κατηγορία 4, πέντε ασθενείς στην κατηγορία 5 και ένας ασθενής στην κατηγορία 6. Επιπλέον, 6 υγιείς μάρτυρες (3 άνδρες και 3 γυναίκες) με διάμεση ηλικία τα 50 έτη (εύρος 38-67 έτη) υποβλήθηκαν στην ίδια εξέταση. Κανείς από τους παραπάνω δεν είχε ιστορικό ή προδιαθεσικούς παράγοντες για ΠΑΝ. Η επαναγγείωση ήταν τεχνικά επιτυχής σε όλους τους ασθενείς και ο μέσος σφυροβραχιόνιος δείκτης (ABI) αυξήθηκε από 0,35 ± 0,2 σε 0,76 ± 0,25, p <0,05. Μετά την επιτυχή επαναγγείωση, το D* αυξήθηκε από 279.88 ± 13.47 10^{-5} mm^2/s σε 331.51 ± 31 10^{-5} mm^2/s, p<0.05. Επιπλέον, οι υγιείς μάρτυρες παρουσίασαν υψηλότερη τιμή D* σε σύγκριση με τους ασθενείς με ΠΑΝ (μέση τιμή 332.47 ± 22.95 10^{-5} mm^2/s έναντι 279.88 ± 13.47 10^{-5} mm^2/s αντίστοιχα p<0.05).

Συμπέρασμα

Οι τεχνικές αιματικής διήθησης με χρήση υπολογιστικής ή μαγνητικής τομογραφίας είναι αξιόπιστες εφαρμογές που μπορούν να αποτελέσουν χρήσιμα εργαλεία για την αξιολόγηση της υποαιμάτωσης των κάτω άκρων και την εκτίμηση των αποτελεσμάτων της διαδερμικής αγγειοπλαστικής σε ασθενείς με ΚΙΑ. Οι πληροφορίες που παρέχονται από αυτές τις εξετάσεις μπορεί να βοηθήσουν στην αξιόπιστη πρόβλεψη της ανταπόκρισης στη θεραπεία επαναγγείωσης ή σε επικείμενο ακρωτηριασμό άκρου σε ασθενείς με ΚΙΑ. Τέλος, θα μπορούσαν να χρησιμοποιηθούν ως εργαλεία για την παρακολούθηση των αποτελεσμάτων της ενδαγγειακής ή χειρουργικής θεραπείας και του σχεδιασμού της στρατηγικής επαναγγείωσης.

Abstract

Introduction

Peripheral arterial disease (PAD) describes the impairment of blood flow to lower extremities as a result of stenoses or occlusions in lower limb arteries on a basis of atherosclerotic disease. The prevalence of PAD varies in general population from 3-10% in individuals younger than 70 years to 15-20% in elder people older than 70 years. The main risk factor for PAD include diabetes mellitus (DM), hypertension (HT), hyperlipidemia (HL), coronary arterial disease (CAD) and smoking. The classic presenting symptom of PAD is intermittent claudication (IC) and less commonly patients presented with critical limb ischemia (CLI) which requires revascularization in order to prevent amputation. CLI refers to the end stage of PAD, in which macrovascular lesions of lower limb arteries induce significant reduction of distal perfusion pressure. It can be presented as ischemic rest pain, gangrene or ulceration of foot. Revascularization strategies include either endovascular procedures such as percutaneous transluminal angioplasty (PTA) with or without stent deployment or surgical procedures such as lower extremity by-pass (using autologous venous or synthetic grafts). The selection of the appropriate treatment is based on patient clinical status, limb threat assessment and anatomic pattern of the disease. Evaluation of PAD includes medical history, clinical examination, functional tests such as ankle-brachial index (ABI) and segmental limb pressures and anatomic/radiologic tests such as color duplex ultrasound (CDUS), computed tomography angiography (CTA) and magnetic resonance angiography (MRA). These modalities provide significant information about the distribution of macrovascular lesions of the limbs (stenoses, occlusions) but not for the local microvascular perfusion of the extremities. They can be used in clinical practice to assess the extent of disease, plan the revascularization strategy and finally confirm the

patency of the main arteries after treatment. However, they cannot measure blood flow (BF) to the limb or estimate the influence of collateral vessels on end-organ perfusion. These modalities are also incapable of estimating the response to therapeutic interventions regarding the improvement in tissue perfusion.

Purpose

The goals of PhD thesis are:

- to emerge hypoperfusion of lower extremities in patients with CLI and estimate PTA results using CT and MR perfusion techniques.
- to compare the abilities of different MR perfusion techniques .
- to correlate the lower limb perfusion results with the clinical outcome of patients after PTA and their imaging studies (CDUS, CTA) as part of their follow-up to determine the potential prognostic value of CT/MR perfusion techniques.

Materials and Methods

Selective patients with CLI (either rest pain or minor/major tissue loss, Rutherford categories 4-6) were enrolled in this research. The anatomic distribution of atherosclerotic lesions and patient's comorbidities/overall clinical status should make them suitable for endovascular revascularization. Patients presenting less advanced PAD (not classified as CLI) or acute lower limb ischemia were excluded. Similarly, patients that underwent surgical revascularization or those in whom either a conservative approach or a primary amputation was performed, were also excluded.

The patients that fulfilled the abovementioned criteria were subjected to CT perfusion examination (CTFP) or MR perfusion examination including dynamic contrast-enhanced MRI (DCE-MRI) and diffusion weighted MRI (DW-MRI) before and after PTA. All patients were followed-up with clinical examination at 1, 3, 6 and 12 months and color Doppler ultrasound combined with clinical examination on an annual basis.

CTFP examinations were performed on a 128-slice CT scanner (Revolution GSI, GE Healthcare, USA). Images were obtained after injection of 40 ml of iodinated non-ionic contrast medium followed by 30 mL of saline solution at a flow rate of 4 mL/s. CT perfusion images were transferred to a dedicated workstation (AW server 3.2, GE Medical Systems) and analyzed using commercial CT software (CT-Perfusion-4D, GE Medical Systems). CT perfusion maps of various hemodynamic parameters such as blood volume [BV], blood flow [BF] and permeability surface [PS] were created via deconvolution algorithm and the change in the relative perfusion parameters before and after endovascular treatment was calculated. Moreover, studies from 6 patients were examined by a second observer to determine inter-observer reproducibility.

MR perfusion examinations were performed on a 1.5T clinical MR Scanner (Vision/Sonata Hybrid system, Siemens, Erlangen, Germany) enforced with a powerful 3T equivalent gradient system. The MR perfusion protocol included:

- Conventional T1w 3D GRE VIBE and T2/T1w 3D GRE CISS sequences.
- Diffusion weighted (DW) sagittal images utilizing a high resolution HASTE (Half-Fourier Acquisition Single-shot Turbo spin Echo) sequence with diffusion sensitizing gradients with b values (b = 0, 50, 100, 150, 200, 500, 800, 1000 s/mm2).
- T1w 3D GRE VIBE sequence in sagittal plane with variable flip angles (FA = 5^{o},10^{o},15^{o},20^{o}, 25^{o},30^{o}) for the initial calculation of the parametric T1 maps and T1w 3D GRE VIBE perfusion sequence repeated for ten minutes after the intravenous injection of paramagnetic contrast medium CA (0.1 mmol/kg) for DCE-MRI.

DCE-analysis was performed utilizing an extended Tofts model and quantitative perfusion maps based on pharmacokinetic parameters such us blood flow (BF), K^{trans} and K_{ep} were created from parametric data fitted to the extended Tofts model utilizing a population-based arterial input function (AIF).

As far as the comparison between MR perfusion parameters Linear and nonlinear least squares algorithms, were incorporated for the quantification of the parameters through a variety of widely used models, able to extract physiological information from each imaging technique. All numerical calculations were implemented in Python 3.5 and include the: Intra voxel incoherent motion for diffusion and Patlak's, Extended Toft's and Gamma Capillary Transit time (GCTT) models for perfusion MRI.

DW sagittal images were analyzed in-house software (QMRI Utilities-X) and color parametric maps of tissue diffusion coefficient (D) and flow-related pseudo diffusion inside the capillary network (D*) were constructed on a pixel by pixel basis. The parametric maps (D and D*) were then transferred and evaluated with a commercially available software (nordicICE v4.0, NNL, Bergen, Norway).

Results

As far as CTFP examination, 22 patients enrolled in the study. Technical success was achieved in 19 patients, CTFP evaluation was not feasible in 5 examinations and one patient died before post-PTA CTFP. Totally, 13 patients (10 male, 3 female) were included in the analysis. The median age was 72 years (range 51-84 years). According to Rutherford classification of PAD, one patient was allocated to class 4, eight patients to class 5 and four patients to class 6 PAD. Revascularization was technically successful in all patients, and mean ankle–brachial index (ABI) increased from 0.36 ± 0.16 to 0.75 ± 0.22. After revascularization, mean BV increased from 1.55 mL/100 g ± 0.83 to 4.51 mL/100 g ± 1.53, BF increased from 16.28mL/100 g/min ± 4.97 to 31.49 mL/100 g/min ± 6.86, and PS increased from 3.1 mL/min/100 g ± 1.95 to 8.67 mL/min/100 g ± 3.85 ($P < .05$). Perfusion parameters increase was greater in dermis compared to muscle tissue regions ($p=0.0016$ for BV increase, $p=0.0333$ for BF increase and $p=0.0027$ for PS increase). Moreover, patients with poor response to revascularization who finally

underwent amputation presented lower post-PTA perfusion parameters values than patients with significant clinical improvement (P <.05). All measurements demonstrated very good interobserver reproducibility, and intraclass correlation coefficients were 0.91 for BV, 0.94 for BF, and 0.95 for PS respectively. The mean dose-length product of CTFP was 1430.4 mGy*cm and the mean effective dose was 0.29 mSv.

As far DCE-MRI, 16 selective patients enrolled in the study. Technical success was achieved in 13 patients, one patient died and another patient underwent amputation before post-PTA examination and DCE analysis was not feasible in one case. Totally, 10 patients (6 male, 4 female) with a median age of 68 years (range 58-79 years) were included in the final analysis. According to Rutherford classification of PAD, two patients were allocated to class 4, six patients to class 5 and two patients to class 6 PAD. Revascularization was technically successful in all patients and mean ABI increased from 0.37 ± 0.18 to 0.76 ± 0.23, p < 0.05. After PTA, mean BF increased from 6.232 ± 2.867–9.867 ± 2.965 mL/min/100 g, K^{trans} increased from 0.060 ± 0.022 to 0.107 ± 0.041 min−1 and K_{ep} increased from 0.103 ± 0.024 to 0.148 ± 0.024 min−1, p < 0.05. All measurements demonstrated very good inter-observer reliability with an ICC > 0.85 for all perfusion parameters.

As far as the comparison between diffusion and perfusion parameters, voxel by voxel correlation analysis didn't show any significant correlation based on the Pearson's correlation. When a Gaussian filter was applied to the parametric maps, a good correlation (> 0.5) of diffusion and perfusion parameters was achieved.

Finally, 8 patients (5 male, 3 female) with a median age of 69 years (range 56-79 years) underwent DW-MRI before and after PTA. According to Rutherford classification of PAD, two patients were allocated to class 4, five patients to class 5 and one patients to class 6 PAD. Moreover 6 healthy volunteers (3 male, 3 female) with a median age of 50 years (range 38-67 years) underwent the same examination. Neither of these volunteers had history of PAD or predisposing factors for PAD such as diabetes mellitus, hypertension

or history of smoking. Technical success was also achieved in all patients, included in the final analysis (8/8). After PTA, mean ABI increased from 0.35 ± 0.2 to 0.76 ± 0.25 ($p<0.05$). After successful revascularization, D* increased from 279.88 ± 13.47 10^{-5} mm^2/s to 331.51 ± 31 10^{-5} mm^2/s, $p<0.05$. Moreover, healthy volunteers presented higher D* in comparison with PAD patients (332.47 ± 22.95 10^{-5} mm^2/s versus 279.88 ± 13.47 10^{-5} mm^2/s respectively, $p<0.05$).

Conclusion

CT perfusion, DCE-MRI and DW-MRI are reproducible techniques which can be useful tools for evaluation of lower limb hypoperfusion and estimation of PTA outcome in patients with CLI. The information provided by these examinations may aid reliable prediction of poor response to revascularization or an imminent amputation in patients with CLI. Moreover, they could be promising tools for monitoring of endovascular or surgical treatment and planning of revascularization strategy.

Peripheral arterial disease

Peripheral arterial disease (PAD) describes the impairment of blood flow to lower extremities as a result of atherosclerotic disease [1]. Atherosclerosis is a complex process which includes endothelial dysfunction, platelet activation, thrombosis, oxidative stress, smooth muscle activation, lipid disturbances and genetic factors [2]. Inflammation has also a significant role in all phases of atherosclerotic process as biological data implicate inflammatory pathways in early atherogenesis, in lesion progression and in the thrombotic complications of the disease. Moreover there is correlation between inflammatory markers and ischemic events which can be an important tool for risk stratification [3].

Epidemiology

The incidence of PAD varies in general population from 3 -10% in individuals younger than 70 years to 15-20% in elder people older than 70 years, whereas the prevalence in this age group is between 14 and 29% [4]. Figure 1 shows the prevalence of PAD by age group and sex in high-income and low-income counties. Moreover, PAD is a significant manifestation of systemic atherosclerosis and is associated with increased rate of cardiovascular ischemic disease and death [5]. However, 40% of patients with PAD are asymptomatic and only 10% present intermittent claudication (IC), a cramping leg pain which is the typical symptom of the disease. Moreover 50% have atypical lower extremity symptoms [6]. This heterogenity of clinical presentation is the main reason for under-diagnosis of PAD and the difficult estimation of its incidence in general population. Furthermore, only 25% of patients with PAD seek treatment, which leads to functional decline, limitation of physical activity and in serious cases to limb amputation [5]. The 10-year risk of death in PAD patients is over 40% and about 20% of patients will suffer a heart attack, stroke or death within 1 year [7] .

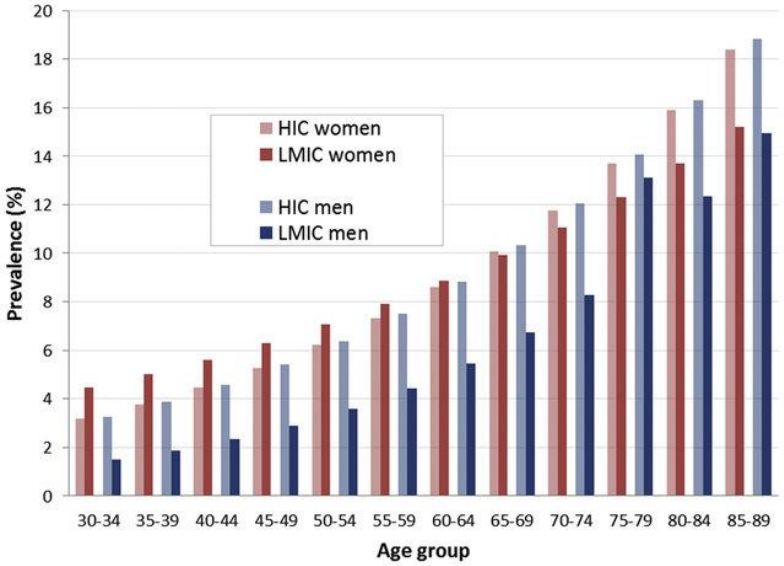

Fig. 1: Prevalence of peripheral artery disease (PAD; ankle-brachial index [ABI] <0.9) by age and sex in high-income countries (HICs) and in low-and middle-income countries (LMICs).

Conte MS, Bradbury AW, Kolh P, et al. Global vascular guidelines on the management of chronic limb-threatening ischemia. J Vasc Surg. 2019;693

Risk factors

The risk of PAD can be predicted by age and the knowledge of atherosclerotic risk factors such as diabetes mellitus (DM), hypertension (HT), hyperlipidemia (HL), coronary arterial disease (CAD) and smoking. The early identification of these risk factors is useful in determining populations and patients at risk. The relative risk of PAD by contributing risk factor is shown in figure 2.

Age, sex, race

As it is referred in the previous paragraph, the incidence of PAD increased with age. Data from the Framingham Heart study showed than the prevalence of PAD increased 10-fold from men aged 30-44 years to men aged 65-74 years and 20-fold in women in the same age groups [8]. PAD was traditionally identified as a male-dominant disease with a male: female prevalence ratio to be reported as 2:1 for PAD [4]. However, recent population

trends and studies revealed that women are affected at least as often as men with PAD [9]. Black race is also associated with PAD. The prevalence rate increased in black race in comparison with Hispanic white and non-Hispanic white race [4]. Furthermore a recent study showed that the high prevalence of PAD in black race is not explained by increased prevalence of DM, HT, HL or other cardiovascular risk factors in this group. As a result, black ethnicity seems to be a strong and independent risk factor for PAD [10].

Diabetes mellitus

DM is a significant risk factor for PAD and cardiovascular diseases. DM affects the vessel wall by multiples ways (derangement of endothelials cells, proatherogenic activity in smooth muscle cells, oxidative stress) but also effects blood cells causing aggregation of enhanced platelets, increased blood viscosity and hypercoagulable state [11]. Rotterdam study showed that DM presents in about 12% and 16% in male and female patients with PAD in comparison with non-PAD patients (6.7% and 6.3% respectively) [12]. A metanalysis also revealed that a 1 % increase in glycated hemoglobin is associated with a 26% increase of the possibility to develop PAD [13]. Moreover, there is association between PAD and foot ulcers in patients with DM and these patients should be evaluated by a multisciplinary diabetic foot team. Complications of foot ulcers are the leading cause of hospitalization and amputation in DM patients and approximately 20-40% of the healthcare resources which were spent for DM are related to treatment of diabetic feet [14].

Hypertension

HT is another significant risk factor for cardiovascular diseases including PAD. About 35-55% of patients with PAD at presentation, also have HT [15]. The risk of IC increased 2.5-fold in men and 4-fold in women with HT [8]. Moreover patients with both PAD and

HT have high risk for stroke or myocardial infarction, so the efficient blood pressure control is important to prevent progression of PAD and fatal complications [15].

Hyperlipidemia

HL is strongly associated with symptoms and sings of PAD. The Lipid Research Clinics Program Prevalence Study compared lipid levels of individuals with and without claudication and with normal or pathological ABI and confirmed the association between HL and PAD [16]. The Framingham Heart Study, showed that there is a 1.2-fold increase in the risk of symptomatic PAD for every 40 mg/dL elevation of total cholesterol levels [8]. However, the strongest lipoprotein risk factor is the low concentration of HDL. Both Rotterdam and Framingham studies revealed this correlation [12,8], whereas the Cardiovascular Health Study showed a 1% increased odds of PAD for every 1mg/dl decrease in HDL [17].

Hyperhomocysteinemia

Multiple studies suggested than increased plasma homocysteine concentration is an independent risk factor for PAD, as it promotes oxidative damage to vascular wall and increased proliferation of vascular smooth muscles cells [18]. A metanalysis which included 33 studies showed that homocysteine levels were significantly elevated in patients with PAD compared to controls [19]. In the same way, a prospective blinded study demonstrated that elevated levels of plasma homocysteine are associated with cardiovascular death and progression of coronary artery disease in patients with symptomatic PAD [20].

Chronic kidney disease

Patients with CKD present a higher risk to develop PAD and its adverse outcomes in comparison with individuals with normal renal function. The prevalence of PAD is increased in patients with CKD and especially in patients requiring dialysis [21],

whereas it exceed 45% in elder patients older than 70 years who undergoing dialysis treatment [22]. Furthermore, patients with both CKD and PAD have a significantly higher risk for death in comparison with patients with one of the above mentioned diseases [23].

Smoking

Smoking is the most important modifiable risk factor for PAD. Smoking increases several folds the risk of PAD and it is also more influential risk factor for PAD compared to CAD [24]. It affects the normal function by multiple ways such as endothelial dysfunction and alteration of coagulation, platelet function and lipoprotein metabolism [25]. A metanalysis which included 55 studies showed that there is significant correlation between smoking and PAD which is greater than the reported for CAD. Moreover it revealed that the risk is lower in ex-smokers but it remains high compared to never-smokers [26].

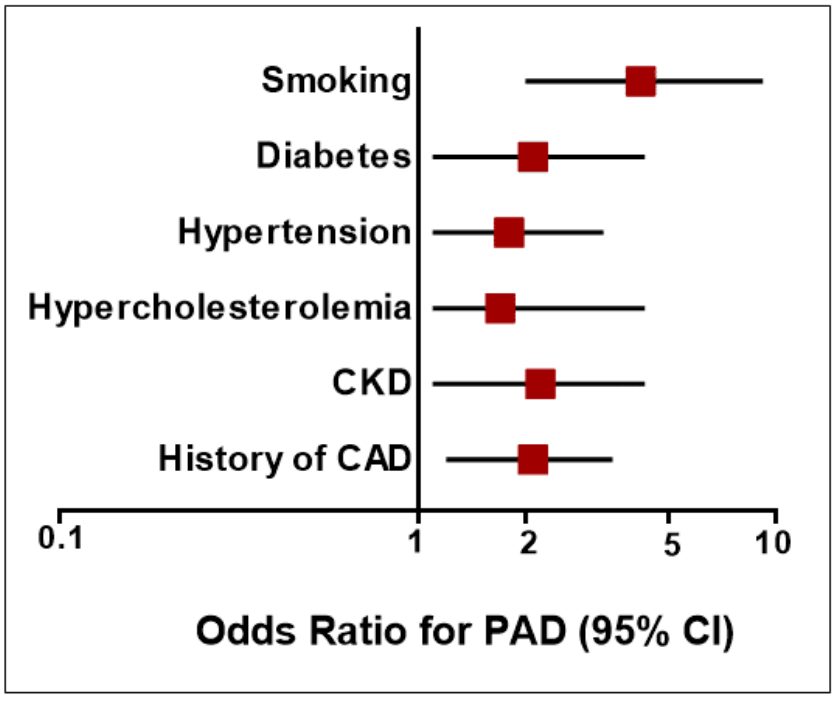

Fig. 2: Risk factors and Odds ratio for PAD

Selvin E, Erlinger TP. Prevalence of and risk factors for peripheral arterial disease in the United States: results from the National Health and Nutrition Examination Survey, 1999-2000 Circulation 2004;110:738-43.

References

[1] Schirmang TC, Ahn SH, Murphy TP et al. Peripheral arterial disease: update of overview and treatment. Med Health R I 2009;92:398-402.

[2] Faxon DP, Fuster V, Libby P et al. Atherosclerotic vascular disease conference: Writing Group III: pathophysiology. Circulation 2004;109:2617-25.

[3] Libby P, Ridker PM, Maseri A. Inflammation and atherosclerosis. Circulation 2002;105:1135-43.

[4] Selvin E, Erlinger TP. Prevalence of and risk factors for peripheral arterial disease in the United States: results from the National Health and Nutrition Examination Survey, 1999-2000 Circulation 2004;110:738-43.

[5] Hirsch AT, Criqui MH, Treat-Jacobson D, et al. Peripheral arterial disease detection, awareness, and treatment in primary care. JAMA 2001;286(11):1317-1324.

[6] Hiatt WR. Medical treatment of peripheral arterial disease and claudication. N Engl J Med 2001;344(21):1608-1621.

[7] Steg PG, Bhatt DL, Wilson PW, et al. One-year cardiovascular event rates in outpatients with atherothrombosis. JAMA 2007;297(11):1197-1206

[8] Murabito JM, D'Agostino RB, Silbershatz H, Wilson WF. Intermittent claudication: a risk profile from the Framingham Heart Study. Circulation 1997; 96:44–49.

[9] Schramm K, Rochon PJ. Gender Differences in Peripheral Vascular Disease. Semin Intervent Radiol 2018;35(1):9-16.

[10] Criqui MH, Vargas V, Denenberg JO, et al. Ethnicity and peripheral arterial disease: the San Diego Population Study. Circulation 2005;112(17):2703-2707.

[11]American Diabetes Association. Peripheral arterial disease in people with diabetes. Diabetes Care 2003;26:3333-3341.

[12] Meijer WT, Grobbee DE, Hunink MG, Hofman A, Hoes AW. Determinants of peripheral arterial disease in the elderly: the Rotterdam study. Arch Intern Med 2000; 160:2934 –2938.

[13] Selvin E, Marinopoulos S, Berkenblit G, Rami T, Brancati FL, Powe NR, et al. Meta analysis: glycosylated hemoglobin and cardiovascular disease in diabetes mellitus. Ann Intern Med 2004;141:421-31

[14] Boulton AJ, Vileikyte L, Ragnarson-Tennvall G, Apelqvist J. The global burden of diabetic foot disease. Lancet 2005;366(9498):1719-24.

[15] Clement DL, De Buyzere ML, Duprez DA. Hypertension in peripheral arterial disease. Curr Pharm Des 2004;10(29):3615-3620.

[16] Pomrehn P, Duncan B, Weissfeld L, et al. The association of dyslipoproteinemia with symptoms and signs of peripheral arterial disease. The Lipid Research Clinics Program Prevalence Study. Circulation 1986;73(suppl): I100 -I107.

[17] Newman AB, Siscovick DS, Manolio TA, Polak J, Fried LP, Borhani NO, et al. Ankle-arm index as a marker of atherosclerosis in the Cardiovascular Health Study. Cardiovascular Heart Study (CHS) Collaborative Research Group. Circulation 1993;88:837-845.

[18] Welch GN, Loscalzo J. Homocysteine and atherothrombosis. N Engl J Med 1998; 338:1042-1050.

[19] Khandanpour N, Loke YK, Meyer FJ, Jennings B, Armon MP. Homocysteine and peripheral arterial disease: systematic review and meta-analysis. Eur J Vasc Endovasc Surg 2009;38(3):316-322.

[20] Taylor LM Jr, Moneta GL, Sexton GJ, Schuff RA, Porter JM. Prospective blinded study of the relationship between plasma homocysteine and progression of symptomatic peripheral arterial disease. J Vasc Surg 1999;29:8-19

[21] Leskinen Y, Salenius JP, Lehtimaki T, Huhtala H, Saha H. The prevalence of peripheral arterial disease and medial arterial calcification in patients with chronic renal failure: requirements for diagnostics. Am J Kidney Dis 2002;40:472 -479.

[22]Lamping DL, Constantinovici N, Roderick P, et al. Clinical outcomes, quality of life, and costs in the North Thames Dialysis Study of elderly people on dialysis: a prospective cohort study. Lancet 2000;356(9241):1543-1550.

[23] Liew YP, Bartholomew JR, Demirjian S, Michaels J, Schreiber MJ Jr. Combined effect of chronic kidney disease and peripheral arterial disease on all-cause mortality in a high-risk population. Clin J Am Soc Nephrol 2008;3(4):1084-1089.

[24] Lu JT, Creager MA. The relationship of cigarette smoking to peripheral arterial disease. Rev Cardiovasc Med. 2004;5(4):189-193.

[25] Newby DE, Wright RA, Labinjoh C, et al. Endothelial dysfunction, impaired endogenous fibrinolysis, and cigarette smoking: a mechanism for arterial in a defined population. Circulation1985;71:516 -522.

[26] Lu L, Mackay DF, Pell JP. Meta-analysis of the association between cigarette smoking and peripheral arterial disease. Heart 2014;100(5):414-423.

Clinical presentation and classification of PAD

The majority of patients with PAD (about 65-75%) are asymptomatic. Whether symptoms develop or not depends on the level of activity of the individuals. The classic presenting symptom is intermittent claudication (IC) and less commonly patients presented with critical limb ischemia (CLI) which requires revascularization in order to prevent amputation or other PAD complications [1].

Intermittent claudication

The most typical presentation of PAD is intermittent claudication (IC), which is characterized by pain in lower extremities, especially in the calves, which increased by walking or exercise and relieved by rest. The symptoms location often indicates the level of arterial involvement. In patients with proximal arterial lesions (aortoiliac segment), the pain extends into the thighs and buttocks. It is also important to distinguish IC from pain related to venous diseases, arthritis and peripheral neuropathy [2]. The Edinburgh Claudication Questionnaire is a helpful tool for diagnosis of IC with high specificity and acceptable sensitivity [3]. However, the diagnosis of PAD may be missed because many patients are asymptomatic or present atypical symptoms. Moreover, although PAD is a progressive disease, its clinical course is stable in the majority of cases. That is a result of collateral vessels development, metabolic adaption of ischemic muscle and movement altering in favor of non-ischemic muscles [4]. Fortunately, amputation is a rare complication of IC (<2%) but closed follow-up and risk factors modification is necessary because it is difficult to predict the risk of deterioration in PAD patients [1].

Ischemic rest pain

In more severe cases of PAD, pain is not only present during exercise but also at rest. It is a continuous, burning pain which increased in supine position and relieved by sitting or placing the extremity in a dependent position [2]. Nocturnal rest pain often occurs after the patient has fallen asleep, as systemic blood pressure decreases, which causes further reduction of limb perfusion [5].

Gangrene and ulceration

Gangrene and ulcers represent the most severe presentation of PAD. Gangrene is a type of tissue necrosis as a result of significant reduction of blood supply [2]. It usually affects digits or the heel but in severe cases may involve the whole foot (figure 1). Symptoms include red or black color of foot, numbness, pain, skin breakdown and coolness [6]. There are two main types of gangrene, dry and wet. Dry gangrene is characterized by dry and shriveled skin and is associated with severe PAD. It also develops slowly. On the other hand, wet gangrene refers to bacterial infection of the affected tissue. Swelling and wet appearance by blisters oozing fluid are features of this type. Moreover, it may be associated with PAD but it can be also a result of frostbite, burn or trauma. Wet gangrene usually develops rapidly and has poorer prognosis compared to dry-gangrene due to systemic manifestation of sepsis. A salvage amputation may be necessary to prevent death [7].

Arterial ulcers are also associated with severe PAD as a result of lower extremity hypoperfusion. They are extremely painful and they are often presented after local trauma. However, pain is absent in patients with peripheral neuropathy [2]. Ulceration typically located on the toes and forefoot, but other areas may also be affected in patients with diabetic neuropathy or foot deformity [6]. Ulcers have gray or yellow fibrotic base and undermining skin margins (figure 2). They are often associated with skin and muscle tissue changes such as skin thinness, muscle atrophy and absence of

hair and they can also be complicated by local infection and inflammation [8]. However, there are also foot ulcers which are caused by venous diseases or diabetes (neuropathic/neuroischemic) and differential diagnosis is critical in order to provide the optimal medical treatment [1].

Fig. 1: Dry gangrene of left foot

Fig. 2: Two patients with arterial heel ulceration and mixed arterial-venous ulceration of toes and dorsal aspect of the foot respectively.

Critical limb ischemia

Critical limb ischemia (CLI) refers to the end stage of PAD, in which macrovascular lesions of lower limb arteries induce significant reduction of distal perfusion pressure that microcirculation and nutrient blood flow to tissues are significantly disturbed. The definition of CLI has involved from the initial definition by Bell et al on 1982 to TASC I and TASC II and the recent published GLOBAL vascular guidelines [14]. TASC II suggests the term of CLI to be used for all patients with chronic ischemic rest pain, ulcers or gangrene attributable to objectively proven arterial occlusive disease and the diagnosis should be supported by objective tests [1]. Global vascular guidelines which were published on 2019, proposed the term critical limb threatening ischemia (CLTI) which included a broader and more heterogeneous group of patients with various degrees of limb ischemia with increased amputation risk. CLTI is associated with chronic limb hypoperfusion on a basis of athreosclerotic disease, so patients with acute limb ischemia, vasculitides, venous diseases, neoplastic diseases and radiation arteritis are excluded. The diagnosis of CLTI requires both objectively documented atherosclerotic PAD and ischemic rest pain or tissue loss (gangrene, ulceration) [6].

Acute lower limb ischemia

Acute lower limb ischemia (ALLI) represents a quickly developing or sudden decrease in limb perfusion, resulting in a potential threat to the viability of the extremity [1]. The hypoperfusion also impairs cardiopulmonary and renal function due to systemic acid-base and electrolyte abnormalities [9]. The causes of ALLI include acute thrombosis of a limb artery or bypass graft, embolism from the heart, dissection and trauma [10]. A limb-threatening ischemic event is characterized acute if the duration of symptoms is less than 14 days, subacute between 15 days and 3 months and chronic after 3 months [11]. A patient with ALLI often presents with the “5 P’s” of parasthesia, pain, pallor,

pulselessness, and paralysis (figure 3) and the incidence is about 1.5 cases per 10,000 individuals per year [12]. Patients with ALLI have poor short-term outcomes, with a risk of amputation between 10% and 30% and a mortality rate of approximately 15% to 20% in the first year, mainly in the peri-operative period [1,13].

Fig. 3: A patient with acute limb ischemia of right lower extremity

Classification

During the first meeting of the European Society for Cardiovascular Surgery, in 1952, Fontaine et al. introduced a simple clinical classification of patients with chronic PAD. At that time hemodynamic measurements were not available, so the classification was based on the symptoms, signs and clinical presentation of PAD [15]. The Fontaine classification has 4 grades and is displayed in figure 4. Two decades later, in 1969, Yao et al presented the measurement of ankle-brachial index (ABI) using a 10 MHz Doppler probe suggesting an alternative way for the evaluation of PAD [16]. During the same period, Carter et al introduced the systolic pressure measurement in toe, ankle and arm using pneumatic cuffs. They demonstrated that systolic pressures were decreased in patients with atherosclerosis, thromboangiitis obliterans, or Raynaud's phenomena. Moreover, they found that systolic pressure expressed as percentage of brachial pressure was a good index for the evaluation of the overall disease compared to ankle-to-toe pressure which could be a useful index for small distal artery disease [17]. Rutherford classification was proposed as a staging system for PAD, in the Society for Vascular Surgery/International Society for CardioVascular Surgery (SVS/ISCVS) Standards which were published in 1986 [18]. The classification was revised in 1997. Rutherford classified PAD into acute and chronic disease and associated clinical symptoms with objective findings such as ABI, toe pressure and pulse volume recordings. Rutherford's classification resembles Fontaine's classification, with the addition of objective noninvasive data [19]. The classification is demonstrated in figure 4.

On 2019, the Society of Vascular Surgery (SVS) Lower Extremity Guidelines Committee created the SVS Lower Extremity Threatened Limb Classification System [26]. This system correlates amputation risk with parameters such as wound extension, degree of ischemia and severity of foot infection (figure 5) and is titled WIFi (wound, ischemia, foot infection). Each of this fields takes a separate grade and the three grades are

combined to calculate the amputation risk and estimate the benefit of revascularization. WIFi classification has been evaluated in multiple trials and is also suggested for clinical use in the recent Global Vascular Guidelines of Chronic Limb-Threatening Ischemia [6].

Fontaine classification		Rutherford classification	
Stage	**Symptoms**	**Category**	**Symptoms**
I	Asymptomatic	0	Asymptomatic
II	Intermittent claudication	I	Mild claudication
		2	Moderate claudication
		3	Severe claudication
III	Ischemic rest pain	4	Ischemic rest pain
IV	Ulceration or gangrene	5	Ischemic ulceration (minor tissue loss)
		6	Ischemic gangrene (major tissue loss)

Fig. 4: Fontaine stages and Rutherford categories for PAD

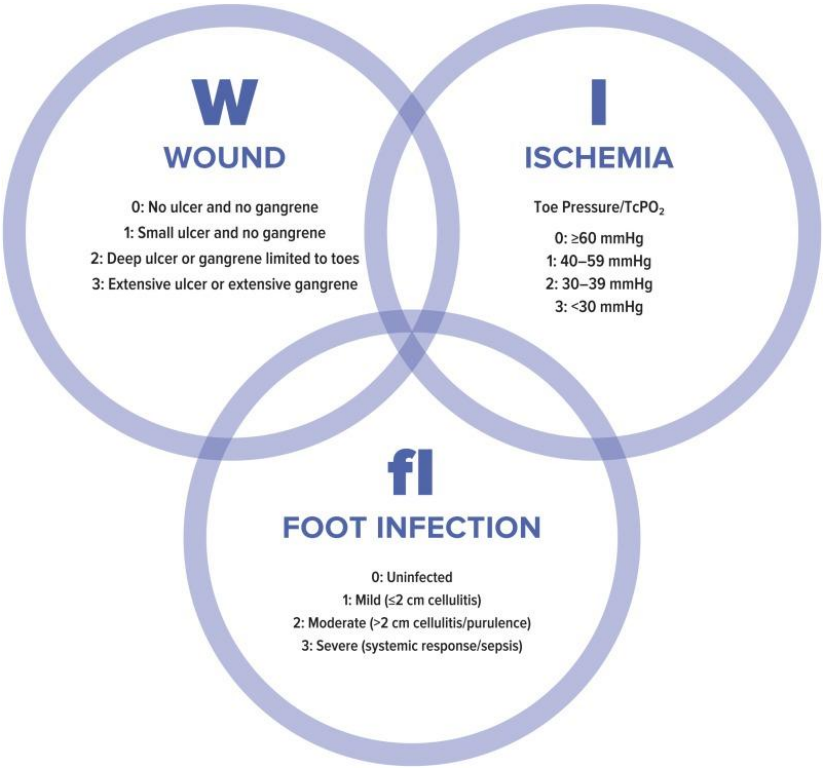

Fig. 5: SVS WIFi classification system

Anatomic classification

Fontaine's and Rutherford's classification are based on clinical history and physical examination of PAD patients. In order to select and plan the appropriate revascularization strategy, anatomic classifications systems have been introduced based on angiographic findings. The first classification system was proposed in 1975. It divided peripheral arteries into pelvic, thigh and calf vessels and each of these three segments took a score from 1 to 9 depending on the atherosclerotic lesions. The maximum score for each extremity is 27 [20]. Bollinger et al suggested an anatomic classification system with many similarities with the previous one, but it divided limb arteries into smaller defined segments which were given a score from 1 to 4 depending on the severity of atherosclerotic lesions. This system took also into consideration the number of atherosclerotic lesions (from single lesions to multiple lesions encompassing the majority of the segment) [21]. It has been reported in a small number of studies or trials but nowadays it is not used in clinical practice. Patients with DM presented different distribution of atherosclerotic lesions compared to patients without DM. Graziani et al, suggested an anatomic classification system which focused mainly on bellow-the-knee arteries (BTK). However, this system has been only used on DM patients with CLI and it was not validated for predicting symptom severity [22]. In 2000, 14 societies from Europe and North America representing vascular surgery, interventional radiology and cardiology formed a consensus for the classification and treatment of PAD which was referred as Trans-Atlantic Inter-Society Consensus Document (TASC). This consensus was updated on 2007 (TASC II) included also societies from Australia, South Africa and Japan. TASC II divided lower extremities arteries into aoro-iliac and femoral-popliteal area and lesions were grouped into 4 categories (A-D) according to the number of lesions, their length and their severity (figure 6). TASC A lesions are treated effectively with endovascular procedures. TASC B lesions have good results with endovascular procedures and this treatment must be the

first approach. TASC C lesions should be treated with surgical procedures and endovascular procedures can be performed in high risk patients and finally TASC D lesions should be always treated by open surgery [1]. However, multiple trials have shown excellent results in TASC C and D lesions using endovascular procedures [23-25]. The Global Vascular Guidelines of Chronic Limb-Threatening Ischemia which were published on 2019 introduced the Global Limb Anatomic Staging System (GLASS) as a new angiographic scoring system. GLASS was developed to facilitate clinical decision in CLI. It defines a preferred target artery path, and establishes stages of complexity for intervention. Overall, it can predict the likelihood of limb salvage and on the same time to propose the best way to achieve it [6].

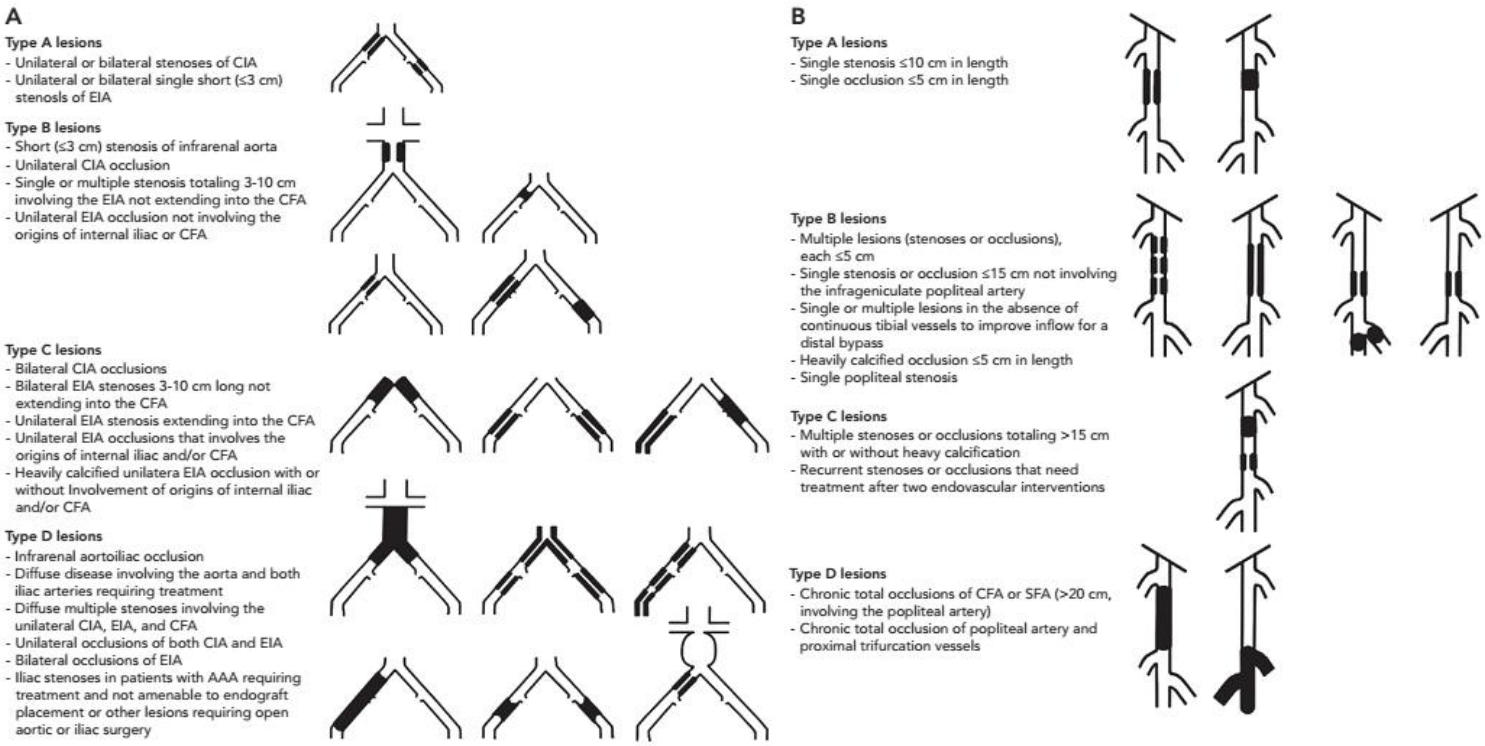

Fig. 6: Trans-Atlantic Inter-Society Consensus II classifications for (A) Aorto-iliac and Femoro-Popliteal PAD

References

[1] Norgren L, Hiatt WR, Dormandy JA et al. Inter-society consensus for the management of peripheral arterial disease (TASC II). J Vasc Surg 2007;45(Suppl. S):S5–67.

[2] Aboyans V, Ricco JB, Bartelink MEL, et al. 2017 ESC Guidelines on the Diagnosis and Treatment of Peripheral Arterial Diseases, in collaboration with the European Society for Vascular Surgery (ESVS): Document covering atherosclerotic disease of extracranial carotid and vertebral, mesenteric, renal, upper and lower extremity arteries. Endorsed by: the European Stroke Organization (ESO)The Task Force for the Diagnosis and Treatment of Peripheral Arterial Diseases of the European Society of Cardiology (ESC) and of the European Society for Vascular Surgery (ESVS). Eur Heart J 2018;39(9):763-816.

[3] Leng GC, Fowkes FG. The Edinburgh Claudication Questionnaire: an improved version of the WHO/Rose Questionnaire for use in epidemiological surveys. J Clin Epidemiol 1992;45:1101-1109.

[4] McDermott MM, Criqui MH, Greenland P, Guralnik JM, Liu K, Pearce WH, et al. Leg strength in peripheral arterial disease: associations with disease severity and lower-extremity performance. J Vasc Surg 2004;39(3):523-30.

[5] Beard JD. Chronic lower limb ischemia. West J Med 2000;173(1):60-63.

[6] Conte MS, Bradbury AW, Kolh P, et al. Global vascular guidelines on the management of chronic limb-threatening ischemia. J Vasc Surg 2019;69(6S):3S-125S.e40.

[7] Al Wahbi A. Autoamputation of diabetic toe with dry gangrene: a myth or a fact?. Diabetes Metab Syndr Obes 2018;11:255-264.

[8] Hampton S. An introduction to various types of leg ulcers and their management.. Br J Nurs 2006;15(11):S9-S13.

[9] Kasirajan K, Ouriel K. Current options in the diagnosis and management of acute limb ischemia. Progress in cardiovascular nursing 2002;17(1):26-34.

[10] Creager MA, Kaufman JA, Conte MS. Clinical practice. Acute limb ischemia. The New England journal of medicine 2012;366(23):2198-206.

[11] Patel N, Sacks D, Patel RI, Moresco KP, Ouriel K, Gray R et al. SIR reporting standards for the treatment of acute limb ischemia with use of transluminal removal of arterial thrombus. Journal of vascular and interventional radiology : JVIR 2003;14(9 Pt 2):S453-65.

[12] Walker TG. Acute limb ischemia. Techniques in vascular and interventional radiology 2009;12(2):117-29.

[13] Earnshaw JJ, Whitman B, Foy C. National Audit of Thrombolysis for Acute Leg Ischemia (NATALI): clinical factors associated with early outcome. Journal of vascular surgery 2004;39(5):1018-25.

[14] Becker F, Robert-Ebadi H, Ricco JB, et al. Chapter I: Definitions, epidemiology, clinical presentation and prognosis. Eur J Vasc Endovasc Surg 2011;42 Suppl 2:S4-S12.

[15] Fontaine R, Kim M, Kieny R. Surgical treatment of peripheral circulation disorders. Helv Chir Acta 1954;21:499-533.

[16] Yao ST, Hobbs JT, Irvine WT. Ankle systolic pressure measurements in arterial disease affecting the lower extremities. Br J Surg 1969;56:676-9.

[17]Carter SA, Lezack JD. Digital systolic pressures in the lower limb in arterial disease. Circulation 1971;43:905-14.

[18] Suggested standards for reports dealing with lower extremity ischemia. Prepared by the Ad Hoc Committee on Reporting Standards, Society for Vascular Surgery/North American Chapter, International Society for Cardiovascular Surgery. J Vasc Surg 1986;4:80-94.

[19] Rutherford RB, Baker JD, Ernst C, et al. Recommended standards for reports dealing with lower extremity ischemia: revised version. J Vasc Surg 1997;26:517-38.

[20]Vogelberg KH, Berchtold P, Berger H, et al. Primary hyperlipoproteinemias as risk factors in peripheral artery disease documented by arteriography. Atherosclerosis 1975;22(2):271-285

[21] Bollinger A, Breddin K, Hess H, et al. Semiquantitative assessment of lower limb atherosclerosis from routine angiographic images. Atherosclerosis 1981;38(3-4):339-346

[22] Graziani L, Silvestro A, Bertone V, et al. Vascular involvement in diabetic subjects with ischemic foot ulcer: a new morphologic categorization of disease severity. Eur J Vasc Endovasc Surg 2007;33(4):453-460

[23] Hans SS, DeSantis D, Siddiqui R, KhouryM. Results of endovascular therapy and aortobifemoral grafting for Transatlantic Inter-Society type C and D aortoiliac occlusive disease. Surgery 2008;144(4):583-589

[24] Balzer JO, Gastinger V, Ritter R, et al. Percutaneous interventional reconstruction of the iliac arteries: primary and long-termsuccess rate in selected TASC C and D lesions. Eur Radiol 2006;16(1):124-131

[25] Baril DT, Chaer RA, Rhee RY, Makaroun MS, Marone LK. Endovascular interventions for TASC II D femoropopliteal lesions. J Vasc Surg 2010;51(6):1406-1412

[26] Mills Sr JL, Conte MS, Armstrong DG, Pomposelli FB, Schanzer A, Sidawy AN, et al. The Society for Vascular Surgery Lower Extremity Threatened Limb Classification System: risk stratification based on wound, ischemia, and foot infection (WIfI). J Vasc Surg 2014;59:220e234.e1-2.

Treatment of PAD

The goals of therapy in patients with PAD are to relieve their exertional symptoms, to prevent the progression of systemic atherosclerotic disease, to decrease the risk for cardiovascular events or amputation and to improve their functional status and their quality of life. The appropriate assessment of risk factors, comorbidities, compliance with medical therapy and the regular follow-up of patients with PAD are important parameters to achieve these goals [1-2].

Risk factors modification

Smoking cessation

The significant association between smoking and cardiovascular diseases or PAD is evaluated and confirmed by multiple studies. Smoking cessation slows the progression to CLI and reduces cardiovascular associated mortality [3]. U.S. Public Health Service has published guidelines for efficient smoking cessation and cardiovascular societies recommend smoking cessation for all PAD patients. Nowadays, there are multiple treatment options including behavioral modification counseling and medical therapy with nicotine supplements (gum, nasal spray, transdermal patches) and antidepressant drugs such as bupropion hydrochloride sustained-release tablets. A combination of the above mentioned treatment options has better results as far as long-term rates of cessation compared to nicotine patches alone [4]. However, in cases of tobacco cessation failure, other methods such as hypnotherapy or acupuncture can be also used [3].

Management of Diabetes Mellitus

DM has a significant role in the development of PAD and cardiovascular diseases [1]. The benefits of glycemic control on microvascular disease such as diabetic retinopathy or

nephropathy in DM patients have been demonstrated in Diabetes Control and Complications Trial and the United Kingdom Prospective Diabetes Study. These studies showed also that intensive glycemic control was associated with reduction of cardiovascular events but had no effect on PAD and the risk for amputation [5-6]. However, glycemic control is essential in all DM patients with PAD. Metformin is used in clinical practice as the initial oral hypoglycemic agent. If additional therapy is necessary, drugs such as sulfonylurea, thiazolidinedione, a-glucosidase can be used. The goal for individuals with DM is to maintain a glycosylated hemoglobin A1c level lower than 7%. However, in patients with severe vascular diseases or limited life expectancy, the acceptable level can be higher (<8%) [2].

Management of Hypertension

Hypertension is a major risk factor for PAD but there are not sufficient data to clarify if hypertension treatment can alter the progression of the disease and its complications [3]. Recent data showed that ACE inhibitors may offer protection against major cardiovascular events (death, MI, stoke) in high risk PAD patients [7]. The International Verapamil-SR/Trandolapril Study (INVEST) also showed that all-cause death, nonfatal MI and nonfatal stroke can be reduced in PAD patients if appropriate control of hypertension is performed [8]. Angiotensin-converting enzyme inhibitors (ACEIs), calcium channel blockers, and diuretics can be effectively used for reduction of blood pressure. The recommended goal is to achieve a systolic blood pressure < 140 mm Hg and diastolic blood pressure < 90 mm Hg in all patients with PAD and especially CLI [2]. However, there are concerns about the possible worsen of ischemia in CLI, as a result of reduction of heart rate and blood pressure but it has not been proved so far.

Management of Hyperlipidemia

Hyperlipidemia is associated with PAD and cardiovascular diseases. Aggressive LDL reduction must be offered to all PAD patients in order to reduce the risk of myocardial infarction, stroke and death as it is suggested by the National Cholesterol Education Program (NCEP) Expert Panel on Detection, Evaluation, and Treatment of High Blood Cholesterol in Adults (Adult Treatment Panel III) [9]. In patients with PAD, therapy with a statin not only reduces cholesterol concentrations, but also improves endothelial function [10]. The Heart Protection Study also demonstrated that allocation to 40 mg simvastatin daily reduced the rates of MI, stroke and revascularization therapies by about one-quarter [11]. Moreover, patients undergoing major lower extremity amputations and were on medium- or high-intensity statin therapy presented improved survival rates at one year in comparison with patients who were on low-intensity therapy [12]. The recommendation for patients with PAD is to achieve a serum LDL cholesterol concentration of less than 100 mg per deciliter and a serum triglyceride concentration of less than 150 mg per deciliter [13]. Therefore, lipid-lowering therapy with moderate or high intensity dose of a statin, is necessary for all patients with PAD to reduce all-cause and cardiovascular mortality [2].

Antithrombotic therapy

Antiplatelet agents are strongly recommended for all symptomatic PAD patients to reduce the risk for major adverse cardiovascular events [2]. A metanalysis form Antiplatelet Trialists' Collaboration showed that antiplatelet therapy reduces the risk of fatal and nonfatal cardiovascular events from 11.9 % in the control group to 9.5 % in antiplatelet therapy group [14]. Aspirin is the traditional antiplatelet therapy in clinical practice and the American college of chest physicians recommended aspirin from 81 to 325 mg daily in PAD patients [15]. However, there are multiple studies showing that alternatives to aspirin such as clopidogrel, ticlopidine, dipyridamole are more effective.

An RCT demonstrated that long-term administration of clopidogrel in patients with PAD is more effective in reducing risk of stroke, MI or cardiovascular death in comparison with aspirin [16]. Other agents such as ticagrelor and vorapaxar have been also evaluated by studies, but their benefits compared to clopidogrel have not been proven [2]. A recent metanalysis which evaluated the effectiveness of different agents such as ticagrelor, ticlopidine, aspirin, picotamide, vorapaxar, and clopidogrel as single or dual antiplatelet therapy with aspirin demonstrated that clopidogrel monotherapy has the most favorable benefit-harm profile. Dual antiplatelet therapy (clopidogrel + aspirin) also reduces the rate of major amputation but increases the risk for severe bleeding [17]. Overall, antiplatelet therapy should be offered in all PAD patients, but there are not enough data to recommend the best antiplatelet agent for these patients [2].

Medical therapy for PAD

Vasodilator drugs such as papaverine have been used for treatment of claudication, but their efficacy has not established. Moreover they lower systemic blood pressure and decrease resistance in normal vessels leading to reduction of blood flow to the affected limb and worsen of ischemia [18].

Pentoxifylline, a xanthine derivative is a competitive nonselective phosphodiesterase inhibitor, which increases intracellular cAMP, activates PKA, inhibits TNF and reduces inflammation and innate immunity. Moreover, it improves red blood cell deformability and reduces blood viscosity and blood clot formation [3]. An RCT showed reduction in rest pain and sleep disturbance in CLI patients using Pentoxifylline [19]. However, recent studies have not confirmed this benefit, so it is not recommended in the treatment of CLI [2].

Cilostazol is a phosphodiesterase III inhibitor which can be used for the treatment of intermittent claudication. It promotes vasodilation, increases HDL and decreases

triglyceride levels [3]. Four RCTs, enrolling patients with claudication, demonstrated improved pain-free and maximal treadmill walking distance using 100 mg of Cilostazol twice daily [18]. As far as CLI patients, a study showed that Cilostazol combined with endovascular revascularization induced higher rates of limb salvage but has no effect in total survival or freedom from further revascularization [20]. Therefore, Cilostazol is recommended as initial therapy for patients with mild to moderate intermittent claudication but not in patients with CLI.

Diet and exercise

In order to prevent the progression of systemic atherosclerotic disease and decrease the risk for cardiovascular events, apart from the above mentioned pharmacologic treatments, diet and exercise can also help to achieve this goal. A diet high in carbohydrates and saturated fats increases the risk for cardiovascular events. On the other hand, a diet with low intake of saturated fats, and high intake of monounsaturated fats, omega-3 fatty acids, antioxidants and other natural plant sterols can reduce effectively the rate of cardiovascular events and mortality [21].

Exercise improves maximal treadmill walking distance and the quality of life in PAD patients. A metanalysis showed that regular exercise increases pain-free walking time by 180% and maximal walking time by 150% in patients with IC [22]. The mechanism is based on the improvement of oxygen extraction in the legs, in endothelial vasodilator function and muscle carnitine metabolism with exercise [18]. Regular aerobic exercise apart from improvement of PAD symptoms, reduces also the risk for cardiovascular events. Therefore a supervised exercise program with at least three sessions per week and daily walking is the most effective symptomatic therapy for patients with IC [3].

Revascularization

In cases without limb threatening ischemia, symptoms of PAD tend to remain stable with medical therapy and lifestyle modifications. In these patients, with mild or moderate intermittent claudication, performing a surgical or endovascular prophylactic intervention, provides little benefit and on the same time increases the risk for vessel damage and other possible complications. On the other hand, patients presenting with severe IC impacting on the quality of life or CLI (rest pain, ulceration, gangrene) must undergo revascularization in order to preserve limb function. However, in patients with extensive ischemic disease and severe comorbidities, the prognosis is poor even with revascularization and may require amputation. Revascularization strategies include either endovascular procedures such as percutaneous transluminal angioplasty (PTA) with or without stent deployment or surgical procedures such as lower extremity by-pass (using autologous venous or synthetic grafts) and endarterectomy [23]. Although there are multiples studies evaluating the results of each revascularization therapy, there are limited high-quality data to support evidence-based revascularization. The traditional method of choice between endovascular or surgery first approach was based on TASC II classification of the disease [1]. However, as it is referred in the previous section, there are multiple trials that demonstrated excellent results in TASC C and D lesions using endovascular procedures. Moreover, some patients would benefit from revascularization treatment and other not. Overall, TASC II focused only on the number, location and severity of atherosclerotic lesions and didn't evaluate the severity of limb ischemia and clinical status of patient. The recently published Global vascular guidelines on the management of chronic limb-threatening ischemia, sponsored by the 3 leading vascular societies [the European Society for Vascular Surgery (ESVS), the Society for Vascular Surgery (SVS), and the World Federation of Vascular Societies (WFVS)], try to approach the patient in a holistic way taking into consideration clinical status, limb threat assessment according to WIFi classification and anatomic assessment of

atherosclerotic lesions according to GLASS classification [2]. Global guidelines propose a three-step integrated approach (PLAN) for the efficient selection of revascularization strategy which is based on patient risk estimation, limb staging and anatomic pattern of disease. Patient risk estimation assesses the patients according to periprocedural risk, life expectancy and candidacy for limb salvage. Limb staging is based on WIFi classification system and anatomic pattern of disease on GLASS classification. The plan framework of clinical decision in CLI is displayed in figure 1. However there are many cases without improvement after revascularization. The presumed benefit of revascularization is associated with the severity of ischemia and limb threat as it is displayed in figure 2. Patients with mild ischemia are successfully treated conservatively with infection control and wound care, whereas patients with severe ischemic lesions and high degree of limb threat according to WIFi stage present the maximum benefit after successful revascularization. As far as the affected areas, inflow disease (which refers to lesions proximal to SFA) is generally treated with endovascular procedures. Surgery is performed only in extensive occlusions or after failed endovascular revascularization. Outflow (infraguinal) disease (distal to SFA origin) is usually treated by endovascular approach and surgery is indicated in patients with GLASS stage III lesions and WIFi stage 3 or 4 as it is displayed in figure 3.

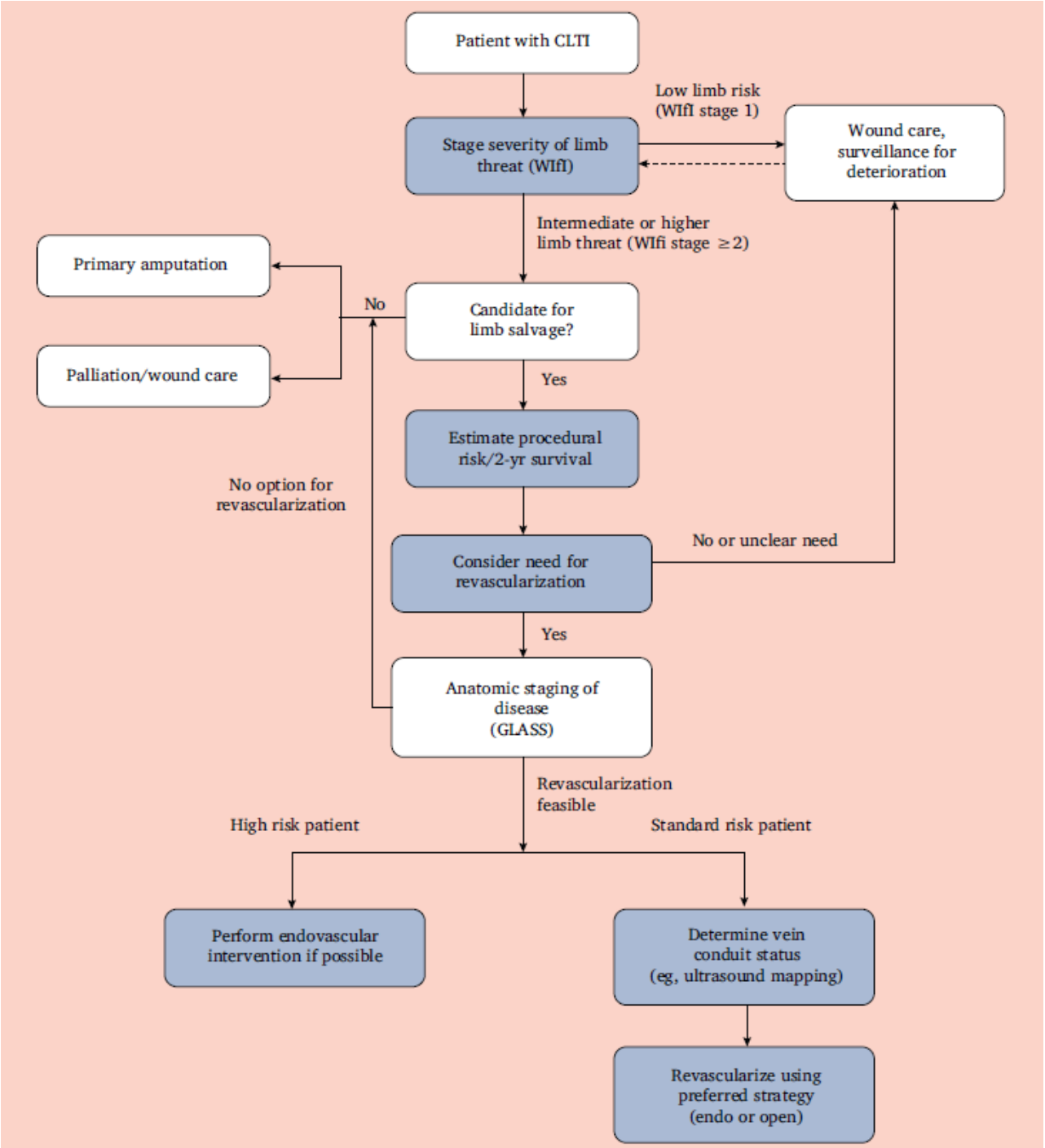

Fig. 1: PLAN framework of clinical decision-making in CLI

Conte MS, Bradbury AW, Kolh P, et al. Global vascular guidelines on the management of chronic limb-threatening ischemia. J Vasc Surg 2019;69(6S):3S-125S.e40.

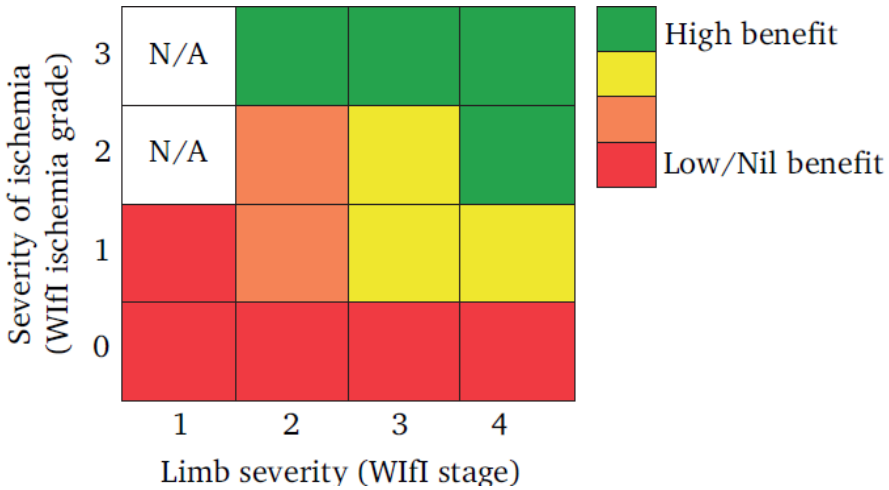

Fig. 2: Benefit of performing revascularization in CLI.

Conte MS, Bradbury AW, Kolh P, et al. Global vascular guidelines on the management of chronic limb-threatening ischemia. J Vasc Surg 2019;69(6S):3S-125S.e40.

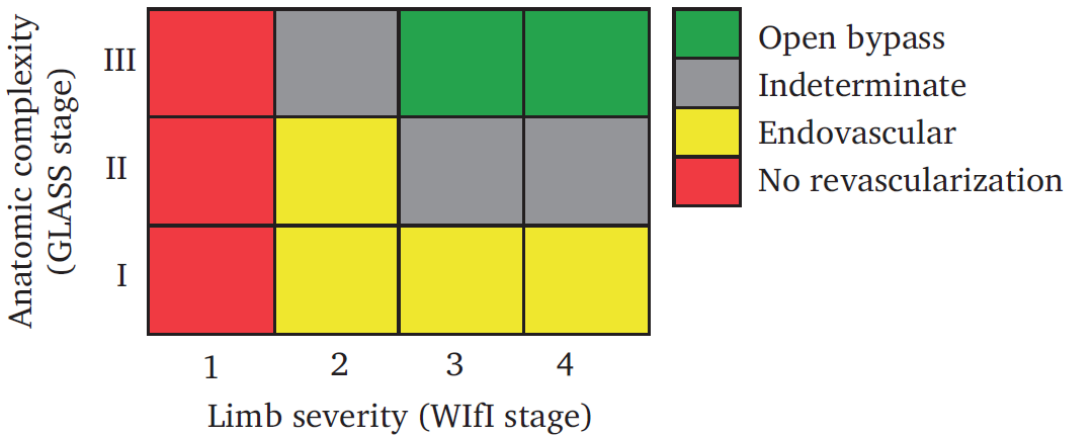

Fig. 3: Preferred initial revascularization strategy for infrainguinal disease.

Conte MS, Bradbury AW, Kolh P, et al. Global vascular guidelines on the management of chronic limb-threatening ischemia. J Vasc Surg 2019;69(6S):3S-125S.e40.

Endovascular Revascularization

Endovascular procedures are the favored approaches in many centers because of the lower mortality and morbidity compared to surgical procedures. IM is usually treated by inflow revascularization whereas CLI is associated with multilevel disease and requires both inflow and outflow revascularization [23].

Aorto-iliac disease should be treated in patients with severe IM, CLI, blue toe syndrome and vasculogenic impotence. Ipsilateral or contralateral approach can be selected and a variety of different catheters and guide-wires can be used to traverse the stenotic or occluded segments. However, the most commonly used vascular access is retrograde CFA access. Stenoses are normally crossed with soft or hydrophilic wires whereas total occlusions may required contralateral access and sometimes subintimal recanalization. Iliac stent placement is indicated after inadequate PTA due to elastic recoil. Significant residual stenosis is defined as an >30% residual stenosis on final angiography or residual peak to peak systolic pressure gradient > 5 mm Hg [24]. Both primary stenting (stent placement after PTA) or direct stenting (stent placement without predilatation) are acceptable for treatment of occlusions in iliac arteries. Various types of stents can be used. Balloon-expandable stents offer greater radial force and a more precise deployment in comparison with self-expanding stents which are useful in long tapered, tortuous and less calcified lesions. Covered stents are useful in cases of isolated iliac aneurysms, iatrogenic ruptures and arteriovenous fistulas. Their role for restenosis prevention is still uncertain [23,24].

SFA is a common site for atherosclerotic disease and the lesions are typically long with diverse clinical presentation. As it previously described, patients with average-risk (anticipated periprocedural mortality < 5%, anticipated 2-year survival >50%) are treated based on WIFi and GLASS stage (figure 3). On the other hand, high-risk patients are treated almost always with endovascular procedures because of lower morbidity and mortality [2]. Ipsilateral antegrade approach can be used for mid and distal

femoropopliteal lesions, whereas contralateral retrograde or ipsilateral retrograde approach via popliteal artery can be performed in proximal SFA lesions. The lesions can be crossed either endoluminally or subintimally using hydrophilic wires. After PTA, multiple stents can be placed across the site of residual stenosis due to long length of SFA lesions [25]. In cases of rigid calcified plaques, stent expansion may be incomplete with significant residual stenosis. In these cases, percutaneous atherectomy can be performed. Atherectomy devices remove atherosclerotic plaque and combined with low-pressure PTA prepare arteries for efficient stent placement. There are multiple atherectomy techniques such as extractional atherectomy, rotational atherectomy, laser atheroablation and orbital atherectomy [26].

As far as tibial disease, it is rarely treated in patients with IM and is more commonly pursued in patients with CLI in order to obtain relief from ischemic rest pain, facilitate ulcer healing and prevent limb loss. A direct antegrade CFA approach is preferable because it offers efficient pushability and trackability for devices to cross extensive calcified lesions. The stenoses are typically crossed with 0.018 or 0.014 inch guide wires and PTA balloon and stent dimensions are chosen according to the reference vessel diameter and lesion length. Efforts should be also focused to improve tibial runoff as the vessels may be occluded rapidly without adequate outflow [27]. Three cases of successful endovascular revascularization are demonstrated in figures 4, 5 and 6.

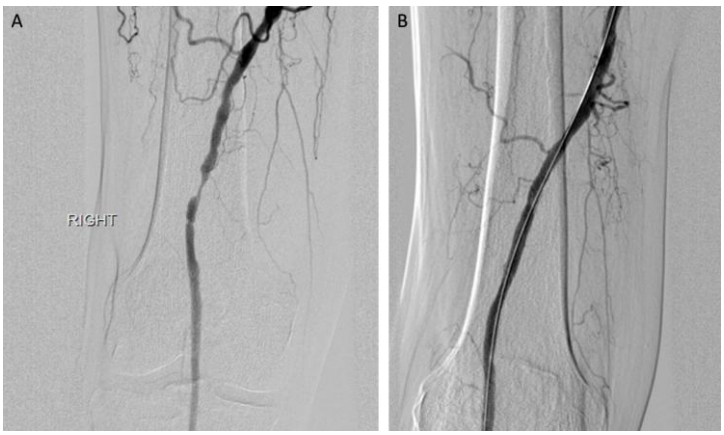

Fig. 4: A 67 year old patient with severe intermittent claudication. (A) DSA showed a hemodynamic significant stenosis in proximal right popliteal artery. (B) The stenotic lesion was successfully treated by PTA and stent deployment

Fig. 5: A 68-year-old male patient with CLI of right lower extremity. (A) DSA showed total occlusion of right SFA and (B) reconstruction of popliteal artery via collaterals. (C) Through percutaneous approach from the left common femoral artery, the occlusion was traversed with a hydrophilic guide wire. (D) The patient underwent successful PTA and stent placement. (E) Final DSA showed significant flow restoration.

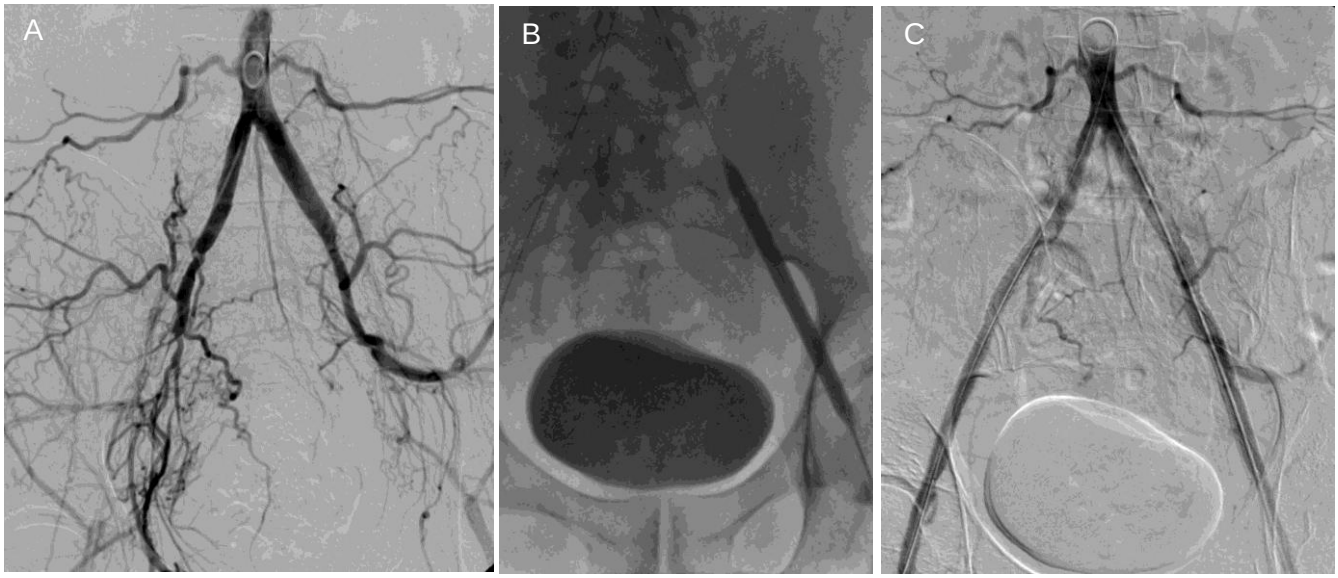

Fig.6: A 56-year-old male patient with CLI of both lower extremities (ischemic rest pain). (A) DSA showed total occlusion of both external iliac arteries. (B) Through retrograde approach from both common femoral arteries, the occlusions were traversed and patient underwent PTA and stent deployment. (C) Final DSA showed significant flow restoration and extinction of collateral vessels.

Angiosome-guided revascularization

Thirty years ago, Taylor and Palme introduced the angiosome theory in their anatomical study [28]. An angiosome is defined as a 3-dimensional block of tissue comprising of the skin, subcutaneous tissue, fascia, muscle, and bone drained by specific vessels (figure 7). During revascularization procedures, target vessel is usually selected based on the quality of outflow and its runoff. Angiosome-guided revascularization characterizes the direct recanalization of the artery that supplies ischemic angiosome and is associated with improved would healing and increased limb salvage in several studies [29-30]. On the other hand, not all lesions can be treated based on the angiosome model because of limitations such as difficult access to the vessel or anatomical anomalies and this theory is also not applicable in by-pass surgery because the least affected artery is selected as the outflow vessel. Moreover many foot lesions have dual supply and whereas wound healing is improved with direct revascularization, major amputation rate is not affected. Angiosome-guided revascularization is still under debate about its benefits for foot perfusion improvement, so further studies including imaging techniques are necessary to evaluate its advantages.

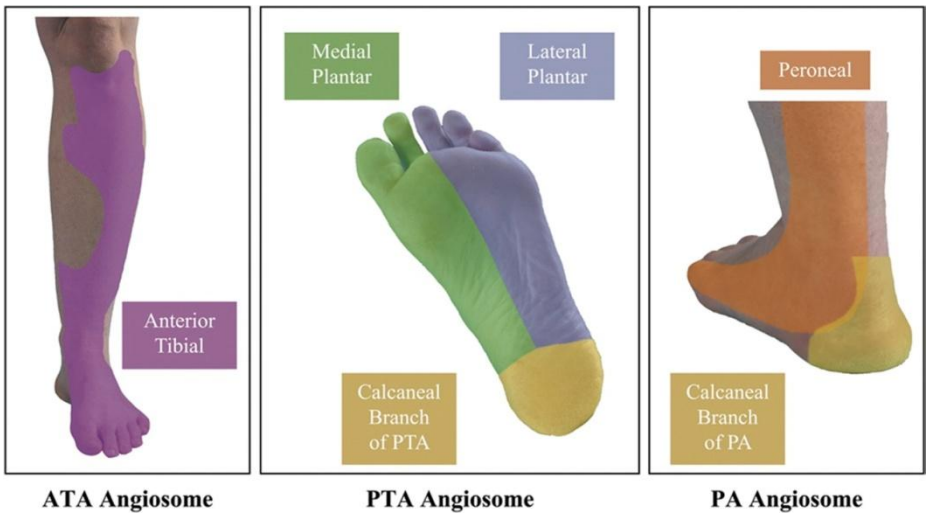

Fig. 7: Angiosomes of the foot and ankle. Three main arteries supply the six angiosomes of the foot and ankle. Bosanquet DC, Glasbey JC, Williams IM, Twine CP. Systematic review and meta-analysis of direct versus indirect angiosomal revascularisation of infrapopliteal arteries. Eur J Vasc Endovasc Surg. 2014;48(1):88-97.

Surgical revascularization

Open surgical revascularization can also increase blood flow to the affected limb, promote wound healing and decrease the risk and level of amputation. Common femoral endarterectomy is the gold standard treatment for CFA lesions with high technical success and long-term patency. In cases that endovascular revascularization is not indicated, lower extremity bypass can be performed. Surgeons create an alternative conduit for blood flow to circumvent the area of atherosclerotic lesions and restore tissue perfusion. There are different procedures according the location of lesions and normal target vessels such as aortobifemoral bypass, contralateral femorofemoral bypass, femoropopliteal bypass and axillary-femoral bypass [31]. Great saphenous vein is typically chosen for bypass because it provides better long-term patency rates but human umbilical vein and prosthetic grafts from polytetrafluoroethylene (PTFE) or Dacron can be also used [23]. However, this is a major surgical procedure which is performed under general anesthesia and is associated with higher rate of periprocedural and postprocedural complications in comparison with endovascular procedures [32]. Multilevel disease may require hybrid revascularization using both endovascular procedures for inflow disease and surgical procedures for outflow disease.

Amputation

In patients with extensive ulcers or gangrene of foot, amputation may be necessary. Minor (toe, metatarsal) amputations can be performed in patients with gangrene or small ulcers but require adequate blood flow to the affected limb and they are usually performed after revascularization. On the other hand, major amputations can be applied in patients with extensive tissue loss or infection after failed revascularization. These amputations limit functional independence and a prosthetic limb is necessary for walking. Moreover they are associated with poor healing and may require further surgical procedures or amputations to treat the affected areas [1,2, 23].

References

[1] Norgren L, Hiatt WR, Dormandy JA et al. Inter-society consensus for the management of peripheral arterial disease (TASC II). J Vasc Surg 2007;45(Suppl. S):S5–67.

[2] Conte MS, Bradbury AW, Kolh P, et al. Global vascular guidelines on the management of chronic limb-threatening ischemia. J Vasc Surg 2019;69(6S):3S-125S.e40.

[3] Stoyioglou A, Jaff MR. Medical treatment of peripheral arterial disease: a comprehensive review. J Vasc Interv Radiol 2004;15(11):1197-1207

[4] A clinical practice guideline for treating tobacco use and dependence: A US Public Health Service report. The Tobacco Use and Dependence Clinical Practice Guideline Panel, Staff, and Consortium Representatives. JAMA 2000;283(24):3244-3254.

[5] Effect of intensive diabetes management on macrovascular events and risk factors in the Diabetes Control and Complications Trial. Am J Cardiol 1995;75:894 –903.

[6] UK Prospective Diabetes Study (UKPDS) Group. Intensive bloodglucose control with sulphonylureas or insulin compared with conventional treatment and risk of complications in patients with type 2 diabetes (UKPDS 33). Lancet 1998;352(9131):837– 853.

[7] Yusuf S, Sleight P, Pogue J, Bosch J, Davies R, Dagenais G. Effects of an angiotensin-converting-enzyme inhibitor, ramipril, on cardiovascular events in high-risk patients. The Heart Outcomes Prevention Evaluation Study Investigators. N Engl J Med 2000;342:145

[8] Bavry AA, Anderson RD, Gong Y, Denardo SJ, Cooper- Dehoff RM, Handberg EM, et al. Outcomes among hypertensive patients with concomitant peripheral and coronary artery disease: findings from the INternational VErapamil-SR/Trandolapril STudy. Hypertension 2010;55:48e53.

[9] National Cholesterol Education Program (NCEP) Expert Panel on Detection, Evaluation, and Treatment of High Blood Cholesterol in Adults (Adult Treatment Panel III). Third Report of the National Cholesterol Education Program (NCEP) Expert Panel

on Detection, Evaluation, and Treatment of High Blood Cholesterol inmAdults (Adult Treatment Panel III) final report. Circulation 2002;106:3143–3421.

[10] Khan F, Litchfield SJ, Belch JJ. Cutaneous microvascular responses are improved after cholesterol-lowering in patients with peripheral arterial disease and hypercholesterolaemia. Adv Exp Med Biol 1997;428:49-54.

[11] Heart Protection Study Collaborative Group. MRC/BHF Heart Protection Study of cholesterol lowering with simvastatin in 20,536 high-risk individuals: a randomised placebo-controlled trial. Lancet 2002;360:7e22.

[12] DeCarlo C, Scher L, Shariff S, Phair J, Lipsitz E, Garg K. Statin use and other factors associated with mortality after major lower extremity amputation. J Vasc Surg 2017;66(1):216-225

[13] Ansell BJ, Watson KE, Fogelman AM. An evidence-based assessment of NCEP Adult Treatment Panel II guidelines: National Cholesterol Education Program. JAMA 1999;282:2051-7.

[14] Collaborative overview of randomised trials of antiplatelet therapy. I. Prevention of death, myocardial infarction, and stroke by prolonged antiplatelet therapy in various categories of patients. BMJ 1994;308:81-106.

[15] Sachdev GP, Ohlrogge KD, Johnson CL. Review of the Fifth American College of Chest Physicians Consensus Conference on Antithrombotic Therapy: outpatient management for adults. Am J Health Syst Pharm 1999;56:1505-14

[16] CAPRIE Steering Committee. A randomised, blinded, trial of clopidogrel versus aspirin in patients at risk of ischaemic events (CAPRIE). CAPRIE Steering Committee. Lancet 1996;348(9038):1329-1339.

[17] Katsanos K, Spiliopoulos S, Saha P, Diamantopoulos A, Karunanithy N, Krokidis M, et al. Comparative efficacy and safety of different antiplatelet agents for prevention of major cardiovascular events and leg amputations in patients with peripheral arterial disease: a systematic review and network metaanalysis. PLoS One 2015;10:e0135692.

[18] Hiatt WR. Medical treatment of peripheral arterial disease and claudication. N Engl J Med 2001;344(21):1608-1621.

[19] Intravenous pentoxifylline for the treatment of chronic critical limb ischaemia. The European Study Group. Eur J Vasc Endovasc Surg 1995;9(4):426-436.

[20] Soga Y, Iida O, Hirano K, Suzuki K, Kawasaki D, Miyashita Y, et al. Impact of cilostazol after endovascular treatment for infrainguinal disease in patients with critical limb ischemia. J Vasc Surg 2011;54:1659e67.

[21] Kok FJ, Kromhout D. Atherosclerosisdepidemiological studies on the health effects of a Mediterranean diet. Eur J Nutr 2004;43(Suppl 1):I/2e5

[22] Girolami B, Bernardi E, Prins MH, et al. Treatment of intermittent claudication with physical training, smoking cessation, pentoxifylline, or nafronyl: a meta-analysis. Arch Intern Med 1999;159:337-45.

[23] Kinlay S. Management of Critical Limb Ischemia. Circ Cardiovasc Interv 2016;9(2):e001946.

[24] Tsetis D, Uberoi R. Quality improvement guidelines for endovascular treatment of iliac artery occlusive disease. Cardiovasc Intervent Radiol 2008;31(2):238-245.

[25] Tsetis D, Belli AM. Guidelines for stenting in infrainguinal arterial disease. Cardiovasc Intervent Radiol 2004;27(3):198-203.

[26] Franzone A, Ferrone M, Carotenuto G, et al. The role of atherectomy in the treatment of lower extremity peripheral artery disease. BMC Surg 2012;12 Suppl 1(Suppl 1):S13.

[27] van Overhagen H, Spiliopoulos S, Tsetis D. Below-the-knee interventions. Cardiovasc Intervent Radiol 2013;36(2):302-311.

[28] Taylor GI, Palmer JH. The vascular territories (angiosomes) of the body: experimental study and clinical applications. Br J Plast Surg 1987;40(2):113-141.

[29] Alexandrescu VA, Hubermont G, Philips Y, et al. Selective primary angioplasty following an angiosome model of reperfusion in the treatment of Wagner 1-4 diabetic

foot lesions: practice in a multidisciplinary diabetic limb service. Journal of Endovascular Therapy 2008 Oct;15(5):580-593.

[30] Jongsma H, Bekken JA, Akkersdijk GP, Hoeks SE, Verhagen HJ, Fioole B. Angiosome-directed revascularization in patients with critical limb ischemia. J Vasc Surg 2017;65(4):1208-1219.

[31] Antoniou GA, Georgiadis GS, Antoniou SA, Makar RR, Smout JD, Torella F. Bypass surgery for chronic lower limb ischaemia. Cochrane Database Syst Rev 2017;4(4):CD002000.

[32] Adam DJ, Beard JD, Cleveland T, et al. Bypass versus angioplasty in severe ischaemia of the leg (BASIL): multicentre, randomised controlled trial. Lancet 2005;366(9501):1925-1934.

Evaluation of PAD

A comprehensive medical history and clinical examination are necessary for patients at increased risk for PAD. According to ACC/AHA guidelines all patients with symptoms such as intermittent claudication, impaired walking function and non-healing wounds should be further evaluated with ankle-brachial index measurement (ABI) and imaging studies [1]. The effective treatment of PAD and especially CLI is based on appropriate classification of the disease which relies on successful evaluation of patients. Recent technologic advances have made the diagnosis and imaging of PAD more accurate which allows better planning for revascularization strategy. Apart from physical examination, there are noninvasive tests for patients screening, stratification and evaluation of outcome after treatment. These tests can be divided in two broad categories: functional tests such as ankle-brachial index (ABI), segmental limb pressures, pulse volume recordings (PVRs) and oxygen testing and anatomic/radiologic tests such as color duplex ultrasound (CDUS), computed tomography angiography (CTA) and magnetic resonance angiography (MRA). The above mentioned tests may differ across hospitals and health systems according to the local practice, availability of the modalities and training of doctors and technologists [2].

Physical examination

Patients with suspected PAD or CLI should be initially evaluated with physical examination. Patients should be relaxed and acclimatized in room temperature. The physicians can recognize sings of the disease such as dry and cool skin, muscle atrophy or dystrophic toenails. Moreover, palpation of lower extremity pulses can depict the extension and distribution of the disease but this a specific and not sensitive clinical test [3]. Auscultation of bruits of femoral artery at the groin and distally can be also performed but it is a poor sensitive examination. It is also very important during clinical

examination to recognize signs of sensory and motor neuropathy because it is associated with progressed PAD or sudden cyanotic discoloration of toes as a result of atherothrombotic microembolism from proximal arteries (blue toe syndrome) [4].

Ankle-brachial index

ABI is calculated by the ankle systolic blood pressure divided by brachial artery systolic blood pressure. Both brachial pressures should be measures and if there is difference between them, the higher pressure is selected. In cases with a greater than 15 mm Hg difference between them, peripheral upper extremity disease is suspected. As far as ankle systolic blood pressure, it is measured from both dorsalis pedis and posterior tibial arteries after the patient has been at rest in the supine position for ten minutes and the greater pressure from each side is used for calculation of ABI. Normal values ranged between 0.9 and 1.29. An ABI between 0.5 and 0.89 is associated with mild or moderate, PAD whereas an ABI lower than 0.5 is associated with severe PAD or CLI. Values greater than 1.4 are a result of noncompressible calcified arteries especially in diabetic or elder patients which also suggest severe PAD and require further evaluation. ABI calculation is a simple, cheap and noninvasive test for the initial screening of suspected population, quantification of the severity of PAD and prediction of the risk for future cardiovascular events. Furthermore, it is also used as a surveillance test during follow-up of PAD patients [3,4]. A prospective cohort study included 3209 patients with a mean follow-up duration of 8 years showed that ABI is a strong and independent predictor of mortality [5]. Moreover, it is found to be a valid method for cardiovascular risk assessment, independent of standard risk factors and other subclinical cardiovascular diseases [6]. However, ABI can underestimate the severity of PAD especially in cases of tissue loss or presents false results in patients with heavily calcified vessels [2].

Segmental limb pressures and segmental pulse volume recordings

Segmental limb pressures can provide an initial indication of the anatomical location of atherosclerotic lesions. A series of blood pressure cuffs are placed at various levels of upper and lower extremities and systolic blood pressure is obtained. The recommended location of the cuffs for lower extremity are the upper thigh, lower thigh, upper calf and ankle. A difference greater than 30 mm Hg between two segments or between the two limbs at the same segments suggests significant stenosis at this area. Segmental limb pressures measurement is useful in patients without calcified vessels because arterial calcification can lead to false results [2,7]. This restriction can be overcome using segmental pulse volume recordings (PVRs) which are not altered by calcium. PVR is a noninvasive test which evaluates extremity flow. It depicts a graph of the pulsatile change in limb blood flow using constant pressure from blood pressure cuffs at various levels like segmental limb pressures. PVRs utilize the principle of plethysmography which detects segmental volume changes during cardiac cycle. This test can be performed as a preliminary test in patients with suspected PAD to evaluate if symptoms are a result of atherosclerotic disease. Moreover it can be used as surveillance test to follow-up patients with PAD and should be considered as a part of complete noninvasive examination [3,8].

Treadmill test

Treadmill test can be performed in patients with borderline ABI with symptoms of PAD. Moreover, it is useful for differential diagnosis between vascular claudication and neurologic claudication and for assessment of treatment efficacy during follow-up. Testing can be performed on a treadmill or in case of unavailability with walking test [4]. There are different variations for treadmill test, but the typical test is performed on a treadmill walking at 3.2 km/h with a 10% slope. A pressure drop > 20% confirms the arterial origin of symptoms [9]. Patients who cannot perform treadmill exercise can be

tested with active plantar flexion which has excellent correlation with treadmill test [10].

Transcutaneous measurement of oxygen partial pressure

Transcutaneous measurement of oxygen partial pressure ($TcPO_2$) is a noninvasive method to measure PO_2 at the skin surface. $TcPO_2$ measurement can assess local oxygen diffusion from the capillary bed through the skin epidermis which reflects the microvacsular status in the skin (figure 1). It is very useful for quantification of PAD, prediction of ulcer healing and determination of the optimum level for amputation. Moreover, it does not disturb tissue around the wound and eliminates the risk of infection as a noninvasive technique [11]. In patients with tissue loss, $TcPO_2$ should be considered before and after revascularization to estimate the benefit of treatment [4]. Furthermore, a recent study demonstrated that a low $TcPO_2$ (<25 mm Hg) is an independent prognostic marker for 1 year mortality in patients with DM and diabetic foot ulcers [12]. However, $TcPO_2$ measurements are affected by tissue edema, inflammation and vasoconstriction. Apart from that, it is not an imaging modality and there is lack of anatomic information, provided by this examination [2].

Fig. 1: $TcPO_2$ recording using an adhesive sensor on the dorsal aspect of the foot

Thottiyen, S. et al. Ankle Brachial Index vs Transcutaneous Partial Pressure of Oxygen for Predicting Healing of Diabetic Foot Ulcers with Peripheral Arterial Disease: a Comparative Study. Indian J Surg (2020).

Color Doppler Ultrasound

Color Doppler Ultrasound (CDUS) uses the combination of grey scale (B-mode) and color pulsed-wave Doppler technique. This combination provides information not only for the anatomic location and extent of disease but also for velocity and flow volume in the vessels [13]. CDUS is a noninvasive, safe and low cost modality and it is usually the first imaging examination for PAD evaluation and the only one available for some health care settings. CDUS is indicated for assessment of stenosis or occlusion in PAD patients, for surveillance of previous endovascular or surgical interventions, for anatomic mapping before intervention and further assessment of vascular abnormalities such as pseudoaneurysms, vascular injuries and malformations [2]. The excellent tolerance and lack of radiation exposure make CDUS the method of choice for routine follow-up (figure 2). Furthermore CDUS is a useful tool for real time guidance during endovascular procedurals [3]. However, there are difficulties and pitfalls during examination as a result of bowel gas and movement, highly calcified vessels and body habitus. Moreover, it is a time-consuming examination and highly operator dependent. It cannot also provide full arterial imaging and another imaging modality is often necessary before endovascular/surgical revascularization [4].

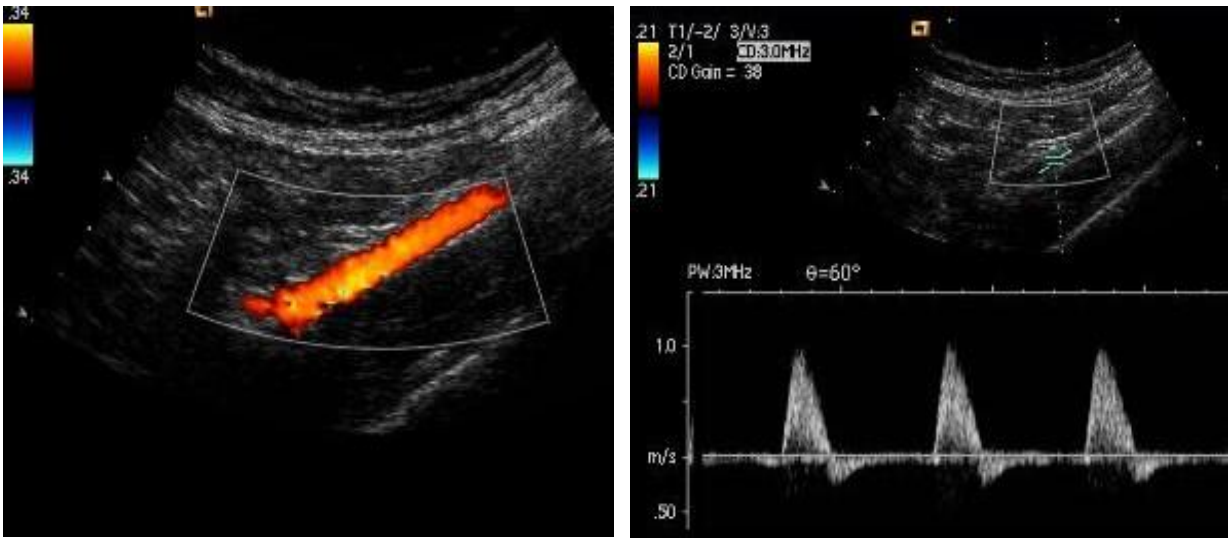

Fig. 2: A 80 year-old female patient with CLI successfully treated with PTA and stent deployment in an occlusion of left common and external iliac artery. CDUS demonstrated excellent stent patency without signs of restenosis.

Computed tomography angiography

Computed tomography angiography (CTA) using multidetector computed tomography (MDCT) quickly generates high-resolution, contrast-enhanced images depicting the arterial tree in multiple planes or in 3-dimensional reconstructions. MDCT evolution resulting in increased speed of scanning and greater longitudinal field of view. Moreover, the development of advance-processing techniques offered maximum intensity projection (MIP) images which are useful for evaluation of the degree of stenosis especially in tortuous vessels and volume rendered (VR) 3D reconstructions which can provide a global overview for the depiction of pathology (figure 3) [13]. It is the primary diagnostic modality for vascular diseases in many institutions and it is used for the evaluation of atherosclerotic lesions in PAD patients but also in cases of congenital abnormalities, traumatic or iatrogenic injuries, inflammatory vascular diseases and aneurysms. Moreover, it is a useful tool for arterial mapping and assessment of revascularization strategy before treatment (figure 4). Finally, it can depict the results of endovascular and surgical procedures and their complications, so it can be performed as a surveillance examination in patients with non-diagnostic CDUS [14]. The accuracy of CTA for assessing atherosclerotic lesions is excellent as it is demonstrated by a metanalysis by Met et al. The reported sensitivity and specificity for aortoiliac stenoses were 96% and 98% respectively and for femoropopliteal region were 97% and 94% respectively [15]. Moreover, CTA is superior to other imaging modalities for evaluation of restenosis inside metallic stents or stent grafts [16]. However, CTA is associated with significant doses of ionizing radiation and the usage of iodinated contrast may induce nephropathy in patients with pre-existing renal insufficiency. On the other hand, modern CT scanners and imaging protocols offer contrast and radiation dose reduction while maintaining image quality [2,3]. Another limitation of CTA is observed in patients with extensive and dense vessels calcifications. These calcification have high attenuation leading to blooming artifact and

overestimation of stenosis. Dual-energy CTA may be a promising technique to minimize this artifact [13].

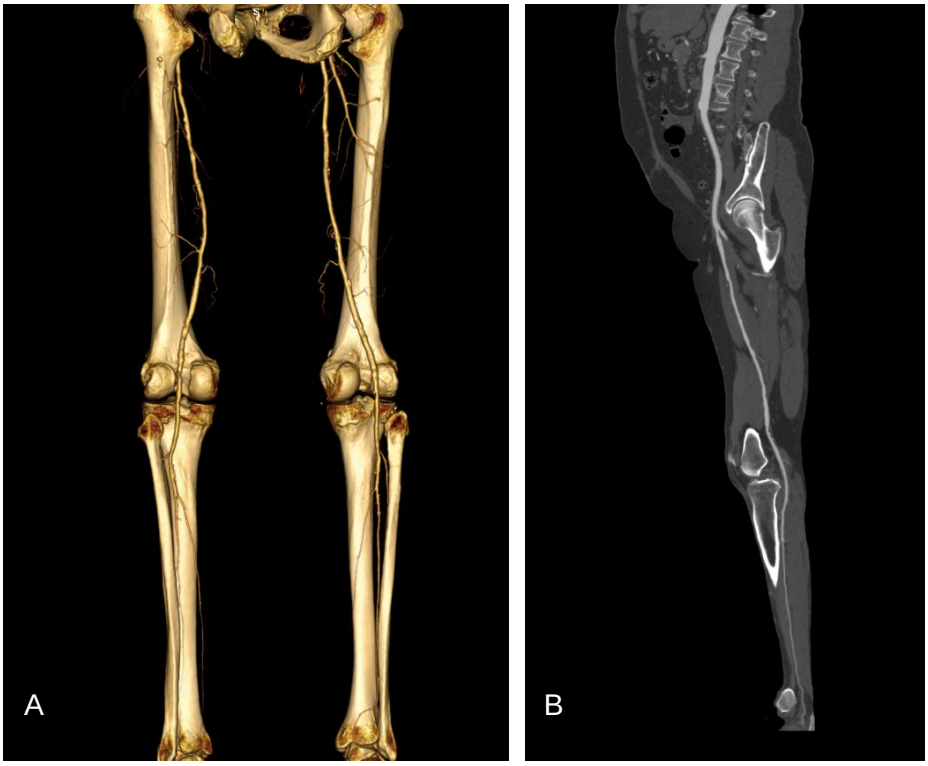

Fig. 3: Peripheral CTA of lower limb arteries. (A) volume rendered (VR) 3D reconstruction image and (B) maximum intensity projection (MIP) image.

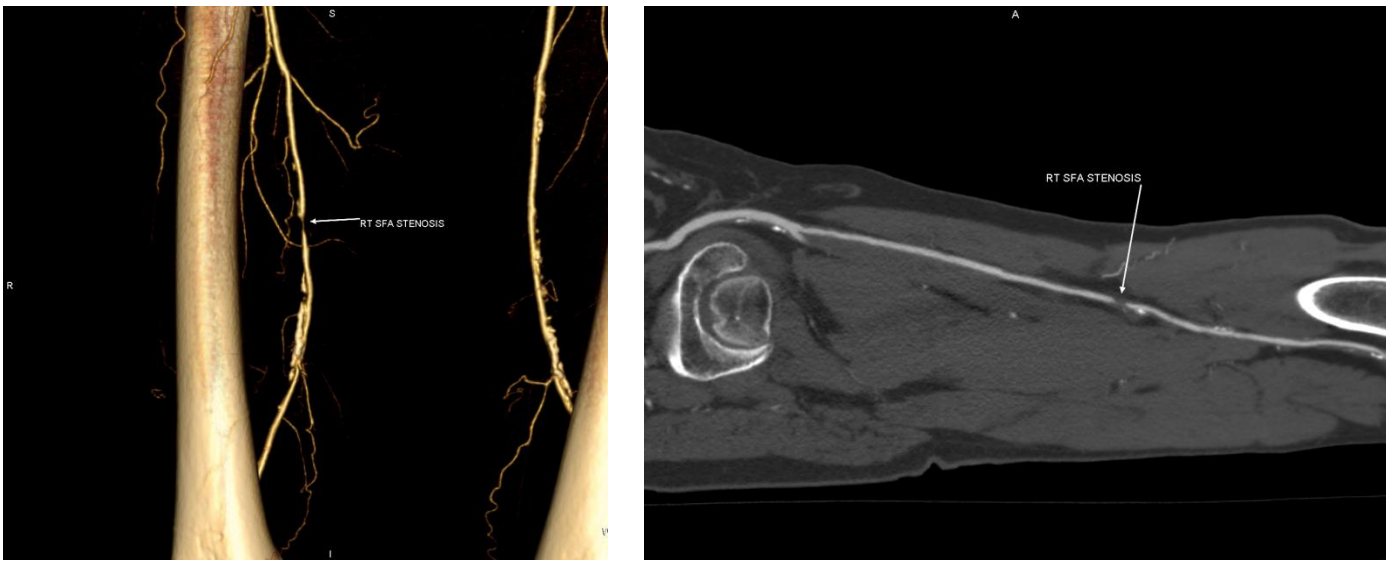

Fig. 4: Peripheral CTA of lower limb arteries in a patient with severe intermittent claudication. (A) VR 3D reconstruction image and (B) MIP image demonstrate a hemodynamic significant stenosis in right superficial femoral artery.

Magnetic resonance angiography

Magnetic resonance angiography (MRA) provides excellent angiographic images without radiation exposure and iodinated contrast administration. It can be performed either using contrast-enhanced (CE-MRA) techniques after intravenous administration of paramagnetic contrast or using non-contrast enhanced, flow-sensitive techniques such as time of flight (TOF) MRA, steady state free precession MRA and phase-contrast MRA [13]. Multiple studies demonstrated significant correlation between MRA and DSA (figure 5). MRA sensitivity and specificity in PAD ranged between 93% and 100% [4]. A metanalysis by Collins et al, also showed that MRA is associated with superior sensitivity and specificity for the detection of >50% stenoses in comparison with CTA and CDUS [17]. As far as, non-contrast MRA, TOF is rarely performed in lower extremity imaging because it is susceptible to motion due to prolonged imaging acquisition times. Phase contrast MRA was the first non-contrast technique for peripheral arterial imaging. It is associated with reduced acquisition time and fewer artifacts in comparison with TOF but it is rarely used nowadays due to more advanced techniques. Electrocardiographically (ECG) gated partial-Fourier fast spin echo (FSE) is a new technique which can exploit the difference in arterial and venous flow during cardiac cycle. However, it has lower sensitivity and specificity compare to CE-MRA. A recent developed technique is Quiescent-interval single-shot (QISS) MRA. It surpasses the disadvantages of the above mentioned techniques, as it includes shorter acquisition time and reduced sensitivity to patient motion (figure 6) [18].

MRA is accompanied by several limitations. It cannot be performed in patients with pacemakers or metal implants, claustrophobia and severe renal failure in cases that a CE-MRA is indicated. Other limitations include overestimation of stenoses and difficulties to visualize in-stent stenosis. Moreover, failure of MRA to depict vessel calcifications may affect the revascularization treatment planning. Finally, there is limited availability of advanced MRI technology in many centers [3].

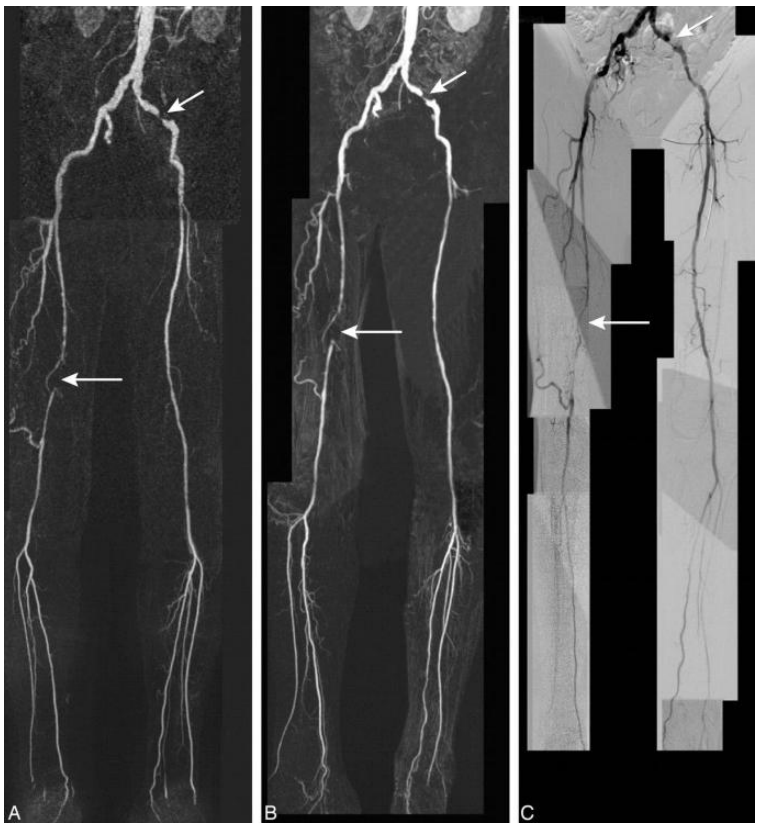

Fig. 5: Coronal contrast-enhanced MR angiographic maximum intensity projection images using (A) 1.5T and (B) 3T contrast-enhanced MR angiography and (C) digital subtraction angiography. Van den Bosch H, et al. 3T versus 1.5T MR angiography in peripheral arterial occlusive disease: an equivalence trial in comparison with digital subtraction angiography. J Cardiovasc Magn Reson. 2012;14(Suppl 1):P139

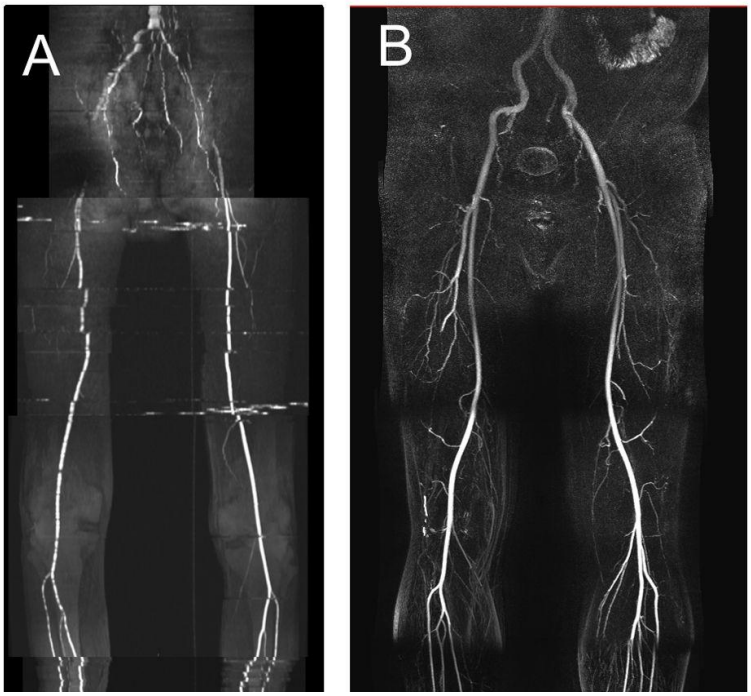

Fig. 6: Non-contrast MRA. (A) TOF and (B) 3D Fast spin echo (FSE) at 3T. Pollak AW, Norton PT, Kramer CM. Multimodality imaging of lower extremity peripheral arterial disease: current role and future directions. Circ Cardiovasc Imaging 2012; 5(6): 797-807.

Digital subtractive angiography

Digital subtractive angiography (DSA) was considered the gold standard modality for vascular imaging for decades. Nowadays, it is rarely performed for diagnosis of PAD, as there is availability of less invasive modalities such as CDUS, CTA and MRA which are accompanied by less radiation and without complication inherent to arterial puncture (hematoma, dissection, pseudoaneurysm) [10]. However, many physicians still prefer it because it allows diagnosis and treatment at the same setting. In DSA, images are produced after contrast administration and radiopaque structures such as bones are subtracted digitally form the image, allowing accurate depiction of vessels. For aorta and peripheral arteries, a retrograde transfemoral approach is usually performed. Transradial or transbrachial approach can be also used if femoral access is not possible [4]. In patients with severe CKD or allergy to iodinated contrast, CO_2 angiography can be performed. The diagnostic accuracy is lower compared to DSA but it can still provide diagnostic images [3].

Fig. 7: Conventional and digital subtractive angiography (DSA) of aortic bifurcation and iliac arteries.

References

[1] Gerhard-Herman MD, Gornik HL, Barrett C, et al. 2016 AHA/ACC Guideline on the Management of Patients With Lower Extremity Peripheral Artery Disease: A Report of the American College of Cardiology/American Heart Association Task Force on Clinical Practice Guidelines [published correction appears in J Am Coll Cardiol. 2017 Mar 21;69(11):1521]. J Am Coll Cardiol 2017;69(11):e71-e126.

[2] Dhanoa D, Baerlocher MO, Benko AJ, et al. Position Statement on Noninvasive Imaging of Peripheral Arterial Disease by the Society of Interventional Radiology and the Canadian Interventional Radiology Association. J Vasc Interv Radiol 2016;27(7):947-951.

[3] Conte MS, Bradbury AW, Kolh P, et al. Global vascular guidelines on the management of chronic limb-threatening ischemia. J Vasc Surg 2019;69(6S):3S-125S.e40.

[4] Aboyans V, Ricco JB, Bartelink MEL, et al. 2017 ESC Guidelines on the Diagnosis and Treatment of Peripheral Arterial Diseases, in collaboration with the European Society for Vascular Surgery (ESVS): Document covering atherosclerotic disease of extracranial carotid and vertebral, mesenteric, renal, upper and lower extremity arteries. Endorsed by: the European Stroke Organization (ESO)The Task Force for the Diagnosis and Treatment of Peripheral Arterial Diseases of the European Society of Cardiology (ESC) and of the European Society for Vascular Surgery (ESVS). Eur Heart J 2018;39(9):763-816.

[5] Feringa HH, Bax JJ, van Waning VH, et al. The long-term prognostic value of the resting and postexercise ankle-brachial index. Arch Intern Med 2006;166(5):529-535.

[6] Criqui MH, McClelland RL, McDermott MM, et al. The ankle-brachial index and incident cardiovascular events in the MESA (Multi-Ethnic Study of Atherosclerosis). J Am Coll Cardiol 2010;56(18):1506-1512.

[7] Gale SS, Scissons RP, Salles-Cunha SX, et al. Lower extremity arterial evaluation: are segmental arterial blood pressures worthwhile?. J Vasc Surg 1998;27(5):831-839.

[8] Sibley RC 3rd, Reis SP, MacFarlane JJ, Reddick MA, Kalva SP, Sutphin PD. Noninvasive Physiologic Vascular Studies: A Guide to Diagnosing Peripheral Arterial Disease. Radiographics 2017;37(1):346-357.

[9] Hiatt WR, Cox L, Greenwalt M, Griffin A, Schechter C. Quality of the assessment of primary and secondary endpoints in claudication and critical leg ischemia trials. Vasc Med 2005;10(3):207-213.

[10] Norgren L, Hiatt WR, Dormandy JA et al. Inter-society consensus for the management of peripheral arterial disease (TASC II). J Vasc Surg 2007;45(Suppl. S):S5 – 67.

[11] Bajwa A, Wesolowski R, Patel A, et al. Assessment of tissue perfusion in the lower limb: current methods and techniques under development. Circ Cardiovasc Imaging 2014;7(5):836-843.

[12] Fagher K, Katzman P, Löndahl M. Transcutaneous oxygen pressure as a predictor for short-term survival in patients with type 2 diabetes and foot ulcers: a comparison with ankle-brachial index and toe blood pressure. Acta Diabetol 2018;55(8):781-788.

[13] Pollak AW, Norton PT, Kramer CM. Multimodality imaging of lower extremity peripheral arterial disease: current role and future directions. Circ Cardiovasc Imaging 2012;5(6):797-807.

[14] Fleischmann D, Hallett RL, Rubin GD. CT angiography of peripheral arterial disease. J Vasc Interv Radiol 2006;17(1):3-26.

[15] Met R, Bipat S, Legemate DA, Reekers JA, Koelemay MJ. Diagnostic performance of computed tomography angiography in peripheral arterial disease: a systematic review and meta-analysis. JAMA 2009;301(4):415-424.

[16] Soulez G, Therasse E, Giroux MF, et al. Management of peripheral arterial disease: role of computed tomography angiography and magnetic resonance angiography. Presse Med 2011;40(9 Pt 2):e437-e452.

[17] Collins R, Burch J, Cranny G, et al. Duplex ultrasonography, magnetic resonance angiography, and computed tomography angiography for diagnosis and assessment of symptomatic, lower limb peripheral arterial disease: systematic review. BMJ 2007;334(7606):1257.

[18] Mathew RC, Kramer CM. Recent advances in magnetic resonance imaging for peripheral artery disease. Vasc Med 2018;23(2):143-152.

PART II

Evaluation of percutaneous transluminal angioplasty outcome in patients with peripheral arterial disease using modern medical imaging techniques (CT and MR perfusion)

Purpose of PhD Thesis

The goals of PhD thesis are:

- to emerge hypoperfusion of lower extremities in patients with CLI using CT and MR perfusion techniques.
- to estimate PTA results using CT and MR perfusion techniques.
- to compare the abilities of different MR perfusion techniques.
- to correlate the lower limb perfusion results with the clinical outcome of patients after PTA and their imaging studies (CDUS, CTA) as part of their follow-up to determine the potential prognostic value of CT/MR perfusion techniques.

Evaluation of percutaneous transluminal angioplasty outcome in patients with critical limb ischemia using CT foot perfusion examination

Materials and Methods

Study design

In order to be included in this protocol, patients had to present with CLI (either rest pain or minor/major tissue loss, Rutherford categories 4-6). Additionally, anatomic distribution of atherosclerotic lesions and patients' comorbidities/overall clinical status should make them suitable for endovascular revascularization. Initially, patients underwent diagnostic CTA in order to determine anatomic distribution of arterial disease and then the treatment plan was decided in a multidisciplinary manner, according to standard institutional protocols and common practice. Moreover, patients had to be in a position to understand the purpose of the study, comply with the follow-up protocol and provide informed consent.

Patients presenting less advanced PAD, not classified as CLI were excluded. Similarly, patients that underwent surgical revascularization or those in whom either a conservative approach or a primary amputation was performed, were also excluded. Patients presenting with acute limb ischemia (duration of symptoms <2 weeks, according to TASC II definition) were not considered to comply with the aim of the study. Allergy to iodinated contrast, moderate or severe renal impairment (GFR < 45 mL/min), congestive heart failure and severe cardiac rhythm anomalies, were also considered as exclusion criteria.

Selective patients that fulfilled the abovementioned criteria were subjected to CT foot perfusion examination (CTFP) of the affected foot. Subsequently, the endovascular procedure was carried out and technical success was defined as a residual stenosis less

than 30% without flow-limiting dissection in the target lesion. Enrolled patients underwent a second CTFP examination within 1st week after treatment. All patients were followed-up with clinical examination at 1, 3, 6 and 12 months and color Doppler ultrasound combined with clinical examination on an annual basis.

Clinical evaluation and measurement of ABI was performed by vascular surgeons before PTA, after PTA and during follow-up. Analysis and evaluation of CTFP was performed by two blinded radiologists, a resident in radiology with 4 years experience in CT and a senior professor of Radiology and Interventional Radiology with 29 years experience in vascular imaging.

The study was approved by the local ethic committee and all patients provided written informed consent prior to study enrollment.

Study population

Between April 2016 and May 2017, 22 selective patients enrolled in this study. Technical success was achieved in 19 patients and thus 3 patients were excluded from subsequent analysis. These patients presented multilevel occlusive disease (TASC D) with extensively calcified vessels and were initially judged high risk for surgical revascularization. Subsequently, after failed endovascular intervention and following extensive discussion of the procedural risks, these patients underwent successful surgical revascularization (2 axillo-femoral and 1 femoro-popliteal bypass). Moreover one patient, who underwent successful PTA, died before post-PTA CTFP. Totally, 13 subjects (10 male, 3 female) were included in the analysis, because CTFP evaluation was not feasible in 5 examinations. The median age was 72 years (range 51-84 years). According to Rutherford classification of PAD, one patient was allocated to class 4, eight patients to class 5 and four patients to class 6 PAD. Patients' main risk factors were hypertension (n=10), hyperlipidemia (n=9), diabetes mellitus (n=9), smoking (n=11),

coronary artery disease (n=4) and previous endovascular or surgical procedure (n=4). Clinical data of patients are displayed in table 1.

Table 1: Clinical data of study population

Pt No	Sex	Age	Risk Factors	Lesion location	Rutherford Classification	Rutherford Classification (6 months after PTA)	ABI pre-PTA	ABI post-PTA
1	M	64	HT, DM, HL, SM, CAD	(L) SFA,POPA	6	2	0.4	1
2	M	75	HT, SM	(L) CIA,EIA	4	2	0.27	0.5
3	M	72	DM, HL,CAD	(R) EIA,SFA	5	5	0.4	0.6
4	M	84	HT, DM, HL, SM	(R) SFA,POPA	5	2	0.7	0.9
5	F	62	HT, SM	(R) EIA	5	1	0.2	0.5
6	M	83	DM, HL, SM, CAD	(R) SFA	6	3	0.35	0.55
7	F	51	SM	(L) CIA,POPA	5	1	0.3	1
8	M	60	HT, DM, HL, SM	(R) SFA,POPA	5	2	0.3	0.9
9	F	78	HT, DM, HL, SM	(R) CIA, EIA, SFA, POPA	5	2	0.1	1.1
10	M	80	HT, DM, HL, CAD	(R) SFA,POPA	5	3	0.27	0.75
11	M	55	HT, DM, HL, SM	(L) CIA,EIA	6	5	0.5	0.6
12	M	57	HT, SM	(L) CIA,EIA	5	5	0.58	0.66
13	M	74	HT, DM, HL, SM	(R) SFA, POPA,TPT	6	3	0.3	0.7

Imaging protocol

All studies were performed on a 128-slice CT scanner (Revolution GSI, GE Healthcare, USA) at a room temperature. Patients were examined in the supine position and the angiography scan was obtained in the craniocaudal direction. The position of both feet was stabilized with an adhesive tape during the examination. CTA was performed with a standard CTA protocol from the diaphragm to the feet after injection of 110 ml of iodinated non-ionic contrast medium (Ultravist 370, iodine at 370 mg/ml Bayer

Schering Pharma AG, Leverkusen, Germany) followed by 50 mL of saline solution at a flow rate of 4 mL/s.

The patients also underwent foot perfusion examination before and within the 1st week after endovascular treatment. The acquisition scanning length was 14 cm, enabling imaging of the entire foot and ankle. A shuttle mode technique was employed with the following parameters: 0.625 mm×64 mm collimation (coverage 40 mm), 0.4 s gantry rotation time, pitch of 1.375, 1.25 mm reconstruction interval thickness, number of passes 28, time per pass 1.7 s, 80 kVp tube voltage, reference tube current 220 mAs and total acquisition time 47.7 s. Images were obtained after injection of 40 ml of iodinated non-ionic contrast medium followed by 30 mL of saline solution at a flow rate of 4 mL/s. Scan delay was individualized for each patient, using GE's proprietary bolus-tracking software (SmartPrep) to capture 100 HU in ascending thoracic aorta in order to assess the arrival of contrast medium in the examined area.

The dose-length product (DLP) of each CT perfusion examination was recorded. The mean DLP was used to estimate the mean effective dose using a conversion coefficient of 0.0002 $mSv \cdot mGy^{-1} \cdot cm^{-1}$ [1].

Image analysis

CT perfusion images were transferred to a dedicated workstation (AW server 3.2, GE Medical Systems) and analyzed using commercial CT software (CT-Perfusion-4D, GE Medical Systems). CT-Perfusion-4D utilizes two computational algorithms: deconvolution and standard algorithm. CT perfusion maps of various hemodynamic parameters such as blood volume [BV], blood flow [BF] and permeability surface [PS] were created (figure 1) via deconvolution algorithm which is based on the convolution model. Deconvolution analysis uses arterial and tissue time-concentrations curves to compute impulse residue function (IRF) for the tissue. The advantage of this algorithm is that it corrects time delay in contrast kinetics taking into account the actual injection

rate of contrast and offers a more accurate estimation of IRF. In this study, the time-attenuation curve of the input artery was obtained by placing a region of interest (ROI) on the posterior tibial artery of the affected limb. If this artery was occluded or highly calcified, the ROI was placed in anterior tibial artery or peroneal artery at the ankle level. Subsequently, multiple ROIs of same size were placed around the entire foot, on the dermis and muscle tissues on the dorsal and plantar aspect of the foot and the heel in the same region in the pre- and post-procedure examination. The change in the relative perfusion parameters before and after endovascular treatment was calculated. Studies from 6 patients were examined by a second observer to determine inter-observer reproducibility.

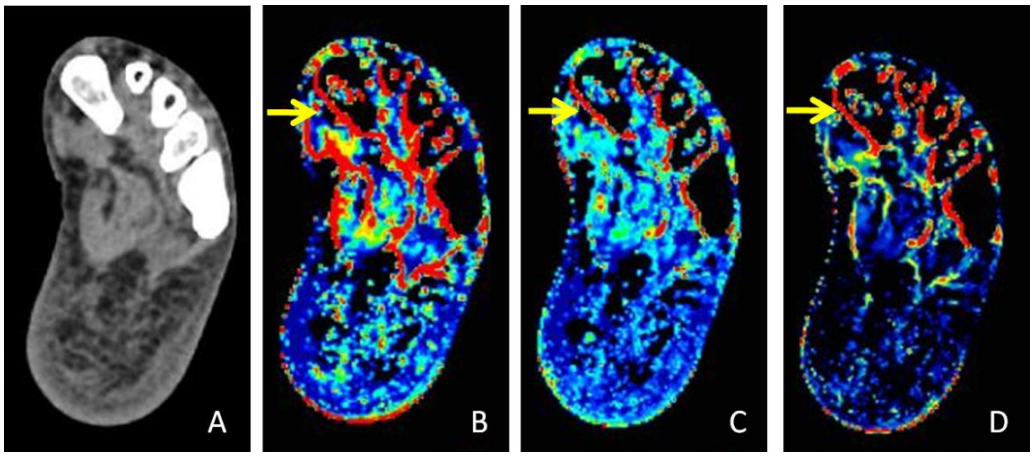

Fig 1: (A) Axial CT image of left foot. Axial perfusion maps of left foot for hemodynamic parameters such as permeability surface (B), blood volume (C) and blood flow (D). Note the "red" pseudo-hyperpefusing lines along the margins of bones which are typical signs of motion artifacts on a perfusion map (arrows).

Statistical analysis

Statistical analysis was performed with MedCalc (version Medcalc Software, Mariakerke, Belgium). Wilcoxon signed rank tests were used to compare pre- and post-procedure perfusion parameters i.e. BV, BF and PS. The increase of ABI was also tested with Wilcoxon signed rank test. Mann-Whitney test was employed to compare perfusion parameters percent change between dermis and muscle tissue regions, which was defined as the percentage change of parameter values between pre- and post-PTA CTFP.

It was also used to compare perfusion parameters values between patients with clinical improvement, without any amputation after PTA and patients who finally underwent amputation. Correlation between perfusion parameters increase and ABI increase was evaluated with Spearman's rank correlation coefficient, due to the fact that the distribution of data was not normal, as it was tested with Kolmogorov-Smirrnov test. ROC analysis was performed to evaluate the potential of each perfusion parameter to discriminate patients with clinical improvement, without any amputation and patients with poor clinical improvement who underwent an amputation after PTA. Interobserver agreement was measured with intra-class correlation coefficient (ICC). Amputation-free survival was evaluated using Kaplan–Meier statistics. Amputation-free survival is a composite metric which incorporates the hard endpoints of mortality and major amputation. Toe and distal foot amputations were considered minor amputations. A p-value < 0.05 was required to consider a test statistically significant.

Results

Procedural details – Clinical outcome

Distribution of atherosclerotic lesions as determined by the diagnostic CTA involved stenoses >50% or occlusions in common iliac artery (n=5), external iliac artery (n=6), superficial femoral artery (n=8) and popliteal artery (n=7), taking into consideration that some patients had more than one arterial lesion. Morphological classification of the target-lesions was conducted according to the TASC II classification system and encompassed one TASC A, eight TASC B, two TASC C and two TASC D lesions. Technical success was achieved in all patients (13/13) included in final analysis. There were no major complications after endovascular treatment, apart from one femoral artery pseudoaneurysm treated with US-guided compression and thrombin injection. PTA was

successfully performed in all patients and provisional stent placement using self-expanding nitinol stents (Luminexx, Bard), (Protege Everflex, Covidien) was performed in seven patients. Three patients underwent additional PTA using drug-eluting balloons (Lutonix, Bard). After successful revascularization mean ABI increased from 0.36±0.16 to 0.75±0.22 (p=0.0002). The patients were followed-up with clinical examination and color Duplex ultrasonography for a mean duration period of 9.1 months (range 6-15 months). During follow up, three patients died due to non-procedure related causes (colon cancer, myocardial infarction and pulmonary embolism). Moreover, the clinical status improved greatly (≧+3 Rutherford categories) in eight patients and moderate (+2 Rutherford categories) in two patients (group A), 6 months after PTA. However, three patients had not clinical improvement (<+1 Rutherford categories) after PTA (group B). In this group, two patients underwent minor amputation (toe, transmetatarsal) while one patient underwent major (above-knee) amputation due to extensive gangrene and tissue necrosis. The major and minor amputations took place during the first year after the procedure. The 6- and 12-month amputation-free survival rates, estimated by Kaplan-Meier analysis, were 100 % and 62.5% respectively.

Perfusion evaluation

Successful revascularization led to a significant change in perfusion parameters (figure 2) Qualitative changes in perfusion parameter maps were found in all patients post-procedurally (table 2).

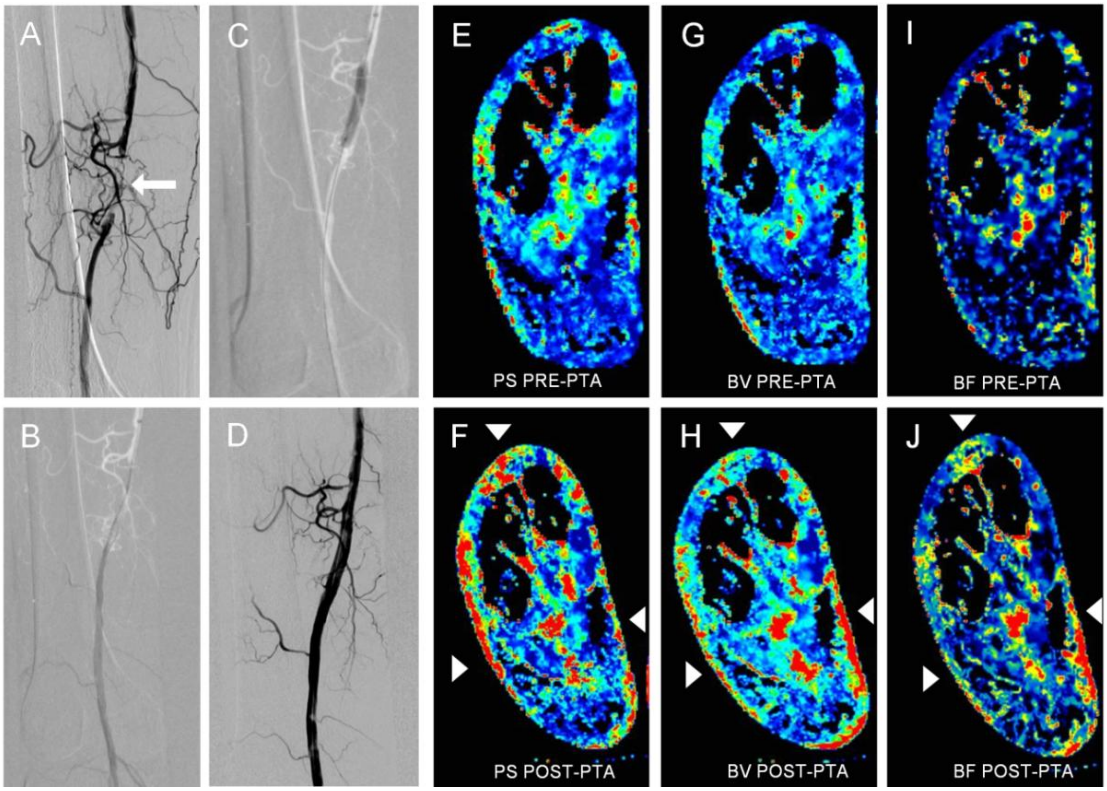

Fig. 2: A 84-year-old male patient with CLI of right lower extremity. (A) DSA showed total occlusion of right distal SFA (arrow). (B) Through percutaneous ipsilateral approach from the right common femoral artery, the occlusion was traversed with a hydrophilic guide wire. (C) The patient underwent PTA using a PTA balloon catheter and a drug-eluting balloon to prevent restenosis. (D) Final DSA showed significant flow restoration without complications. Axial perfusion maps of the foot demonstrated significant increase in Permeability Surface (E,F) Blood Volume (G,H) and Blood Flow (I,J) after PTA especially in the peripheral dermal layer (arrow heads).

Table 2: Results of CTFP examinations in the study population.

Pt No	BV pre-PTA (ml/100g)	BV post-PTA (ml/100g)	BF pre-PTA (ml/100g/min)	BF post-PTA (ml/100g/min)	PS pre-PTA (ml/min/100g)	PS post-PTA (ml/min/100g)
1	0.55	6.61	8.72	36.42	1.11	12.89
2	1.43	5.08	10.95	27.03	1.50	10.15
3	1.40	3.85	15.19	22.26	3.19	5.57
4	1.21	3.35	18.49	31.27	2.49	7.38
5	1.59	3.64	18.87	28.05	6.19	16.15
6	2.62	6.70	21.95	36.80	4.14	8.20
7	0.84	7.31	12.80	43.94	1.27	7.07
8	3.47	4.24	26.94	33.33	7.63	11.62
9	1.22	4.13	14.00	42.66	1.26	6.49
10	1.43	3.89	20.15	31.52	2.70	6.22
11	1.46	3.17	16.74	25.45	2.48	4.02
12	0.58	2.12	12.19	25.67	2.76	3.65
13	2.35	4.48	14.59	24.97	3.57	13.26
Median	1.43	4.13	15.19	31.27	2.70	7.38
Mean ± SD	1.55±0.83	4.51±1.53	16.28±4.97	31.49±6.86	3.1±1.95	8.67±3.85

After PTA, mean BV increased from 1.55±0.83 to 4.51±1.53 ml/100g (p=0.0002), BF increased from 16.28±4.97 to 31.49±6.86 ml/100g/min (p=0.0002) and PS increased from 3.1±1.95 to 8.67±3.85 ml/min/100g, (p=0.0002), (figure 3).

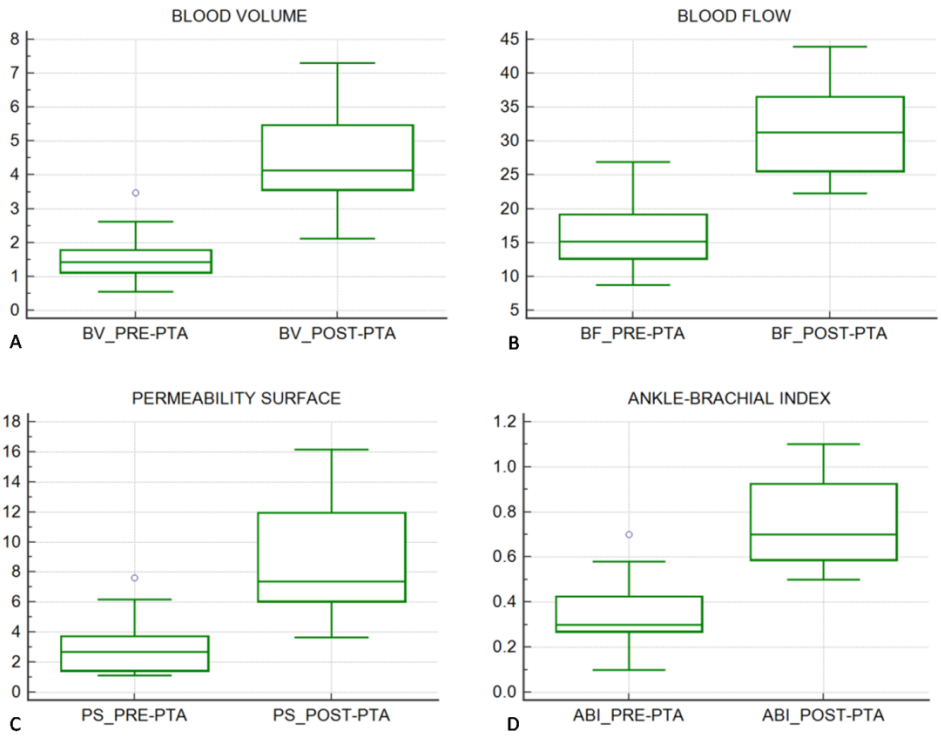

Fig.3: Box-and-whisker plots depicting the median values and the quartile ranges of various perfusion parameters such as Blood Volume (A), Blood Flow (B) and Permeability Surface (C) as well as the values of ankle-brachial index (D) before and after PTA. The boxes stretch from the 25th percentile at the lower edge up to the 75th percentile at the upper edge. The median value is depicted as a line across the box. Outliers are depicted as lines at the outer area of the box plot.

Perfusion parameters increase was greater in dermis compared to muscle tissue regions (p=0.0016 for BV increase, p=0.0333 for BF increase and p=0.0027 for PS increase), (table 3).

Table 3: Comparison of CTFP parameter values (mean ± SD) and mean percent increase of these parameters (in the study poluation) between dermis and muscle tissue regions.

	Dermis			Muscle tissue			p value*
	Pre-PTA	Post-PTA	Increase	Pre-PTA	Post-PTA	Increase	
BV	1.5 ± 0.86	5.44 ± 1.55	345.24%	1.65 ± 0.88	2.73 ± 0.83	114.03%	0.0016
BF	17.39 ± 7.12	37.37 ± 9.61	139.14%	14.85 ± 5.53	22.84 ± 2.88	73.59	0.0333
PS	2.62 ± 1.49	10.88 ± 5.85	395.45%	3.49 ± 2.25	5.7 ± 2.32	130.31%	0.0027

There was no significant correlation between perfusion parameters increase and ABI increase, as it was tested with Spearman's rho (r=0.0413, p=0.8935 for BV, r=0.215, p=0.4814 for BF and r=0.462, p=0.1118 for PS) (figure 4).

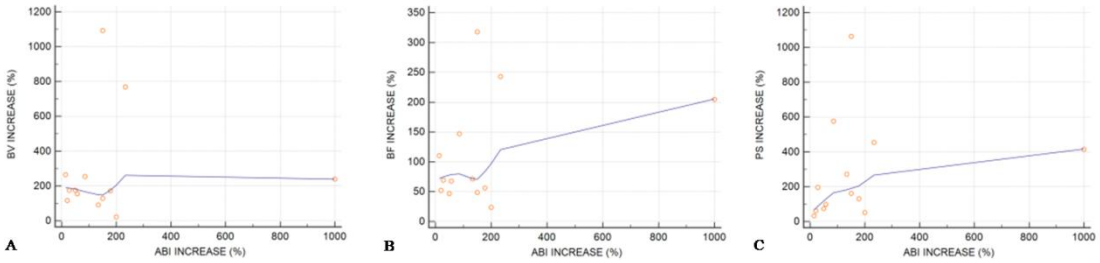

Fig 4: Correlation analyses between ABI increase and perfusion parameters increase [BV (A), BF (B), PS (C)]. The correlation analysis graphs demonstrate no significant correlation between these parameters.

On the other hand, the patients who presented significant clinical improvement without any amputation during follow-up (group A) presented higher post-PTA perfusion values in comparison with patients who finally underwent an amputation (group B), (p=0.028 for BV, p=0.028 for BF and p=0.0112 for PS respectively). A non significant difference on pre-PTA perfusion values was observed between these groups (p=0.499 for BV, p=0.6121 for BF and p=0.8658 for PS respectively). Moreover, only PS increase was statistically significant higher in group A compared to group B (p=0.028), (table 4).

Table 4: Comparison of CTFP parameters values (mean ± SD) and mean percent increase of these parameters between patients with clinical improvement, without any amputation after PTA (group A) and patients with poor response to PTA, who underwent an amputation (group B).

		group A	group B	p value
Pre-PTA	BV	1.67 ± 0.89	1.15 ± 0.49	0.4990
	BF	16.75 ± 5.54	14.71 ± 2.31	0.6121
	PS	3.19 ± 2.24	2.81 ± 0.36	0.8658
Post-PTA	BV	4.94 ± 1.42	3.05 ± 0.87	0.0280
	BF	33.6 ± 6.37	24.46 ± 1.91	0.0280
	PS	9.94 ± 3.41	4.41 ± 1.02	0.0112
Increase (%)	BV	310.32 ± 342.95	185.88 ± 74.71	1
	BF	124.93 ± 98.93	69.74 ± 35.55	0.3105
	PS	342.08 ± 305.92	56.31 ± 21.86	0.0280

ROC analysis results are presented in table 5 and ROC curves are displayed in figure 5. All perfusion parameters were found to have high sensitivity and specificity to predict poor clinical improvement and the occurence of amputation after PTA ($p<0.0001$). However, the small number of patients in the study is inadequate to support the reported cut-off values.

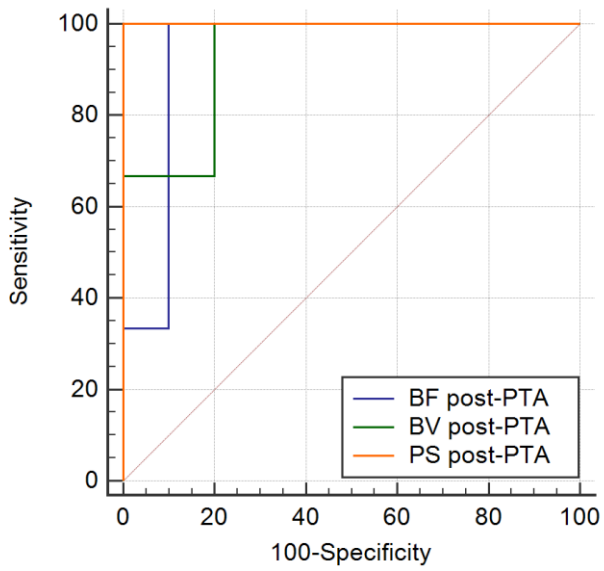

Fig. 5: ROC curves for post-PTA perfusion parameters (BV, BF and PS) regarding the ability to predict the occurence of amputation after PTA.

Table 5: ROC analysis of post-PTA perfusion parameters regarding the ability to predict poor response to revascularization and the occurence of amputation after PTA.

	AUC	p value	Sensitivity	Specificity	Cut-off value
BV	0.933	<0.0001	100 %	80 %	≤3.85
BF	0.933	<0.0001	100 %	90 %	≤25.67
PS	1	<0.0001	100 %	100 %	≤5.57

All measurements demonstrated very good inter-observer reproducibility and ICC was 0.91 (95% CI 0.64-0.97) for BV, 0.94 (95% CI 0.83-0.98) for BF, and 0.95 (95% CI 0.86-0.98) for PS.

CTFP analysis was not feasible in 5 examinations (13.9% of total CTFP examinations) due to: a) diffuse calcification or total occlusion of the lower limb arteries and inability to place the arterial ROI and b) motion artifacts which compromised image evaluation in either the pre-procedural (n=4) or the post-procedural (n=1) CTFP. Additionally, there was one case of a patient who died due to myocardial infarction before post-procedural examination. The mean dose-length product of CTFP was 1430.4 mGy*cm and the mean effective dose was 0.29 mSv.

References

[1] Saltybaeva N, Jafari ME, Hupfer M, Kalender WA. Estimates of effective dose for CT scans of the lower extremities. Radiology 2014;273:153-9.

Evaluation of percutaneous transluminal angioplasty outcome in patients with critical limb ischemia using dynamic contrast-enhanced MRI

Materials and Methods

Study design

The study included patients with CLI (Rutherford categories 4-6) with either rest pain or minor/major tissue loss and anatomic distribution of atherosclerotic lesions which should make them suitable for endovascular treatment. Initially, patients underwent CDUS and diagnostic CTA in order to determine anatomic distribution of atherosclerotic lesions. In general, a primary endovascular approach was preferred whenever possible, even in selected cases with TASC C and D lesions which were judged as poor surgical candidates.

Patients with acute limb ischemia or less advanced PAD (Rutherford categories 1-3) as well those who underwent surgical or conservative treatment were excluded. The exclusion criteria included also all common contraindications to MRI such as ferromagnetic implants, pacemakers and severe claustrophobia and contraindications for gadolinium contrast medium injection such as previous severe allergic/anaphylactoid reaction, severe renal disease (eGFR <30 mL/min/1.73 m^2) or acutely deteriorating renal function and pregnancy.

Selective patients that fulfilled these criteria were subjected to dynamic contrast-enhanced MRI (DCE-MRI) of the affected foot. The patients also underwent a second DCE-MRI examination within 1st month after endovascular treatment. All patients were

followed-up with clinical examination at 1, 3, 6 and 12 months and color Doppler ultrasound combined with clinical examination on an annual basis.

The study was approved by the local ethic and written informed consent was obtained from every patient before entering the study.

Study population

Between March 2015 and April 2019, 16 selective patients enrolled in the study. Technical success was achieved in 13/16 patients. Three cases with multilevel occlusive disease (TASC D), who underwent surgical revascularization after failed endovascular revascularization, were excluded from subsequent analysis. Moreover, there was one patient who died before post-procedural examination due to ischemic stroke and one patient who underwent amputation due to extensive ulcers and osteomyelitis before post-procedural examination. DCE analysis was not feasible in one case due to motion artifacts which compromised image evaluation. Totally, 10 patients (6 male, 4 female) with a median age of 68 years (range 58-79 years) were included in the final analysis. Patient's main risk factors were hypertension (n=8), hyperlipidemia (n=10), diabetes mellitus (n=8), smoking (n=9) and coronary artery disease (n=5). According to Rutherford classification of PAD, two patients were allocated to class 4, six patients to class 5 and two patients to class 6 PAD. The study population's baseline characteristics are summarized in Table 1.

Table 1: Clinical data of study population

Pt No	Sex	Age	Risk Factors	Rutherford Classification
1	M	76	HT, HL, SM	5
2	M	75	DM, HL, SM,CAD	5
3	M	66	DM, HT, HL,SM, CAD	5
4	M	68	DM, HT, HL,SM, CAD	4
5	F	68	DM, HT, HL,SM	6
6	F	66	DM, HT, HL,SM, CAD	4
7	F	79	DM, HT, HL,SM	5
8	M	58	DM, HT, HL,SM, CAD	5
9	M	64	DM, HL	6
10	F	72	HT, HL, SM	5

Imaging protocol

Studies were performed on a 1.5T clinical MR Scanner (Vision/Sonata Hybrid system, Siemens, Erlangen, Germany) enforced with a powerful 3T equivalent gradient system (Gradient strength : 45 mT/m, Gradient Slew rate : 200 mT/m/ms). A standard quadrature RF bird cage body coil was used for signal excitation and a two channel array Head Coil was used for signal detection.

Conventional and quantitative MR imaging protocols include:

The conventional qualitative imaging protocol consisted of a T1 weighted 3D GRE VIBE (Volume Interpolated Breath hold Examination) sequence (TR/TE/FA: 9.5ms/3.4ms/15^{o}) and a T2/T1 weighted 3D GRE CISS (Constructive Interference in Steady State) sequence (TR/TE/FA: 9.3ms/4.2ms/70^{o}), obtained both in sagittal planes at the area of lower limb. Forty (40) consecutive slices of 2 mm slice thickness and in-

plane spatial resolution (pixel size) of 0.49 mm^2 (FOV=250X250mm, Matrix size=512X512 interpolated) were obtained utilizing either T1 or T2/T1 weighted sequences. Pixel band width was 130 Hz/pxl in both T1 and T2/T1 weighted sequences. Acquisition times were approximately 2.5 min for both sequences.

The quantitative DCE-MRI protocol of the lower limb was performed utilizing firstly a PD to T1 weighted 3D GRE VIBE sequence (TR/TE: 7.8ms/2.7ms) in the sagittal plane with variable flip angles (FA = 5^o,10^o,15^o,20^o, 25^o,30^o) for the initial calculation of the parametric T1 maps. Twenty six (26) consecutive slices of 3 mm slice thickness and in-plane spatial resolution (pixel size) of 0.49 mm^2 (FOV=250X250mm, Matrix size=512X512 interpolated) were obtained. Pixel bandwidth was 150 Hz/pxl. The acquisition time was 21 sec for each flip angle. Each flip angle was obtained separately and therefore, the sequence was repeated 6 times. The total acquisition time for all the set of flip angles was approximately 2 min. The final outcome of this sequence is the production of 26 consecutive slices depicting the calculated T1 parametric maps with the same anatomical characteristics (slice thickness, pixel size) of the base aforementioned sequence. These maps serve as the basis of the calculation of $T1_0$ in DCE-MRI perfusion imaging [1].

The actual T1 weighted DCE perfusion MR imaging of the lower limb was performed utilizing a T1 weighted 3D GRE VIBE sequence (TR/TE/FA: 9.5ms/3.4ms/15^o) in sagittal plane. Twenty six (26) consecutive slices of 3 mm slice thickness and in-plane spatial resolution (pixel size) of 0.49 mm^2 (FOV=250X250mm, Matrix size=512X512 interpolated) were obtained. Pixel bandwidth was 150 Hz/pxl. The acquisition time was 15 sec. The sequence was repeated 40 times. The first 3 repetitions were used for the calculation of the baseline signal. Consequently, during the rest 37 repetitions of the aforementioned sequence, an intravenous continual injection of paramagnetic contrast medium [(Magnevist, Gadopentetate Dimeglumine, Bayer Healthcare, Bayer, 0.2 ml/kg, (0.1 mmol/kg)] was administered for approximately one minute. The mean dose of

paramagnetic contrast medium delivered during the examination was 16.5 ml (range 14-20 ml). The total acquisition time for the 40 repetitions was approximately 10 min. All images were transformed to a separate dedicated workstation for further analysis.

Image analysis

MR images were transferred and analyzed with a commercially available software (nordicICE v4.0, NNL, Bergen, Norway). DCE-analysis was performed utilizing an extended Tofts model (3-parameter fitting). Initially, T1 parametric maps were calculated using a 3D spoiled gradient echo sequence (3D GRE VIBE) with variable flip angles, as previously discussed. Fast T1 calculations using variable flip angles is based on the method proposed by Fram EK et al [2]. This method is incorporated as a standard T1 measurement procedure on the (nordicICE) platform. T1 parametric maps are used for the calculation of the base $T1_0$ maps of the anatomic regions (slices) prior to perfusion analyses.

Quantitative perfusion maps based on pharmacokinetic parameters such as blood flow (BF), K^{trans} and K_{ep} were created from parametric data fitted to the extended Tofts model utilizing a population-based arterial input function [1]. K^{trans} express the volume transfer coefficient between blood plasma and extravascular extracellular space (EES), K_{ep} the exchange rate constant between EES and blood plasma (backflux exchange rate) and finally BF express flow of blood per unit mass of tissue [3]. K^{trans} and K_{ep} are expressed in min^{-1} and BF in ml/min/100g of tissue. Subsequently, multiple ROIs were placed around the entire foot, on the dermis and muscles tissues in the pre- and post-procedure examination and the change in the relative perfusion parameters was calculated. Analysis and evaluation of DCE-MRI was performed by two blinded radiologists to determine inter-observer reliability.

Statistical analysis

Statistical analysis was performed with MedCalc (version Medcalc Software, Mariakerke, Belgium). Wilcoxon signed rank tests were used to compare perfusion parameters such as BF K^{trans} and K_{ep} before and after endovascular treatment. The relative change in ABI was also tested with Wilcoxon signed rank test. Correlation between perfusion parameters and ABI was evaluated with Pearson's correlation coefficient and normal distribution of data was tested with Kolmogorov-Smirnov test. Amputation-free survival was calculated using Kaplan–Meier method. Interobserver agreement was assessed using the interclass correlation coefficient (ICC). A p-value < 0.05 was considered as statistically significant.

Results

Procedural details – Clinical outcome

Patients presented hemodynamically significant stenoses or occlusions in common iliac artery (n=4), external iliac artery (n=5), superficial femoral artery (n=7), popliteal artery (n=4) and below the knee arteries (n=4) taking into consideration that some patients had more than one arterial lesion. The majority of patients had multilevel arterial disease but we only refer the targeted vessels for endovascular recanalization. Technical success was achieved in all patients included in final analysis, without major complications. PTA was successfully performed in all patients, drug coated balloons (Lutonix, Bard) were used in two patients and provisional stenting using self- expanding nitinol stents (Luminexx, Bard), (Protege Everflex, Covidien) was performed in seven patients (table 2). There was significant hemodynamic improvement in all patients and mean ABI increased from 0.37 ± 0.18 to 0.76 ± 0.23 after revascularization ($p<0.05$). All patients received the optimal medical treatment for hypertension, hyperlipidemia and diabetes mellitus. After PTA they received single or dual antiplatelet therapy as it is

displayed in table 2. The patients were followed-up with clinical examination and color Duplex ultrasonography for a mean duration period of 24 months (range 6-48). No recurrent hemodynamically significant stenoses were found at the site of the intervention during US examination, except patient No5 who underwent a second PTA with successful restoration of flow. During follow up one patient died due to acute myocardial infarction, one patient underwent major (above-knee) amputation due to extensive tissue necrosis and there were also two patients who underwent minor (toe) amputations (table 2). The 12-month amputation-free survival rate, estimated by Kaplan-Meier analysis, was 80%,

Table 2: Procedural and Follow-up data of study population

Pt No	Lesion location	Endovascular procedure	Medical therapy after PTA	ABI pre-PTA	ABI post-PTA	Follow-up Rutherford classification (ABI) or event		
						1 month	6 month	1 year
1	(R) CIA,EIA	PTA Stenting	Clopidogrel	(0.25)	(0.6)	Minor (toe) amputation (0.6)	3 (0.5)	3 (0.5)
2	(L) SFA, POPA, TPT, PA	PTA	Aspirin+ Clopidogrel	(0.33)	(0.55)	(0.5)	Death (AMI)	-
3	(R) SFA	DCB PTA	Aspirin+ Clopidogrel	(0.55)	(0.73)	(0.7)	2 (0.7)	2 (0.8)
4	(R) SFA, POPA	PTA Stenting	Aspirin+ Clopidogrel	(0.53)	(0.9)	(0.9)	1 (0.9)	2 (0.8)
5	(R) CIA, EIA, CFA	PTA Stenting	Clopidogrel	(0.2)	(0.4)	Minor (toe) amputation (0.5)	5 (0.4)	5 (0.3)
6	(L) EIA, SFA	PTA Stenting	Aspirin+ Clopidogrel	(0.64)	(1.1)	(1)	2 (0.9)	2 (0.9)
7	(L) CIA, EIA, SFA, POPA	PTA Stenting	Aspirin+ Clopidogrel	(0.1)	(1.1)	(1.1)	1 (1)	1 (0.9)
8	(R) SFA, POPA, PTA, ATA	PTA Stenting	Aspirin+ Clopidogrel	(0.2)	(0.7)	(0.7)	3 (0.7)	3 (0.6)
9	(L) SFA	DCB PTA	Aspirin+ Clopidogrel	(0.4)	(0.8)	(0.7)	2 (0.6)	2 (0.6)
10	(R) CIA, EIA	PTA Stenting	Clopidogrel	(0.5)	(0.7)	(0.5)	Major amputation	-

Perfusion evaluation

Successful revascularization led to a significant change in perfusion parameters (figure 1).

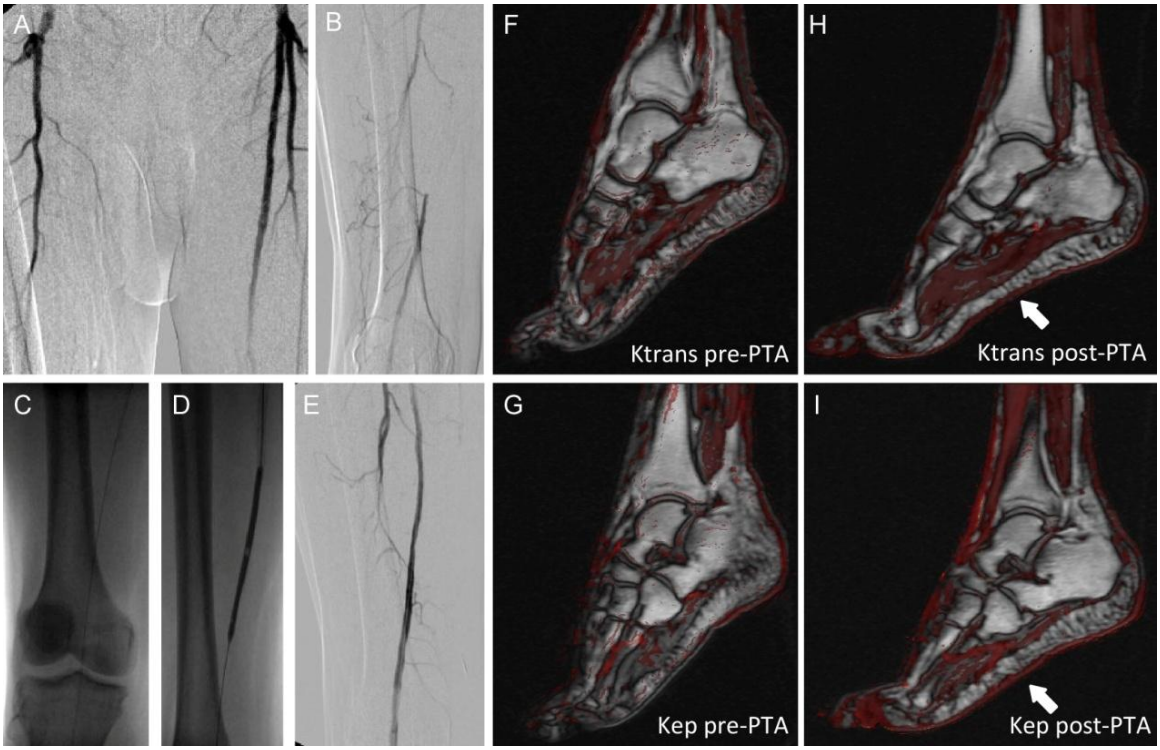

Fig. 1: A 68-year-old male patient with CLI of right lower extremity. DSA showed total occlusion of right SFA (A) and reconstruction of popliteal artery via collaterals (B). Through percutaneous approach from the left common femoral artery, the occlusion was traversed with a hydrophilic guide wire (C). The patient underwent successful PTA and stent placement (D) Final DSA showed significant flow restoration (E). Co-registration of anatomic sagittal T1w sequences combined with K^{trans} and K_{ep} parametric maps before (F,G) and after PTA (H,I) showed significant increase of perfusion parameters after revascularization, especially in the peripheral dermal layer (arrow).

After PTA, mean BF increased from 6.232 ± 2.867 to 9.867 ± 2.965 ml/min/100g, K^{trans} increased from 0.060 ± 0.022 to 0.107 ± 0.041 min^{-1} and K_{ep} increased from 0.103 ± 0.024 to 0.148 ± 0.024 min^{-1}, $p<0.05$. (table 3, Fig. 2).

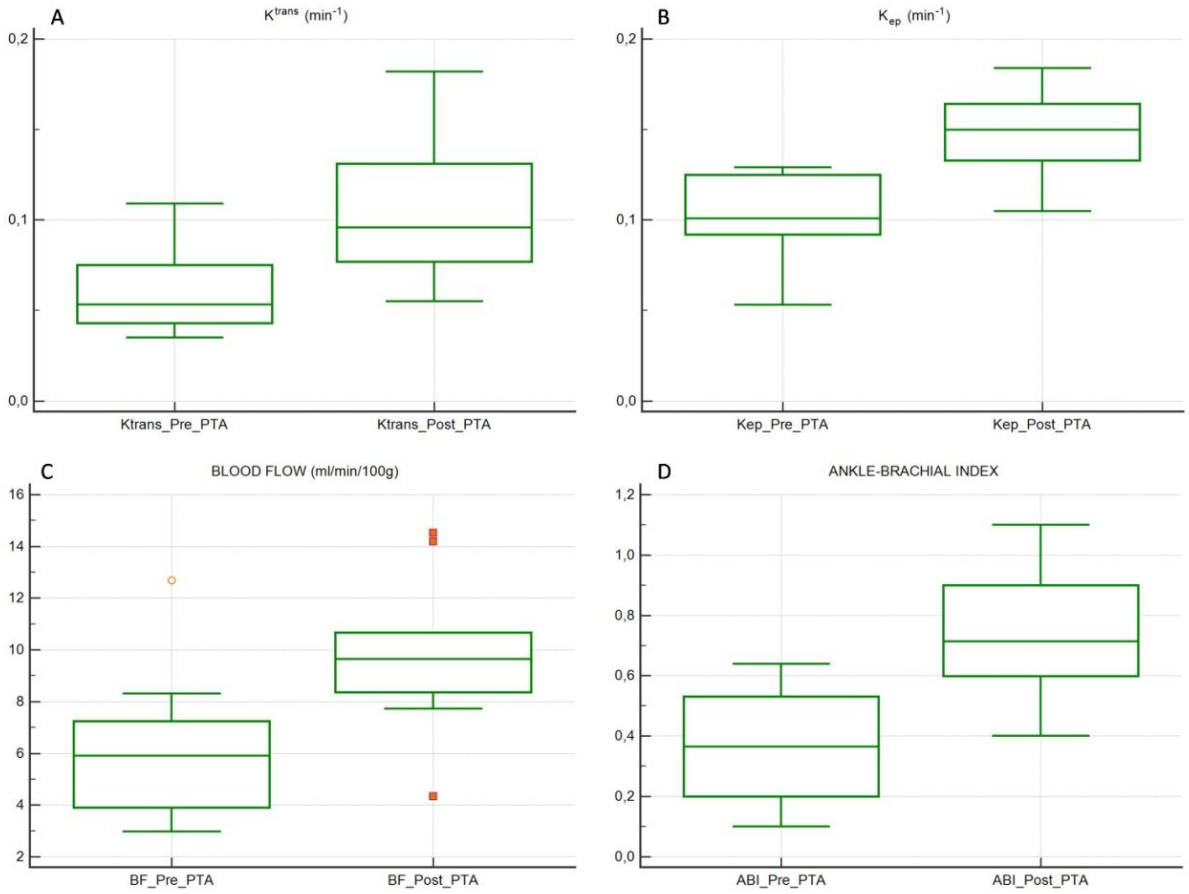

Fig.2: Box-and-whisker plots depicting the median values and the quartile ranges of various perfusion parameters such as K^{trans} (A), K_{ep} (B) and Blood Flow (C), as well as the values of ankle-brachial index (D) before and after PTA. The boxes stretch from the 25th percentile at the lower edge up to the 75th percentile at the upper edge. The median value is depicted as a line across the box. Outliers are depicted as lines at the outer area of the box plot.

Table 3: Results of DCE-MRI examinations in the study population.

Pt No	Gd contrast medium dose (ml)	BF pre-PTA (ml/min/100g)	BF post-PTA (ml/min/100g)	K^{trans} (min^{-1})	K^{trans} (min^{-1})	K_{ep} (min^{-1})	K_{ep} (min^{-1})
1	16	7.234	10.673	0.050	0.055	0.103	0.184
2	15	6.164	10.282	0.035	0.115	0.053	0.133
3	20	6.991	9.255	0.058	0.065	0.129	0.142
4	18	12.682	14.527	0.109	0.182	0.125	0.149
5	15	3.909	8.373	0.080	0.163	0.128	0.151
6	14	3.218	7.727	0.055	0.095	0.093	0.120
7	15	5.182	9.627	0.042	0.077	0.084	0.105
8	18	8.309	14.182	0.075	0.097	0.099	0.175
9	20	5.645	9.693	0.043	0.094	0.092	0.164
10	14	2.982	4.327	0.052	0.131	0.124	0.158
Mean±SD	16.5±2.32	6.232±2.867	9.867±2.965	0.06±0.022	0.107±0.041	0.103±0.024	0.148±0.024

There was no significant correlation between perfusion parameters and ABI, as it was tested with Pearson's correlation coefficient (r=0.37, p=0.106 for K^{trans}, r=0.39, p=0.085 for K_{ep} and r= 0.41, p=0.074 for BF), (figure 3).

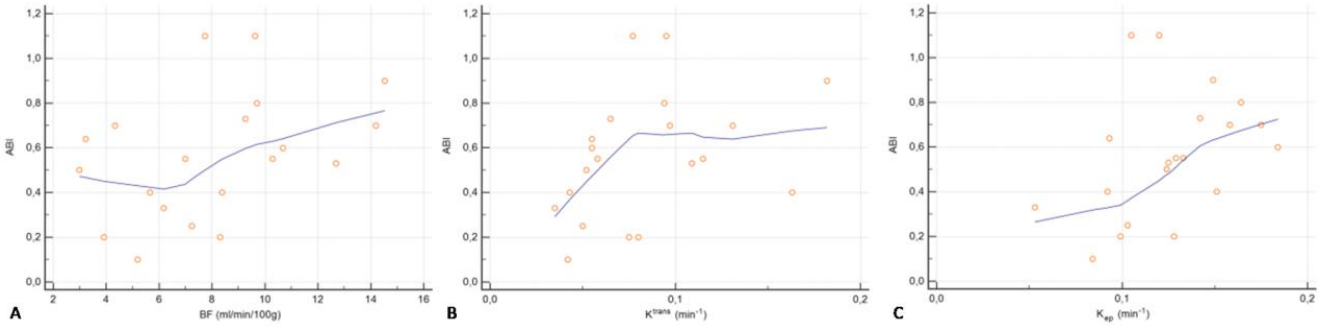

Fig.3: Scatter plots showing the correlation between ABI and perfusion parameters such as BF (A), K^{trans} (B) and K_{ep} (C). The correlation analysis demonstrates no significant correlation between these parameters.

The studies were also analyzed by a second observer to determine inter-observer reliability. All perfusion parameter measurements presented very good inter-observer reliability with an ICC greater than 0.85 for all perfusion parameters and specifically 0.92 (95% CI 0.82-0.97) for K^{trans}, 0.87 (95% CI 0.7-0.95) for K_{ep}, and 0.89 (95% CI 0.73-0.95) for BF.

References

[1] Tofts PS, Kermode AG. Measurement of the blood-brain barrier permeability and leakage space using dynamic MR imaging. 1. Fundamental concepts. Magnetic resonance in medicine 1991; 17:357-67.

[2] Fram EK, Herfkens RJ, Johnson GA, et al. Rapid calculation of T1 using variable flip angle gradient refocused imaging. Magnetic resonance imaging 1987; 5:201-8.

[3] Brix G, Semmler W, Port R, Schad LR, Layer G, Lorenz WJ. Pharmacokinetic parameters in CNS Gd-DTPA enhanced MR imaging. Journal of computer assisted tomography 1991; 15:621-8.

Correlation between diffusion and perfusion MR imaging parameters on peripheral arterial disease

Materials and methods

Study population

Thirteen patients (8 male, 5 female) with PAD with a median age of 68 years (range 56-78 years) underwent MR examination of lower limb using both dynamic contrast-enhanced MRI (DCE-MRI) and diffusion weighted MRI (DW-MRI). According to Fontaine classification, 4 patients presented with stage III and 9 patients with stage IV PAD. The exclusion criteria included all common contraindications to MRI such as ferromagnetic implants, pacemakers and severe claustrophobia and contraindications for gadolinium contrast medium injection such as previous severe allergic/anaphylactoid reaction, severe renal disease (eGFR <30 mL/min/1.73 m^2) or acutely deteriorating renal function and pregnancy.

Imaging protocol

Studies were performed on a 1.5T clinical MR Scanner (Vision/Sonata Hybrid system, Siemens, Erlangen, Germany) enforced with a powerful 3T equivalent gradient system (Gradient strength : 45 mT/m, Gradient Slew rate : 200 mT/m/ms). A standard quadrature RF bird cage body coil was used for signal excitation and a two channel array Head Coil was used for signal detection.

Conventional and quantitative MR imaging protocols include:

The conventional qualitative imaging protocol consisted of a T1 weighted 3D GRE VIBE (Volume Interpolated Breath hold Examination) sequence (TR/TE/FA: 9.5ms/3.4ms/15^{o}) and a T2/T1 weighted 3D GRE CISS (Constructive Interference in Steady State) sequence (TR/TE/FA: 9.3ms/4.2ms/70^{o}), obtained both in sagittal planes at the area of lower limb. Forty (40) consecutive slices of 2 mm slice thickness and in-plane spatial resolution (pixel size) of 0.49 mm^{2} (FOV=250X250mm, Matrix size=512X512 interpolated) were obtained utilizing either T1 or T2/T1 weighted sequences. Pixel band width was 130 Hz/pxl in both T1 and T2/T1 weighted sequences. Acquisition times were approximately 2.5 min for both sequences.

Diffusion weighted (DW) sagittal images of the lower limb were acquired utilizing a high resolution HASTE (Half-Fourier Acquisition Single-shot Turbo spin Echo) sequence with diffusion sensitizing gradients with different b-values (b = 0, 50, 100, 150, 200, 500, 800, 1000 s/mm2), number of slices = 13, echo time (TE) =105 ms, repetition time (TR) = 2000 ms, matrix size =384×384, field of view (FOV)=250×250, slice thickness=5mm. Additionally, a reverse polarization gradient technique was applied by acquiring two sets of sagittal DW images, each time altering the polarization direction of the frequency encoding gradient A P and P-A (Anterior-Posterior).

DCE-MRI of the lower limb was performed utilizing a 3D VIBE (volume interpolated breath hold examination) sequence in the sagittal plane with variable flip angles (FA=5°,10°,15°, 20°, 25°, 30°) for the initial calculation of the parametric T1 maps. Consequently, an intravenous continual injection of the paramagnetic CA (Magnevist, Gadopentetate Dimeglumine, Bayer Healthcare, Bayer, 0.1 mmol/kg) was administered for approximately 1 min. The aforementioned T1W DCE VIBE perfusion sequence was continuously repeated for 10min (20s temporal resolution) after the intravenous

injection of the CA with the following imaging parameters: number of slices=26, FA=15°, TE=2.73 ms, TR=7.8 ms, matrix size=512×512, FOV=250×250 and slice thickness=3 mm. All images were transformed to a separate dedicated workstation for further analysis.

Image analysis

The quantification of both diffusion and perfusion parameters was implemented using python 3.5. According to the Intra-Voxel Incoherent Motion (IVIM) model the DWI signal as a function of the b-value is expressed in $S(b)/S(0) = (1 - f)e^{-bD} + fe^{-bD*}$. S(b) is the measured signal intensity at the current b-value and S(0) is the measured signal intensity without diffusion gradient attenuation factor (typically a T2 image), D is the diffusion coefficient, D* is the pseudodiffusion coefficient and f is the micro-perfusion fraction denoting the ratio of water flowing in capillaries to the total water contained in a voxel [1]. The quantification of the DW signal with the IVIM model is mainly succeeded by two different fitting methods. The first method is a direct estimation of the IVIM parameters using a nonlinear fitting algorithm and the second method is relied on the fact that for b-values greater than 200 s/mm^{2}the micro-perfusion effect is eliminated and does not contribute to the DW signal decay [2]. The procedure for the quantification of the DCE-MRI signal has two important steps. First, the concentration curve as a function of time of the CA is calculated ($C_t(t)$) and then, after the choice of a suitable pharmacokinetic model, nonlinear fitting of the concentration curve is required in order to produce tissue perfusion parameters [3]. In order to provide information about tissue perfusion to patients with PAD a variety of pharmacokinetic models were used such as, the extended Tofts model (ETM) [4], the Patlak model (PM) [5], the steady state model (SSM) [6] and the Gamma capillary transit time model (GCTT) [7]. Except from its complex form, the GCTT model was included in this study since it is a more recently suggested physiological model unifying well-known models such as the Tofts Model [8] the ETM and the adiabatic tissue homogeneity (ATH) model [9]. Except from the

previous models, two semi quantitative parameters were also calculated from the signal intensity curve over time $SI(t)$ such as the area under the curve (AUC) and the relative enhancement ratio (RER) .

Statistical analysis

Two statistical metrics were used, the adjusted R squared ($R^{-}{}^{2}$) and the root mean squared error (RMSE), to determine the goodness of fit for every voxel. Correlation analysis was performed using Pearson's r correlation coefficient taking into account the slices from perfusion and diffusion sequences with the same slice location dicom tag, while rejecting all voxels from tissues without significant blood supply (non-perfused) such as the osseous structures ($v_p = 0$). The effects of noise, after the fitting process, led to parametric maps that exhibit large variations within voxels in small neighborhoods . Thus, in order to examine the relationship between DCE and DWI parameters in a more effective and qualitative way, a 5 × 5 Gaussian filter ($\sigma = 0.9$) was applied on the derived parametric maps.

Results

Metrics from the statistical analysis, showed that regarding the DWI fitting, both the first and the second fitting method were quite accurate since RMSE and $R^{-}{}^{2}$ were as expected at the desired levels, meaning low RMSE and high $R^{-}{}^{2}$. More precisely, for the first fitting method, RMSE = 0.081± (0.048), $R^{-}{}^{2}$ =0.637 ± (0.292) and for the second method, RMSE = 0.085 ± (0.05), $R^{-}{}^{2}$ = 0.627± (0.285). A graphical representation of each aforementioned model fit in a region of the peroneus brevis muscle for DWI and DCE-MRI is depicted in figures 1A and 1B respectively.

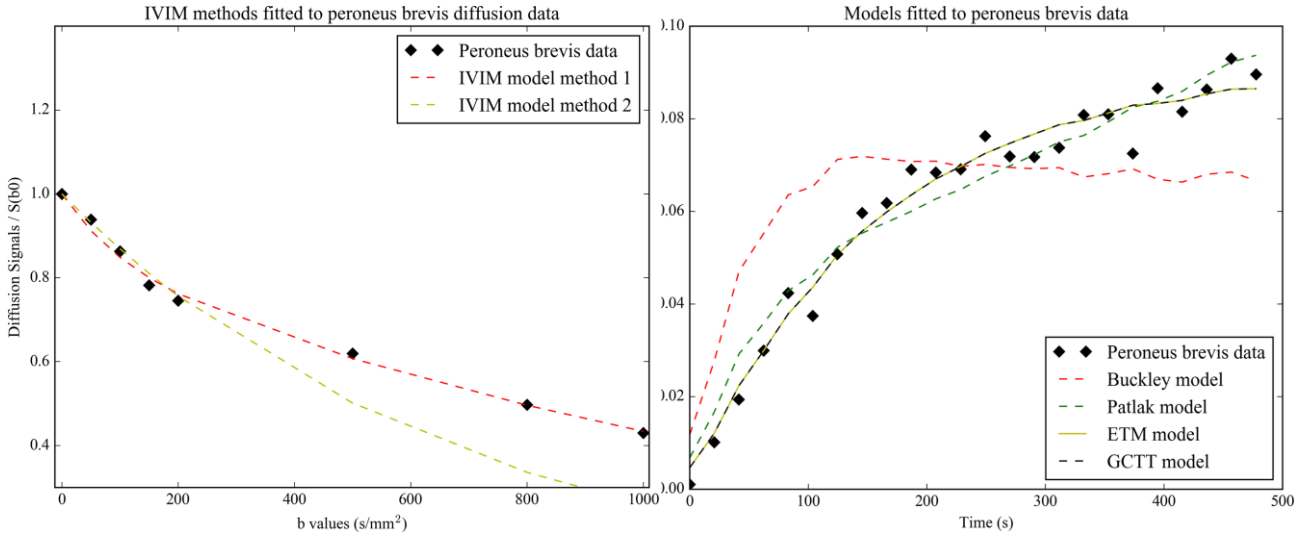

Fig. 1: (A) IVIM model method 1 and 2 fitted to DWI data obtained from the peroneus brevis muscle. (B) Pharmacokinetic models fitted to DCE data derived from the peroneus brevis muscle.

Pearson's correlation (r) coefficient was calculated for every perfusion and diffusion model based parametric map and was displayed in table 1. Pearson's correlation coefficient r, is presented between the parameter (f-IVIM) and the perfusion plasma volume parameters. A graphical illustration of the normalized parametric maps is depicted in figure 2. After the application of the Gaussian filter on the parametric maps the smoothed parametric maps are shown in figure 3. All p values of the correlation analysis for both tables were lower than 0.05.

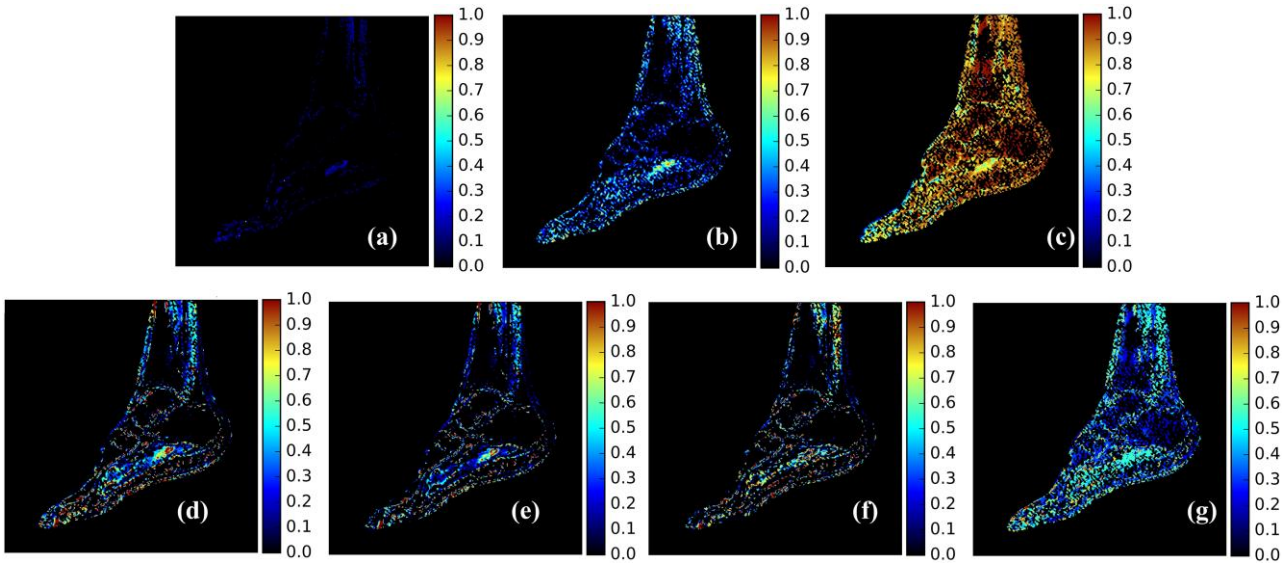

Fig. 2: Blood plasma volume related parametric maps. (b) f-IVIM, semi- quantitative: (a) RER and (c) AUC and (d)-(g) SSM (vp), PM (vp), ETM (vp), GCTT (E) respectively.

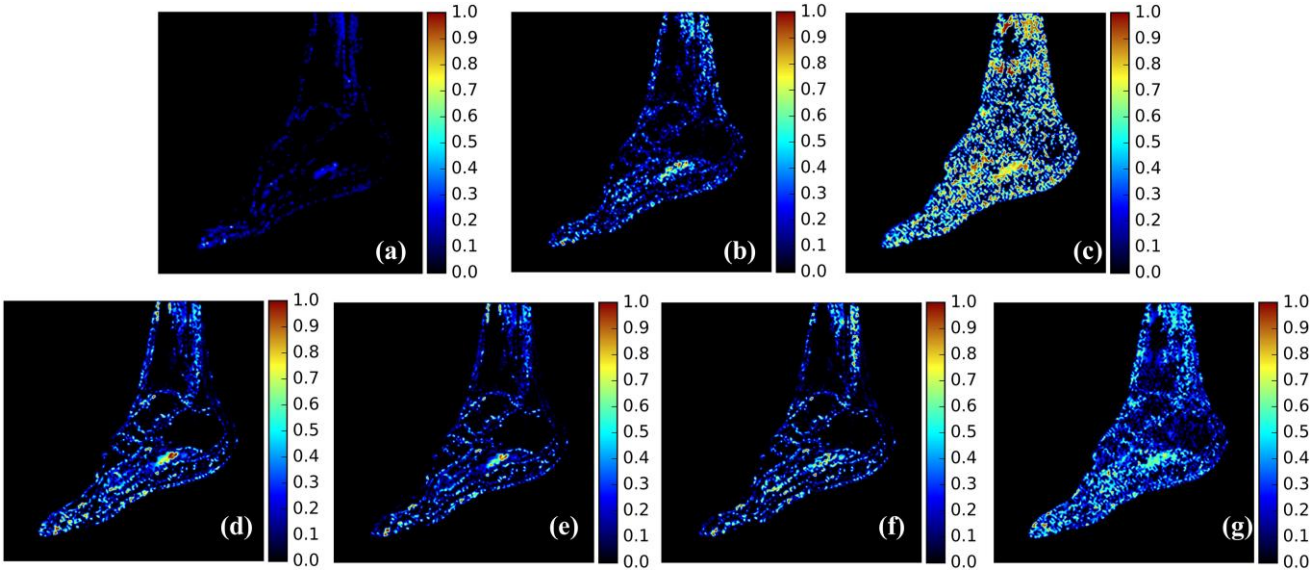

Fig. 3: Blood plasma volume related parametric maps after the application of a 5x5 Gaussian filter (σ = 0.9). (b) f-IVIM, semi- quantitative: (a) RER and (c) AUC and (d)-(g) SSM (vp), PM (vp), ETM (vp), GCTT (E) respectively.

Table 1: Pearson's Correlation coefficient r with and without Gaussian Filtering to the parametric maps.

	Fitting model (parameter) DWI	DWI - Method 1 (f)	DWI - Method 2 (f)
without Gaussian Filtering	SSM (vp)	0.082	0.086
	PM (vp)	0.073	0.071
	ETM (vp)	0.046	0.043
	GCTT (E)	0.039	0.045
	AUC	0.011	0.013
	RER	-0.114	-0.107
with Gaussian Filtering	SSM (vp)	0.429	0.427
	PM (vp)	0.379	0.366
	ETM (vp)	0.406	0.397
	GCTT (E)	0.544	0.551
	AUC	0.254	0.252
	RER	0.592	0.601

References

[1] Le Bihan, Denis, Eric Breton DL. Seperation of Diffusion and Perfusion in Intravoxel Incoherent Motion MR Imaging. Radiology 1988;168:497–505.

[2] Hu Y-C, Yan L-F, Wu L, Du P, Chen B-Y, Wang L, et al. Intravoxel incoherent motion diffusion weighted MR imaging of gliomas: efficacy in preoperative grading. Sci Rep 2014;4:7208

[3] Tofts PS, Kermode AG. Measurement of the blood-brain barrier permeability and leakage space using dynamic MR imaging. 1. Fundamental concepts. Magnetic resonance in medicine 1991;17:357-67.

[4] Tofts PS, Brix G, Buckley DL, Evelhoch JL, Henderson E, Knopp M V, et al. Estimating kinetic parameters from dynamic contrast-enhanced T(1)-weighted MRI of a diffusable tracer: standardized quantities and symbols. J Magn Reson Imaging 1999;10:223–32.

[5] Patlak CS, Blasberg RG, Fenstermacher JD. Graphical Evaluation of Blood-to-Brain Transfer Constants from Multiple-Time Uptake Data. J Cereb Blood Flow Metab 1983;3:1-7.

[6] Sourbron SP, Buckley DL. Classic models for dynamic contrast-enhanced MRI. NMR Biomed 2013;26:1004–27.

[7] Schabel MC. A unified impulse response model for DCE-MRI. Magn Reson Med 2012;68:1632–46.

[8] Tofts PS. Modeling tracer kinetics in dynamic Gd-DTPA MR imaging. J Magn Reson Imaging 1997;7:91–101.

[9] St Lawrence KS, Lee T-Y. An Adiabatic Approximation to the Tissue Homogeneity Model for Water Exchange in the Brain: I. Theoretical Derivation. J Cereb Blood Flow Metab n.d.;18:1365–77.

Evaluation of percutaneous transluminal angioplasty outcome in patients with critical limb ischemia using diffusion weighted magnetic resonance imaging

Materials and methods

Study design

The study included patients with CLI (Rutherford categories 4-6) with either rest pain or minor/major tissue loss and anatomic distribution of atherosclerotic lesions which should make them suitable for endovascular treatment. Initially, patients underwent CDUS and diagnostic CTA in order to determine anatomic distribution of atherosclerotic lesions.

Patients with acute limb ischemia or less advanced PAD (Rutherford categories 1-3) as well those who underwent surgical or conservative treatment were excluded. The exclusion criteria included also all common contraindications to MRI such as ferromagnetic implants, pacemakers and severe claustrophobia. Selective patients that fulfilled these criteria were subjected to diffusion weighted magnetic resonance imaging (DW-MRI) of the affected foot. The patients also underwent a second DW-MRI examination within 1st month after endovascular treatment. All patients were followed-up with clinical examination at 1, 3, 6 and 12 months and color Doppler ultrasound combined with clinical examination on an annual basis. Moreover healthy volunteers without PAD (control group) underwent the same examination during the study period.

The study was approved by the local ethic committee and both patients and healthy volunteers provided written informed consent prior to study enrollment.

Study population

Between April 2016 and December 2019, 10 selective patients and 6 healthy volunteers enrolled in the study. Technical success was achieved in 9 patients (9/10). One patient with multilevel occlusive disease (TASC D) underwent surgical revascularization after failed PTA and excluded from subsequent analysis. Moreover one patient underwent amputation due to extensive ulcers and osteomyelitis before post-procedural examination. Totally, 8 patients (5 male, 3 female) with a median age of 69 years (range 56-79 years) were included in the final analysis. Patients' main risk factors were hypertension (n=7), hyperlipidemia (n=8), diabetes mellitus (n=7), smoking (n=8) and coronary artery disease (n=5). According to Rutherford classification of PAD, two patients were allocated to class 4, five patients to class 5 and one patients to class 6 PAD. The control group consisted of 6 volunteers (3 male, 3 female) with a median age of 50 years (range 38-67 years). Neither of these volunteers had history of PAD or predisposing factors for PAD such as diabetes mellitus, hypertension or history of smoking.

Imaging protocol

Studies were performed on a 1.5T clinical MR Scanner (Vision/Sonata Hybrid system, Siemens, Erlangen, Germany) enforced with a powerful 3T equivalent gradient system (Gradient strength : 45 mT/m, Gradient Slew rate : 200 mT/m/ms). A standard quadrature RF bird cage body coil was used for signal excitation and a two channel array Head Coil was used for signal detection.

Conventional and quantitative MR imaging protocols include:

The conventional qualitative imaging protocol consisted of a T1 weighted 3D GRE VIBE (Volume Interpolated Breath hold Examination) sequence (TR/TE/FA: 9.5ms/3.4ms/15^{o}) and a T2/T1 weighted 3D GRE CISS (Constructive Interference in Steady State) sequence (TR/TE/FA: 9.3ms/4.2ms/70^{o}), obtained both in sagittal planes at the area of lower limb. Forty (40) consecutive slices of 2 mm slice thickness and in-plane spatial resolution (pixel size) of 0.49 mm^{2} (FOV=250X250mm, Matrix size=512X512 interpolated) were obtained utilizing either T1 or T2/T1 weighted sequences. Pixel bandwidth was 130 Hz/pxl in both T1 and T2/T1 weighted sequences. Acquisition times were approximately 2.5 min for both sequences.

DW sagittal images of the lower limb were acquired utilizing a high resolution HASTE (Half- Fourier Acquisition Single-shot Turbo spin Echo) sequence with diffusion sensitizing gradients with different b values (b = 0, 50, 100, 150, 200, 500, 800, 1000 s/mm^{2}), number of slices = 13, echo time (TE) =105 ms, repetition time (TR) = 2000 ms, matrix size =384×384, field of view (FOV)=250×250, slice thickness=5mm. Additionally, a reverse polarization gradient technique was applied by acquiring two sets of sagittal DW images, each time altering the polarization direction of the frequency encoding gradient A P and P-A (Anterior-Posterior).

Image analysis

A significant characteristic of the DW-MRI that can describe the molecular diffusion of water is the Apparent Diffusion Coefficient (ADC) [1]. However, it is possible to examine that diffusion decay curve in a more complex and advanced way using the following equation Eq.(1) as described in the study of Lemke et al [2]:

$$S(b) = S(0) \cdot [(1-f) \cdot e^{-b \cdot D} + f \cdot e^{-b \cdot (\mathrm{D} + \mathrm{D}*)}] \quad (1)$$

where b value is the user selectable parameter that controls the degree of sensitivity of DWI images to water diffusion and it is expressed in s/mm2. S(b) is the signal intensity

of the image of a homogenous system decays with b values, (D) the real diffusion, (D*) the micro-circulation of blood inside the capillary network and (f) the perfusion fraction. Thus this way, it is feasible to extract additional parameters and information from a single diffusion decay curve. This includes both the real diffusion, that means the tissue diffusion coefficient (D) and the micro-circulation of blood which is the flow-related pseudo diffusion inside the capillary network (D*).

D* and D color parametric maps were constructed on a pixel by pixel basis utilizing an in-house software (QMRI Utilities-X) on a separate workstation. These parametric maps (D and D*) were obtained by fitting with double exponential decay curves to the signal intensities of the corresponding pixel against b values.

The parametric maps (D and D*) were then transferred and evaluated with a commercially available software (nordicICE v4.0, NNL, Bergen, Norway). Subsequently, multiple Regions Of Interest (ROI)s were placed around the entire foot, on the dermis and muscles tissues in the pre- and post-procedure examination in patients with PAD and healthy volunteers and the change in the relative perfusion parameters was calculated.

Statistical analysis

Statistical analysis was performed with MedCalc (version Medcalc Software, Mariakerke, Belgium). Wilcoxon signed rank tests were used to compare D* before and after PTA. The relative change in ABI was also tested with Wilcoxon signed rank test. Mann-Whitney test was employed to compare D* between patients with PAD and healthy volunteers. Amputation-free survival was calculated using Kaplan–Meier method. Interobserver agreement was assessed using the interclass correlation coefficient (ICC). A p-value < 0.05 was considered as statistically significant.

Results

Procedural details – Clinical outcome

Patients with PAD presented occlusions or hemodynamically significant stenoses in common iliac artery (n=3), external iliac artery (n=4), superficial femoral artery (n=6), popliteal artery (n=4) and below the knee arteries (n=4). Many patients presented with multilevel arterial disease but only the targeted lesions for PTA were referred. Technical success was achieved in all patients included in final analysis (8/8), without major complications. Percutaneous vascular access was achieved by either an antegrade puncture (n=3) or retrograde puncture (n=5) of common femoral artery. PTA was performed in all patients and stent deployment using self- expanding nitinol stents (Luminexx, Bard), (Protege Everflex, Covidien) was performed in six patients. Moreover drug coated balloon (Lutonix, Bard) was used in one patient. After PTA, there was significant hemodynamic improvement in all patients and mean ABI increased from 0.35 ± 0.2 to 0.76 ± 0.25 after revascularization ($p<0.05$). After PTA, patients received single or dual antiplatelet therapy. The patients were followed-up with clinical examination and CDUS for a mean duration period of 28 months (range 6-48). During follow up one patient died due to acute myocardial infarction and two patients underwent minor (toe) amputations. The 12-month amputation-free survival rate, estimated by Kaplan-Meier analysis, was 87.5%.

Perfusion evaluation

After successful revascularization, there was significant increase of IVIM perfusion parameters (figure 1). D* increased from 279.88 ± 13.47 10^{-5} mm^2/s to 331.51 ± 31 10^{-5} mm^2/s, $p<0.05$. (Figure 2A). Moreover, healthy volunteers presented higher D* values in comparison with PAD patients. The mean D* was 279.88 ± 13.47 10^{-5} mm^2/s in PAD group and 332.47 ± 22.95 10^{-5} mm^2/s in healthy volunteers group, $p<0.05$. (figure 2B). The studies were also analyzed by a second observer and presented very good inter-observer reliability with an ICC > 0.85.

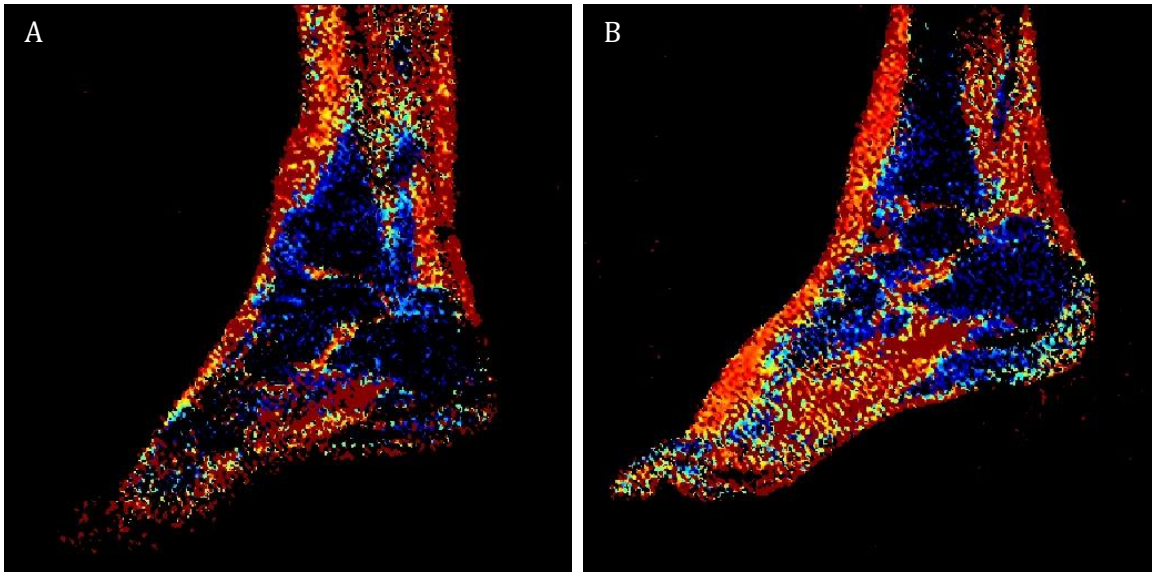

Fig.1: A 70 year-old male patient with CLI of right lower extremity. The patient underwent successful PTA and stent deployment in his right SFA. ABI increased from 0.53 to 0.9 after PTA.

Sagittal IVIM parametric map of flow-related pseudo diffusion inside the capillary network (D*) before (A) and after PTA (B) showed significant increase of D* after revascularization, especially in the peripheral dermal layer.

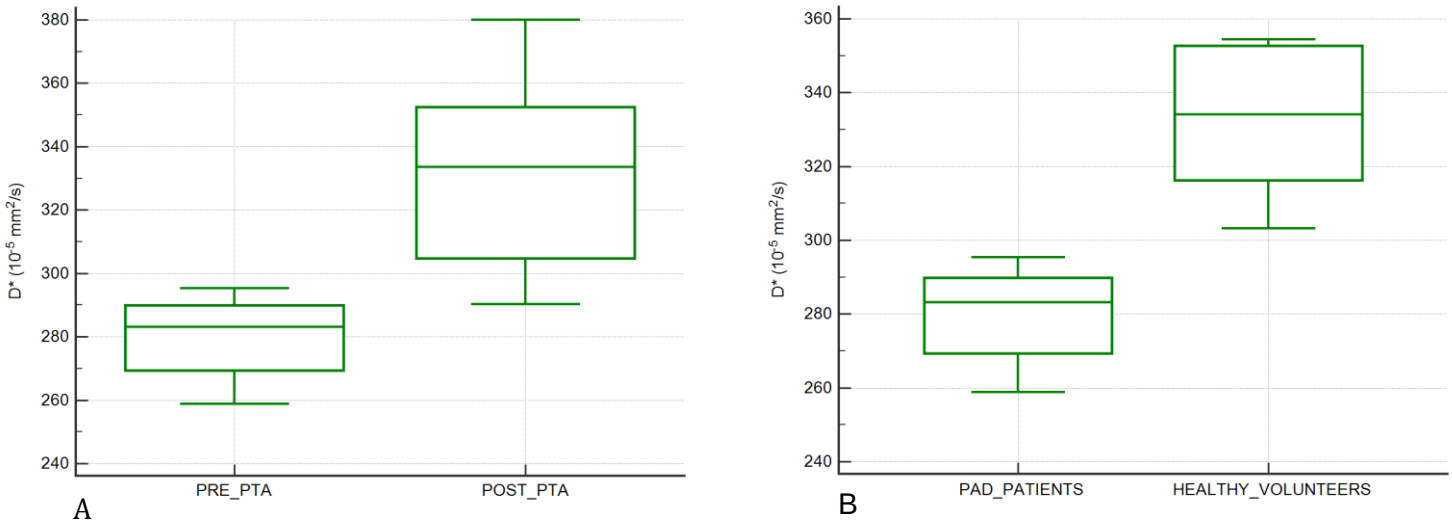

Fig.2: Box-and-whisker plots depicting the median values and the quartile ranges of the flow-related pseudo diffusion inside the capillary network (D*) in patients with PAD before and after PTA (A) and between PAD patients and healthy volunteers (B). The boxes stretch from the 25th percentile at the lower edge up to the 75th percentile at the upper edge. The median value is depicted as a line across the box. Outliers are depicted as lines at the outer area of the box plot.

References

[1] Le Bihan D, Breton E, Lallemand D, Grenier P, Cabanis E, Laval-Jeantet M. MR imaging of intravoxel incoherent motions: application to diffusion and perfusion in neurologic disorders. Radiology 1986;161(2):401-407.

[2] Lemke A, Laun FB, Simon D, Stieltjes B, Schad LR. An in vivo verification of the intravoxel incoherent motion effect in diffusion-weighted imaging of the abdomen. Magn Reson Med 2010;64(6):1580-1585.

Discussion

Imaging modalities such as color duplex ultrasound (CDUS), computed tomography angiography (CTA), magnetic resonance angiography (MRA) and digital subtraction angiography (DSA) provide significant information about the distribution of macrovascular lesions of the limbs (stenoses, occlusions) but not for the local microvascular perfusion of the feet [1]. These modalities are performed in clinical practice to assess the extent of disease, plan the revascularization strategy and finally confirm the patency of the main arteries after treatment [2]. However, they cannot measure blood flow to the limb and estimate the influence of collateral vessels on end-organ perfusion. These modalities are also incapable to estimate the therapeutic results of endovascular or surgical procedures, regarding the improvement in tissue perfusion [3-4].

An accurate measurement of tissue perfusion would be beneficial in patients with PAD both for the diagnosis of limb hypoperfusion and assessment of the severity and extension of disease but also would be helpful for the planning of revascularization strategy and estimation of the results of therapeutic interventions. Different modalities with advantages and disadvantages have been used for evaluation of limb tissue perfusion [5].

Laser Doppler flowmetry (LDF) and imaging (LDI) can measure superficial blood flow in the skin and therefore evaluate microvascular perfusion. LDF is performed using needle probes and enables measurement from a single point of contact. On the other hand, LDI provides a 2-dimensional array of perfusion measurement in a larger area using a scanning motion which can incorporate the entire foot. Moreover, there is no contact with the skin, which is useful in cases of open or infected wounds. These modalities can be used for evaluation of wounds and treatment response in PAD

patients. However, they are associated with low depth of penetration of laser light and measurements are affected by temperature, motion artifacts and consumption of vasoactive substances making comparison of different examinations difficult [6].
Reflection plethysmography allows noninvasive recording of arterial blood volume changes by detecting skin backscattered optical radiation. It can be performed as an alternative of continuous wave Doppler in patients with PAD and especially patients with underlying CKD and diabetes mellitus. However, it does not provide anatomic information and temperature, arteriovenous shunting and inadequate venous drainage may lead to false measurements [7].

Transcutaneous measurement of oxygen partial pressure ($TcPO_2$), as described in a previous section is a noninvasive method that allows assessment of local oxygen diffusion from the capillary bed through the skin epidermidis. It can be performed at the bedside of the patient and it is very useful for quantification of PAD, prediction of ulcer healing and determination of the optimum level for amputation. However, $TcPO_2$ measurements are affected by tissue edema, increased oxygen consumption, inflammation and vasoconstriction. Apart from that, it does not provide anatomic information and measurement electrode analyzes only a small area of skin [8].

Color Doppler Ultrasound (CDUS) is used in clinical practice for the evaluation of PAD patients as a first line imaging modality. Contrast-enhance Ultrasound (CEUS) using microbubble contrast agents can assess muscle tissue perfusion. It is performed with a linear US transducer probe which is placed in the area of interest. After contrast administration, a direct measure of contrast concentration is performed in a region of interest. Using time-CEUS-intensity curves, parameters such as time to peak, maximum contrast and area under time-signal intensity can be evaluated [5]. Amarteifio et al performed CEUS in patients with PAD and healthy volunteers. They demonstrated that

all parameters were different among study groups, thus this examination can be used for PAD diagnosis [9]. Another study also showed that perfusion imaging of lower limb muscles, using CEUS during exercise and measurement of absolute flow reserve can provide valuable information on the severity of PAD, especially in patients with DM [10]. CEUS can be also performed for evaluation of revascularization outcome in patients with PAD. Duerschmied et al, demonstrated that successful revascularization either with surgical or endovascular procedures was associated with significant improvement of perfusion parameters. The authors suggest that CEUS may be a valuable alternative to noninvasive tests such as ABI for estimation of therapeutic results after revascularization. However, like all US techniques, it is operator dependent and is limited by motion artifacts or presence of bones [11].

The technologic advancements in CT systems and the availability of dedicated CT perfusion software enable a wide range of clinical approaches but also give the opportunity for clinical and research investigations. CT is used in clinical practice for a wide range of applications but it can also provide qualitative and quantitative evaluation of tissue perfusion. In patients with acute stroke, neuroimaging has a critical role. The first line imaging technique is non-contrast CT which can differentiate ischemic and hemorrhagic strokes. However, the addition of CT angiography and perfusion imaging can improve the detection of an infract and can identify candidates for thrombolysis or endovascular treatment. MR perfusion and diffusion techniques can also be applied in patients with stroke but CT perfusion is associated with advantages as far as the cost, availability and patient monitoring [12-13]. CT perfusion is also useful for diagnosis and evaluation of the treatment response in patients with tumours. It has a significant role for both differential diagnosis between normal tissue and neoplastic tissue and primary tumor staging [14]. Luczynska et al, demonstrated the efficacy of CT perfusion to detect prostatic carcinoma and distinguish it from normal prostatic tissue [15]. Moreover, it

can be used for therapeutic assessment in multiple tumours and for prediction of response to therapy in head and neck, lung and rectal tumours [16]. It can also be applied in cardiovascular system. CT myocardial perfusion examination in companion with CT coronary angiography can be used for detection of hemodynamically significant coronary stenosis in patients with coronary artery disease [17]. Moreover, its role has been investigated in patients with abdominal aortic aneurysm (AAA) to evaluate the risk for AAA rupture [18] or patients with previous endovascular aneurysm repair (EVAR) for assessment of type II endoleak [19]. The use of this imaging technique in the study of PAD or CLI is not widespread because imaging methods such as CDUS, CTA or MRA are capable of depicting stenoses and/or occlusions of peripheral arteries and in conjunction with clinical examination are decisive in the evaluation of PAD and the selection of the appropriate treatment [1,2]

Dynamic CT perfusion can provide quantitative and qualitative information for hemodynamic perfusion status of the limb. Barfett et al, were the first who used an en bloc volumetric CT perfusion technique of entire foot to emerge the difference of mild and major vascular impairment in 22 healthy volunteers. They used calf blood pressure cuffs to simulate vascular obstruction and demonstrated significant differences of perfusion between unobstructed and obstructed foot [20]. Iezzi et al, evaluated perfusion parameters changes after endovascular treatment in 10 patients with PAD using a CT perfusion technique. They showed that CT perfusion examination is both feasible and reproducible and PTA can induce slight changes in perfusion parameters such as mean transit time (MTT) [21]. Hur et al, also deduced the ability of CT perfusion to measure blood flow of the foot in animals and humans. The authors showed that successful revascularization leads to significant increase of blood flow, especially in the dermal layer and the interpretations of perfusion maps correlated with angiographic findings [22]. A recent study compared CT perfusion parameters in patients with PAD

with either occlusion or high-grade stenosis and correlated them with angiographic and hemodynamic parameters such as ABI and ankle blood pressure. They denoted that perfusion parameters (BV, BF) were higher in patients with stenoses rather than occlusions and there was correlation between BV and ABI [23]. Finally, Cindil et al, also confirmed the role of CT perfusion to detect changes in foot perfusion after successful revascularization. Moreover, they suggested that CT perfusion parameters changes correlated well with clinical improvement after endovascular treatment [24].

Our study, using a CT foot perfusion examination (CTFP) demonstrates statistically significant change in perfusion parameters in patients with CLI after successful revascularization. Compared to other studies, all patients presented with CLI and all but one were allocated to Rutherford 5 or 6 category. As a result of the severe limb ischemia of the study-population, successful PTA may led to improvement in the macro- and microvascular state of the foot which subsequently affected perfusion parameters. In this study, there was no significant correlation between ABI and perfusion parameters increase. Perfusion parameters are influenced both from macrovascular and microvascular function of the foot in comparison with ABI, which reflects the macrovascular status of the limb. Moreover, the perfusion parameters changes were greater in the dermal layer in comparison with muscle tissues, which has been reported in only one study so far [22]. One of the most significant findings, of this study is the correlation between perfusion parameters and clinical outcome after PTA. The patients with significant clinical improvement who did not undergo an amputation presented higher post-PTA perfusion parameters values in comparison with patients with poor response, who finally underwent an amputation after PTA. Moreover, we performed ROC analysis and suggested cut-off values which predict poor response to revascularization and a possible amputation after PTA. As a result, CTFP may have a prognostic role in the evaluation of outcome in patients with CLI and the prediction of

amputation after PTA. These findings were also confirmed by a recent published study, which also evaluated perfusion parameters before and after PTA and compared them with clinical improvement of PAD patients after revascularization and found a significant correlation among them [24].

Radiation exposure should be investigated in the evaluation of the diagnostic value of a CT examination. The mean effective dose of CTFP was found herein to be minor (0.29 mSv), lower than a head CT examination and therefore, the diagnostic benefit of this examination may undoubtedly outweigh any theoretical radiogenic risk associated with the examination. On the other hand, efforts should be focused on further reduction of radiation exposure based on ALARA principle of radiation protection framework. Moreover, a small amount of iodinated non-ionic contrast medium was used in each examination. This should be to taken into consideration in patients with chronic kidney disease to minimize the of contrast–induced nephrotoxicity.

However, this study has also several limitations. CTFP was not feasible in cases of diffuse calcification or absolute occlusion of the lower limb arteries because of the disability to set an arterial ROI. Motion artifact is another significant reason for compromised image evaluation and false results. Five patients were excluded from this study due to above limitations either on the pre-procedural or the post-procedural examination. As this is a prospective study, it is not possible to foresee the outcome of the patients. Three patients were treated with surgical revascularization such as axillo-femoral bypass (n=2) and femoro-popliteal bypass (n=1). Finally, there was one case of a patient who died due to myocardial infarction before post-procedural examination. All these patients were excluded from the study. Another limitation is the absence of correlation between CTFP parameters and measurements from other modalities such as TcPO2, CEUS or MRI, which could be a promising area for future research.

MRI may also have a significant role in the evaluation of tissue perfusion in patients with PAD [5]. Non conventional imaging techniques such as MR diffusion weighted imaging (DWI) and MR perfusion weighted imaging (PWI) are well validated techniques for the diagnosis and the selection of appropriate therapeutic treatment for various diseases, especially as regards the study of brain parenchyma and myocardium. As far as brain imaging, MR perfusion can be used for evaluation of tissue at risk after stroke, for noninvasive histologic assessment of tumours, evaluation of neurodegenerative diseases and assessment of therapeutic results of drugs or surgical treatment in patients with brain tumours [25,26]. MR perfusion techniques are also used during cardiac imaging. They can detect abnormalities in myocardial blood flow which are associated with coronary artery disease [27]. Apart from diagnosis and prognosis of CAD, it can be performed in patients with cardiomyopathy or congenital heart diseases to detect adverse changes in microcirculation or microvascular dysfunction [28]. Moreover, this technique can be used in female pelvis for detection of cervical cancer (primary tumor or recurrence) and staging of endometrial cancers [29]. MR perfusion and diffusion techniques are also valuable tools in male patients with prostate cancer. They can detect and localize tumours, stage and grade these tumors, but also guide biopsies. Moreover, they are useful for treatment decision and therapy evaluation [30]. These techniques can be also used in myoskeletal system. DCE-MRI after intravenous Gadolinium administration enables perfusion measurement of skeletal muscles. It can be used to estimate the treatment response after chemotherapy in patients with skeletal muscle tumours [31]. A study by Soldatos et al, showed that DCE-MRI can increase sensitivity for determination of treatment response of neoadjuvant therapy in patients with soft-tissue sarcomas [32]. Finally, MR perfusion and diffusion techniques can differentiate benign from malignant tumors [33] and they can also evaluate inflammatory diseases such as Charcot foot or vascular abnormalities [31].

On the other hand, these techniques are rarely used in clinical practice for the evaluation of PAD because as it previously referred, imaging methods such as CDUS, CTA or MRA can highlight stenoses or occlusions of lower limb arteries and in companion with clinical examination are used for the diagnosis and the selection of treatment in patients with PAD [1,2]. However, there are efforts by a few researchers to investigate the role of MR perfusion and diffusion techniques for the evaluation of foot hypoperfusion and estimation of PTA outcomes in patients with PAD. Isbell et al, developed a DCE-MRI technique to measure skeletal muscle perfusion in patients with moderate PAD. According to their findings, peak-exercise measurement of limb perfusion with DCE-MRI can distinguish patients with moderate PAD from controls [34]. Another study of Thompson et al, measured the regional distribution of skeletal muscle blood flow during postischemic reactive hyperemia using DCE-MRI. They used an occlusive thigh cuff which delivers a step-input of contrast concentration (onset of reactive hyperemia), when it released and they found an increase in capillary permeability surface during reactive hyperemia [35]. Jiji et al, used also a DCE-MRI technique to evaluate calf muscle perfusion in patients with PAD and healthy volunteers. They confirmed the reproducibility of this technique but did not find any significant differences among these groups [36]. Moreover, Versluis et al, determined arterial flow reserve in patients with intermittent claudication using an MR phase-contrast technique. They demonstrated that this quantitative MR phase-contrast technique can discriminate patients with IC from controls [37].

Non Gd-based techniques for muscle perfusion, like arterial spin labeling (ASL) and blood oxygenation level-dependent (BOLD) allow quantification of the skeletal muscle blood flow in patients with PAD. Pollak et al, used an ASL technique in order to measure blood flow in healthy volunteers and patients with PAD. The study showed that ASL is a reproducible technique which can show statistically significant differences in peak

exercise calf perfusion between study groups [38]. Grözinger et al, evaluated muscle perfusion in 10 patients with PAD before and after PTA, using also an ASL technique and performed perfusion measurements during reactive hyperemia. They concluded that ASL-MRI can detect changes in perfusion parameters such as perfusion value, time-to-peak and duration of hyperemia after successful PTA [39]. A recent study by Edalati et al, also showed that ASL technique can be used to evaluate diabetic feet ulcers and distinguish ischemic regions from normal perfused muscle tissue regions [40]. Furthermore, Wu et al, performed this technique in patients with different stages of PAD and demonstrated that perfusion measurements correlate with the stage of disease, as it is expressed by ABI [41]. Blood oxygenation level-dependent (BOLD) technique can be also used for evaluation of tissue perfusion. Ledermann et al, compared calf muscle perfusion during postischemic reactive hyperemia, in patients with PAD and healthy volunteers using BOLD-MRI. They demonstrated that statistical significant differences in perfusion parameters were found between the two groups [42]. Similarly, Potthast et al, performed BOLD-MRI in patients with IC and volunteers without PAD and showed that PAD patients presented reduced T2* values compared to healthy volunteers [43]. Another study compared BOLD perfusion measurements with laser Doppler flowmetry and $TcPO_2$ in healthy volunteers during ischemia and reactive hyperemia, using a thigh cuff. The authors demonstrated that BOLD measurements present moderate to good correlation with LDF and $TcPO_2$ measurements [44]. Huegli et al, evaluated the results of PTA in patients with PAD using BOLD-MRI. The authors indicated that successful revascularization led to perfusion parameter's alterations, such as T2*max, time to peak and T2* end value [45]. A recent study also tried to determine quantitative changes in microvascular perfusion using IVIM. The study included 8 healthy volunteers who underwent MR IVIM perfusion examination at rest and after 15 min of running/walking. The authors revealed that microvascular blood flow increased significantly from rest to walking, so IVIM MRI can detect muscle tissue activation patterns [46]. Finally, Suo et al

integrated ASL, BOLD and IVIM MRI imaging in patients with PAD and healthy volunteers to investigate their role to diagnose and stage PAD. According to their findings, all the above mentioned methods provide information about tissue perfusion but BOLD MRI was the most sensitive method to located differences between study groups [47].

This is the first time, a DCE-MRI technique was used to evaluate PTA outcome in patients with CLI. Our findings show that a statistically significant change in perfusion parameters is found after successful PTA in CLI patients. Compared to other studies (using both Gd-based and non Gd-based techniques) all patients in this study presented with CLI (Rutherford 4 to 6 category). We suppose that successful revascularization led to significant improvement in the macro- and microvascular status of the foot which improves perfusion parameters. We also noticed that there was no significant correlation between ABI and perfusion parameters, as these parameters are influenced not only by the macrovascular network of the foot (such as ABI) but also from the microvascular status of the limb.

However, DCE-MRI was not feasible in cases with severe motion artifact which compromised image evaluation. Moreover, as this was a prospective study, it was not possible to foresee the outcome of the patients. Three patients did not undergo successful endovascular recanalization and they were treated by surgical revascularization. Moreover, one patient died before post-procedural examination and one patient underwent amputation due to extensive ulcers before post-procedural examination too. These patients (n=6) were excluded from the study. Furthermore, the post-procedural examinations were performed 1 month after PTA, so they did not describe the long-term changes in foot perfusion after PTA.

As far as non Gd-based techniques for evaluation of foot hypoperfusion, our research examined the possible correlation between perfusion parameters which are derived from DCE-MRI and DWI. Gadolinium-based contrast agents improve the diagnostic capabilities of MRI but are associated with adverse effects. The most serious of these complications is nephrogenic systemic fibrosis which is caused by Gd-based contrast administration in patients with CKD or impaired kidney function [48]. Our study showed that IVIM parameters correlate with DCE-MRI perfusion parameters after application of Gaussian filtering. Moreover, the study showed that the best DWI fitting method was the direct estimation of IVIM parameters and the most accurate perfusion model was the Patlak's model.

Based on the above mentioned results, we also compare IVIM perfusion parameters between patients with PAD and healthy volunteers and between patients with PAD before and after PTA. Flow-related pseudo diffusion inside the capillary network (D*) was significantly increased after PTA and there was also a statistically significant difference of D* between patients with PAD and healthy volunteers. Therefore, IVIM can be also used for evaluation of foot hypoperfusion and discrimination between healthy individuals and patients with PAD. Moreover, it can be used for estimation of PTA outcome in PAD patients. This examination is additionally safe for patients, as it does not require Gadolinium contrast administration.

The information of CT and MR perfusion examinations may be also helpful for selection and planning of revascularization strategy. As it is referred in a previous section, after the introduction of angiosome theory by Taylor and Palme [49], a great debate on targeting the procedures based on angiosomes has been started. Many vascular surgeons and interventional radiologists suggest direct revascularization, as it is associated with improved would healing and increased limb salvage in several studies

[50-51]. On the other hand, several studies did not show any significant benefit of direct revascularization. CT and MR perfusion examinations may aid in quantifying and evaluating the angioplasty target area. The parametric perfusion maps can show the differences of the perfusion parameters in the affected angiosome after PTA which could be extensively useful to compare different endovascular therapeutic approaches (direct vs. indirect revascularization). Therefore, this information may be extremely helpful during endovascular revascularization planning.

Conclusion

In conclusion, CT, DCE-MRI and DW-MRI are reliable and reproducible techniques which can be useful tools for evaluation of lower limb hypoperfusion and estimation of PTA outcome in patients with CLI. The information provided by these examinations may aid reliable prediction of poor response to revascularization or an imminent amputation in patients with CLI. Moreover, they could be promising tools for monitoring of endovascular or surgical treatment and planning of revascularization strategy. Further research efforts, including not only CT and MR perfusion techniques but also CEUS, DSA perfusion techniques and nuclear spectroscopy techniques, should be invested into this clinically important field in order to identify the most reliable study regarding the microvascular state of the foot. They could provide important information to the physicians as far as the evaluation of foot hypoperfusion and monitoring of revascularization treatment.

References

[1] Conte MS, Bradbury AW, Kolh P, et al. Global vascular guidelines on the management of chronic limb-threatening ischemia. J Vasc Surg 2019;69(6S):3S-125S.e40.

[2] Aboyans V, Ricco JB, Bartelink MEL, et al. 2017 ESC Guidelines on the Diagnosis and Treatment of Peripheral Arterial Diseases, in collaboration with the European Society for Vascular Surgery (ESVS): Document covering atherosclerotic disease of extracranial carotid and vertebral, mesenteric, renal, upper and lower extremity arteries. Endorsed by: the European Stroke Organization (ESO)The Task Force for the Diagnosis and Treatment of Peripheral Arterial Diseases of the European Society of Cardiology (ESC) and of the European Society for Vascular Surgery (ESVS). Eur Heart J 2018;39(9):763-816.

[3] Dhanoa D, Baerlocher MO, Benko AJ, et al. Position Statement on Noninvasive Imaging of Peripheral Arterial Disease by the Society of Interventional Radiology and the Canadian Interventional Radiology Association. J Vasc Interv Radiol 2016;27(7):947-951.

[4] Pollak AW, Norton PT, Kramer CM. Multimodality imaging of lower extremity peripheral arterial disease: current role and future directions. Circ Cardiovasc Imaging 2012;5(6):797-807.

[5] Bajwa A, Wesolowski R, Patel A, et al. Assessment of tissue perfusion in the lower limb: current methods and techniques under development. Circ Cardiovasc Imaging 2014;7(5):836-843.

[6] Khan F, Newton DJ. Laser Doppler imaging in the investigation of lower limb wounds. Int J Low Extrem Wounds 2003;2(2):74-86.

[7] Khandanpour N, Armon MP, Jennings B, Clark A, Meyer FJ. Photoplethysmography, an easy and accurate method for measuring ankle brachial pressure index: can photoplethysmography replace Doppler?. Vasc Endovascular Surg 2009;43(6):578-582.

[8] Arsenault KA, McDonald J, Devereaux PJ, Thorlund K, Tittley JG, Whitlock RP. The use of transcutaneous oximetry to predict complications of chronic wound healing: a systematic review and meta-analysis. Wound Repair Regen 2011;19(6):657-663.

[9] Amarteifio E, Wormsbecher S, Krix M, et al. Dynamic contrast-enhanced ultrasound and transient arterial occlusion for quantification of arterial perfusion reserve in peripheral arterial disease. Eur J Radiol 2012;81(11):3332-3338.

[10] Lindner JR, Womack L, Barrett EJ, et al. Limb stress-rest perfusion imaging with contrast ultrasound for the assessment of peripheral arterial disease severity. JACC Cardiovasc Imaging 2008;1(3):343-350.

[11] Duerschmied D, Maletzki P, Freund G, Olschewski M, Bode C, Hehrlein C. Success of arterial revascularization determined by contrast ultrasound muscle perfusion imaging. J Vasc Surg 2010;52(6):1531-1536.

[12] Lui YW, Tang ER, Allmendinger AM, Spektor V. Evaluation of CT perfusion in the setting of cerebral ischemia: patterns and pitfalls. AJNR Am J Neuroradiol 2010;31(9):1552-1563.

[13] Konstas AA, Wintermark M, Lev MH. CT perfusion imaging in acute stroke. Neuroimaging Clin N Am 2011;21(2):215-ix.

[14] Petralia G, Bonello L, Viotti S, Preda L, d'Andrea G, Bellomi M. CT perfusion in oncology: how to do it. Cancer Imaging 2010;10(1):8-19.

[15] Luczynska E, Blecharz P, Dyczek S, et al. Perfusion CT is a valuable diagnostic method for prostate cancer: a prospective study of 94 patients. Ecancermedicalscience. 2014;8:476

[16] Kambadakone AR, Sahani DV. Body perfusion CT: technique, clinical applications, and advances. Radiol Clin North Am 2009;47(1):161-178.

[17] Yang DH, Kim YH. CT myocardial perfusion imaging: current status and future perspectives. Int J Cardiovasc Imaging 2017;33(7):1009-1020.

[18] Kontopodis N, Galanakis N, Tsetis D, Ioannou CV. Perfusion computed tomography imaging of abdominal aortic aneurysms may be of value for patient specific rupture risk estimation. Med Hypotheses 2017;101:6-10.

[19] Charalambous S, Kontopodis N, Perisinakis K, et al. Dynamic CT perfusion imaging for type 2 endoleak assessment after endograft placement. Med Hypotheses 2020;139:109701.

[20] Barfett J, Velauthapillai N, Kloeters C, Mikulis DJ, Jaskolka JD. An en bloc approach to CT perfusion for the evaluation of limb ischemia. Int J Cardiovasc Imaging 2012;28(8):2073-2083.

[21] Iezzi R, Santoro M, Dattesi R, et al. Foot CT perfusion in patients with peripheral arterial occlusive disease (PAOD): a feasibility study. Eur J Radiol 2013;82(9):e455-e464.

[22] Hur S, Jae HJ, Jang Y, et al. Quantitative Assessment of Foot Blood Flow by Using Dynamic Volume Perfusion CT Technique: A Feasibility Study. Radiology 2016;279(1):195-206.

[23] Sah BR, Veit-Haibach P, Strobel K, Banyai M, Huellner MW. CT-perfusion in peripheral arterial disease - Correlation with angiographic and hemodynamic parameters. PLoS One 2019;14(9):e0223066.

[24] Cindil E, Erbas G, Akkan K, et al. Dynamic Volume Perfusion CT of the Foot in Critical Limb Ischemia: Response to Percutaneous Revascularization. AJR Am J Roentgenol 2020;214(6):1398-1408.

[25] Petrella JR, Provenzale JM. MR perfusion imaging of the brain: techniques and applications. AJR Am J Roentgenol 2000175(1):207-219.

[26] Vilela P, Rowley HA. Brain ischemia: CT and MRI techniques in acute ischemic stroke. Eur J Radiol 2017;96:162-172.

[27] Klassen C, Nguyen M, Siuciak A, Wilke NM. Magnetic resonance first pass perfusion imaging for detecting coronary artery disease. Eur J Radiol 2006;57(3):412-416.

[28] Coelho-Filho OR, Rickers C, Kwong RY, Jerosch-Herold M. MR myocardial perfusion imaging. Radiology 2013;266(3):701-715.

[29] Thomassin-Naggara I, Siles P, Balvay D, Cuenod CA, Carette MF, Bazot M. MR perfusion for pelvic female imaging. Diagn Interv Imaging 2013;94(12):1291-1298.

[30] Somford DM, Fütterer JJ, Hambrock T, Barentsz JO. Diffusion and perfusion MR imaging of the prostate. Magn Reson Imaging Clin N Am 2008;16(4):685-ix.

[31] Sujlana P, Skrok J, Fayad LM. Review of dynamic contrast-enhanced MRI: Technical aspects and applications in the musculoskeletal system. J Magn Reson Imaging 2018;47(4):875-890.

[32] Soldatos T, Ahlawat S, Montgomery E, Chalian M, Jacobs MA, Fayad LM. Multiparametric Assessment of Treatment Response in High-Grade Soft-Tissue Sarcomas with Anatomic and Functional MR Imaging Sequences. Radiology 2016;278(3):831-840.

[33] Tuncbilek N, Karakas HM, Okten OO. Dynamic contrast enhanced MRI in the differential diagnosis of soft tissue tumors. Eur J Radiol 2005;53(3):500-505.

[34] Isbell DC, Epstein FH, Zhong X, et al. Calf muscle perfusion at peak exercise in peripheral arterial disease: measurement by first-pass contrast-enhanced magnetic resonance imaging. J Magn Reson Imaging 2007;25(5):1013-1020.

[35] Thompson RB, Aviles RJ, Faranesh AZ, et al. Measurement of skeletal muscle perfusion during postischemic reactive hyperemia using contrast-enhanced MRI with a step-input function. Magn Reson Med 2005;54(2):289-298.

[36] Jiji RS, Pollak AW, Epstein FH, et al. Reproducibility of rest and exercise stress contrast-enhanced calf perfusion magnetic resonance imaging in peripheral arterial disease. J Cardiovasc Magn Reson 2013;15(1):14.

[37] Versluis B, Dremmen MH, Nelemans PJ, et al. MRI of arterial flow reserve in patients with intermittent claudication: feasibility and initial experience. PLoS One 2012;7(3):e31514.

[38] Pollak AW, Meyer CH, Epstein FH, et al. Arterial spin labeling MR imaging reproducibly measures peak-exercise calf muscle perfusion: a study in patients with peripheral arterial disease and healthy volunteers. JACC Cardiovasc Imaging 2012;5(12):1224-1230.

[39] Grözinger G, Pohmann R, Schick F, et al. Perfusion measurements of the calf in patients with peripheral arterial occlusive disease before and after percutaneous transluminal angioplasty using MR arterial spin labeling. J Magn Reson Imaging 2014;40(4):980-987.

[40] Edalati M, Hastings MK, Muccigrosso D, et al. Intravenous contrast-free standardized exercise perfusion imaging in diabetic feet with ulcers. J Magn Reson Imaging 2019;50(2):474-480.

[41] Wu WC, Mohler E 3rd, Ratcliffe SJ, Wehrli FW, Detre JA, Floyd TF. Skeletal muscle microvascular flow in progressive peripheral artery disease: assessment with continuous arterial spin-labeling perfusion magnetic resonance imaging. J Am Coll Cardiol 2009;53(25):2372-2377.

[42] Ledermann HP, Schulte AC, Heidecker HG, et al. Blood oxygenation level-dependent magnetic resonance imaging of the skeletal muscle in patients with peripheral arterial occlusive disease. Circulation 2006;113(25):2929-2935.

[43] Potthast S, Schulte A, Kos S, Aschwanden M, Bilecen D. Blood oxygenation level-dependent MRI of the skeletal muscle during ischemia in patients with peripheral arterial occlusive disease. Rofo 2009;181(12):1157-1161.

[44] Ledermann HP, Heidecker HG, Schulte AC, et al. Calf muscles imaged at BOLD MR: correlation with TcPO2 and flowmetry measurements during ischemia and reactive hyperemia--initial experience. Radiology 2006;241(2):477-484.

[45] Huegli RW, Schulte AC, Aschwanden M, et al. Effects of percutaneous transluminal angioplasty on muscle BOLD-MRI in patients with peripheral arterial occlusive disease: preliminary results. Eur Radiol 2009;19(2):509-515.

[46] Jungmann PM, Pfirrmann C, Federau C. Characterization of lower limb muscle activation patterns during walking and running with Intravoxel Incoherent Motion (IVIM) MR perfusion imaging. Magn Reson Imaging 2019;63:12-20.

[47] Suo S, Zhang L, Tang H, et al. Evaluation of skeletal muscle microvascular perfusion of lower extremities by cardiovascular magnetic resonance arterial spin labeling, blood oxygenation level-dependent, and intravoxel incoherent motion techniques. J Cardiovasc Magn Reson 2018;20(1):18.

[48] Rudnick MR, Wahba IM, Leonberg-Yoo AK, Miskulin D, Litt HI. Risks and Options With Gadolinium-Based Contrast Agents in Patients With CKD: A Review. Am J Kidney Dis 2020;S0272-6386(20)30926-4.

[49] Taylor GI, Palmer JH. The vascular territories (angiosomes) of the body: experimental study and clinical applications. Br J Plast Surg 1987;40(2):113-141.

[50] Alexandrescu VA, Hubermont G, Philips Y, et al. Selective primary angioplasty following an angiosome model of reperfusion in the treatment of Wagner 1-4 diabetic foot lesions: practice in a multidisciplinary diabetic limb service. Journal of Endovascular Therapy 2008 Oct;15(5):580-593.

[51] Jongsma H, Bekken JA, Akkersdijk GP, Hoeks SE, Verhagen HJ, Fioole B. Angiosome-directed revascularization in patients with critical limb ischemia. J Vasc Surg 2017;65(4):1208-1219.

Oral and poster presentations related to PhD thesis

Poster, **Dynamic contrast-enhanced magnetic resonance imaging for evaluation of percutaneous transluminal angioplasty outcome in patients with critical limb ischemia**

Nikolaos Galanakis, Thomas G Maris, Nikolaos Kontopodis, Konstantinos Tsetis, Christos Ioannou, Apostolos Karantanas, Dimitrios Tsetis

Cardiovascular and Interventional Radiological Society of Europe's Congress, CIRSE 2020, Online congress 2020

Poster, **The role of dynamic contrast-enhanced MRI in the evaluation of percutaneous transluminal angioplasty outcome in patients with critical limb ischemia**

Nikolaos Galanakis, Thomas G Maris, Nikolaos Kontopodis, Christos Ioannou, Apostolos Karantanas, Dimitrios Tsetis

European Congress of Radiology (ECR) 2020, Vienna (online), 2020

Oral presentation, **Evaluation of PTA outcome in patients with critical limb ischemia using dynamic contrast-enhanced MRI (DCE-MRI)**

Nikolaos Galanakis, Thomas G Maris, Nikolaos Kontopodis, Nikolas Matthaiou, Christos Ioannou, Apostolos Karantanas, Dimitrios Tsetis

XVII Balkan Congress of Radiology, Heraklion, 2019

Oral presentation, **Dynamic contrast-enhanced MRI for evaluation of PTA outcome in patients with critical limb ischemia**

Nikolaos Galanakis, Thomas G Maris, Nikolaos Kontopodis, Christos Ioannou, Apostolos Karantanas, Dimitrios Tsetis

Leading Innovative Vascular Education (LIVE) 2019, Larissa, 2019

Oral presentation, **CT foot perfusion examination for evaluation of PTA outcome in patients with Critical Limb Ischemia**

Galanakis N, Maris TG, Kontopodis N, Kehagias E, Ioannou CV, Kosidekakis N, Perisinakis K, Matthaiou N, Tsetis D

XVI Balkan Congress of Radiology, Kusadasi Turkey, 2018

Poster, **Dynamic contrast-enhanced magnetic resonance imaging for evaluation of percutaneous transluminal angioplasty outcome in patients with critical limb ischemia: Preliminary results**

TG Maris, N Galanakis, N Kontopodis, C Ioannou, A Karantanas, D Tsetis

European Congress of Medical Physics 2018, Copenhagen, 2018

Oral presentation, **Evaluation of percutaneous transluminal angioplasty outcome in patients with Critical Limb Ischemia, using Volumetric CT perfusion technique: A feasibility study**

Galanakis N, Maris TG, Kontopodis N, Kehagias E, Ioannou CV, Matthaiou N, Kosidekakis N, Perisinakis K, Karantanas A, Tsetis DK

Leading Innovative Vascular Education (LIVE) 2018, Patra, 2018

Poster, **Volumetric CT perfusion technique for assessment of PTA outcome in patients with Critical Limb Ischemia: A feasibility study**

Galanakis N, Maris TG, Kontopodis N, Kehagias E, Ioannou CV, Kosidekakis N, Perisinakis K, Karantanas A, Tsetis DK

European Congress of Radiology (ECR) 2018, Vienna, 2018

Oral presentation, **Evaluation of PTA outcome in patients with Critical Limb Ischemia, using Volumetric CT perfusion technique: Preliminary results**

Galanakis N, Maris TG, Kontopodis N, Kehagias E, Ioannou CV, Hatzidakis A, Perisinakis K, Karantanas A, Tsetis DK

Cardiovascular and Interventional Radiological Society of Europe's Congress, CIRSE 2017, Copenhagen, 2017

Ομιλία σε στρογγυλή τράπεζα (ερευνητικό βήμα).

Τίτλος ομιλίας: Εκτίμηση αποτελεσμάτων Διαδερμικής Αγγειοπλαστικής σε Περιφερική Αρτηριακή Νόσο με σύγχρονες τεχνικές Ιατρικής Απεικόνισης

1ο κλινικό φροντιστήριο Ακτινολογίας Μυοσκελετικού, Ηράκλειο 2016

CLINICAL STUDY

CT Foot Perfusion Examination for Evaluation of Percutaneous Transluminal Angioplasty Outcome in Patients with Critical Limb Ischemia: A Feasibility Study

Nikolaos Galanakis, MD, Thomas G. Maris, MSc, PhD, Nikolaos Kontopodis, MD, PhD, Christos V. Ioannou, MD, PhD, Elias Kehagias, MD, EBIR, Nikolas Matthaiou, MD, Antonios E. Papadakis, PhD, Adam Hatzidakis, MD, PhD, Konstantinos Perisinakis, PhD, and Dimitrios Tsetis, MD, PhD, EBIR

ABSTRACT

Purpose: To evaluate foot perfusion in patients with critical limb ischemia (CLI) using quantitative perfusion multi–detector-row CT and estimate perfusion parameter changes before and after percutaneous transluminal angioplasty (PTA).

Materials and Methods: This prospective study investigated 13 patients (10 men; median age, 72 y; range, 51–84 y) with CLI who underwent CT foot perfusion examinations with a 128-slice dual-energy CT scanner 1 day before and 1 week after PTA. Key parameters such as permeability surface (PS), blood volume (BV), and blood flow (BF) were analyzed and compared statistically. The studies were also examined by a second observer to determine interobserver reproducibility.

Results: Revascularization was technically successful in all patients, and mean ankle–brachial index increased from 0.36 ± 0.16 to 0.75 ± 0.22. After revascularization, mean BV increased from 1.55 mL/100 g ± 0.83 to 4.51 mL/100 g ± 1.53, BF increased from 16.28 mL/100 g/min ± 4.97 to 31.49 mL/100 g/min ± 6.86, and PS increased from 3.1 mL/min/100 g ± 1.95 to 8.67 mL/min/100 g ± 3.85 ($P < .05$). Patients with poor response to revascularization who finally underwent amputation presented lower post-PTA perfusion parameters values than patients with significant clinical improvement ($P < .05$). All measurements demonstrated very good interobserver reproducibility, and intraclass correlation coefficients were 0.91 for BV, 0.94 for BF, and 0.95 for PS. The mean effective dose of the examination was estimated at 0.29 mSv.

Conclusions: CT foot perfusion is a reproducible technique that may be a useful modality for the estimation of PTA outcome. Significant restitution of perfusion parameters was observed after successful revascularization.

ABBREVIATIONS

ABI = ankle–brachial index, BF = blood flow, BV = blood volume, CI = confidence interval, CLI = critical limb ischemia, DSA = digital subtraction angiography, PAD = peripheral arterial disease, PS = permeability surface, PTA = percutaneous transluminal angioplasty, ROC = receiver operating characteristic, ROI = region of interest, TASC = Trans-Atlantic Inter-Society Consensus Document on Management of Peripheral Arterial Disease, $TcPO_2$ = transcutaneous oxygen partial pressure

From the Interventional Radiology Unit and Department of Medical Imaging (N.G., E.K., N.M., A.H., D.T.), Department of Medical Physics (T.G.M., A.E.P., K.P.), and Vascular Surgery Unit and Department of Cardiothoracic and Vascular Surgery (N.K., C.V.I.), University Hospital Heraklion, University of Crete Medical School, Voutes, 71110 Heraklion, Greece. Received July 17, 2018; final revision received October 16, 2018; accepted October 17, 2018. **Address correspondence to** D.T.; E-mail: tsetisd@uoc.gr

None of the authors have identified a conflict of interest.

J Vasc Interv Radiol 2019; 30:560–568

https://doi.org/10.1016/j.jvir.2018.10.018

Evaluation of peripheral arterial disease (PAD) includes clinical history, physical examination, and measurement of ankle–brachial index (ABI), segmental pressures, pulse volume recordings, and exercise testing (1–3). There are also noninvasive tests to evaluate the severity of PAD such as venous occlusion plethysmography, transcutaneous oxygen partial pressure ($TcPO_2$) measurement, and contrast-enhanced ultrasound (US). $TcPO_2$ measurement can assess local oxygen diffusion from the capillary bed through the skin epidermis, which reflects the microvascular status in the skin. It is very useful for quantification of PAD, prediction

of ulcer healing, and determination of the optimum level for amputation, but measurements are affected by tissue edema, inflammation, and vasoconstriction. Apart from that, this examination is not an imaging modality, and it is associated with a lack of anatomic information (4). Contrast-enhanced US with the use of microbubble agents can be used to estimate muscle perfusion, but it is an operator-dependent examination and is sometimes associated with artifacts created by patient movement (5).

Radiologic modalities such as color duplex ultrasound (US), computed tomographic (CT) angiography, magnetic resonance (MR) angiography, and digital subtraction angiography (DSA) (1,6) provide significant information about the distribution of macrovascular lesions of the limbs (eg, stenoses, occlusions) but not for the local microvascular perfusion of the feet. These modalities are used in clinical practice to assess the extent of disease, plan the revascularization strategy, and finally confirm the patency of the main arteries after treatment. However, they cannot measure blood flow (BF) to the limb or estimate the influence of collateral vessels on end-organ perfusion. These modalities are also incapable of estimating the response to therapeutic interventions that improve tissue perfusion. CT perfusion calculates the changes in tissue density after intravenous injection of contrast medium and allows functional evaluation of tissue vascularity. However, there are few studies on the role of CT perfusion in PAD (7–9). The purpose of the present study is to evaluate foot hypoperfusion in patients with critical limb ischemia (CLI) with the use of quantitative CT foot perfusion examination and estimate changes in perfusion parameters before and after successful percutaneous transluminal angioplasty (PTA).

MATERIALS AND METHODS

Study Design

The present prospective single-center study was performed to examine the role of CT foot perfusion in the evaluation of baseline and posttreatment foot perfusion in patients with PAD. The study was conducted according to the principles of the Declaration of Helsinki and in accord with the applicable national guidelines, regulations, and acts. The study was approved by the local ethical committee, and all individual participants provided signed informed consent before examination.

To be included in the study, patients had to present with CLI (rest pain or minor/major tissue loss; ie, Rutherford categories 4–6). Additionally, the anatomic distribution of atherosclerotic lesions and the patient's comorbidities and overall clinical status were required to make them suitable for endovascular revascularization. Patients had to be able to understand the purpose of the study, comply with the follow-up protocol, and provide informed consent. Initially, patients underwent diagnostic CT angiography to determine anatomic distribution of arterial disease; the treatment plan was then decided in a multidisciplinary manner according to standard institutional protocols and common practice.

Patients who presented with less advanced PAD not classified as CLI were excluded. Similarly, patients who underwent surgical revascularization, were treated with a conservative approach, or underwent a primary amputation were also excluded. Patients presenting with acute limb ischemia (duration of symptoms < 2 wk per Trans-Atlantic Inter-Society Consensus Document on Management of Peripheral Arterial Disease [TASC] II definition) were excluded because their condition was not considered to comply with the aim of the study. Allergy to iodinated contrast medium, moderate or severe renal impairment (glomerular filtration rate < 45 mL/min), congestive heart failure, and severe cardiac rhythm anomalies were also considered as exclusion criteria.

Patients who fulfilled the aforementioned criteria were subjected to CT foot perfusion measurement in the affected foot. Subsequently, the endovascular procedure was carried out, and technical success was defined as a residual stenosis less than 30% without flow-limiting dissection in the target lesion. Enrolled patients underwent a second CT foot perfusion examination within the first week after treatment. All patients were followed up with clinical examination at 1, 3, 6, and 12 months and color Doppler US combined with clinical examination on an annual basis.

Clinical evaluation and measurement of ABI was performed by vascular surgeons before PTA, after PTA, and during follow-up. Analysis and evaluation of CT foot perfusion was performed by 2 blinded radiologists, a resident in radiology with 4 years' experience in CT and a senior professor of radiology and interventional radiology with 29 years' experience in vascular imaging.

Study Population

Between April 2016 and May 2017, 22 selected patients enrolled in the study. Technical success was achieved in 19 patients, and the other 3 were excluded from subsequent analysis. These patients presented with multilevel occlusive disease (TASC class D) with extensively calcified vessels and were initially judged to be at high risk for surgical revascularization. Subsequently, after failed endovascular intervention and following extensive discussion of the procedural risks, these patients underwent successful surgical revascularization (2 axillofemoral and 1 femoropopliteal bypass). One patient who underwent successful PTA died before post-PTA CT foot perfusion evaluation. In total, 13 subjects (10 men, 3 women) were included in the analysis, as CT foot perfusion evaluation was not feasible in 5 examinations. The median age was 72 years (range, 51–84 y). According to Rutherford classification of PAD, 1 patient was allocated to class 4, 8 to class 5, and 4 to class 6. Patients' main risk factors were hypertension ($n = 10$), hyperlipidemia ($n = 9$), diabetes mellitus ($n = 9$), smoking ($n = 11$), coronary artery disease ($n = 4$), and previous endovascular or surgical procedure ($n = 4$). The study population's baseline characteristics are summarized in **Table 1**.

Table 1. Clinical Data of Study Population

Pt. No./Sex/Age (y)	Risk Factors	Lesion Location*	Rutherford Classification		ABI	
			Before PTA	6 mo after PTA	Before PTA	After PTA
1/M/64	HT, DM, hyperlipidemia, smoking, CAD	(L) SFA, POPA	6	2	0.4	1
2/M/75	HT, smoking	(L) CIA, EIA	4	2	0.27	0.5
3/M/72	DM, hyperlipidemia, CAD	(R) EIA, SFA	5	5	0.4	0.6
4/M/84	HT, DM, hyperlipidemia, smoking	(R) SFA, POPA	5	2	0.7	0.9
5/F/62	HT, smoking	(R) EIA	5	1	0.2	0.5
6/M/83	DM, hyperlipidemia, smoking, CAD	(R) SFA	6	3	0.35	0.55
7/F/51	Smoking	(L) CIA, POPA	5	1	0.3	1
8/M/60	HT, DM, hyperlipidemia, smoking	(R) SFA, POPA	5	2	0.3	0.9
9/F/78	HT, DM, hyperlipidemia, smoking	(R) CIA, EIA, SFA, POPA	5	2	0.1	1.1
10/M/80	HT, DM, hyperlipidemia, CAD	(R) SFA, POPA	5	3	0.27	0.75
11/M/55	HT, DM, hyperlipidemia, smoking	(L) CIA, EIA	6	5	0.5	0.6
12/M/57	HT, smoking	(L) CIA, EIA	5	5	0.58	0.66
13/M/74	HT, DM, hyperlipidemia, smoking	(R) SFA, POPA, TPT	6	3	0.3	0.7

ABI = ankle brachial index; CAD = coronary artery disease; CIA = common iliac artery; DM = diabetes mellitus; EIA = external iliac artery; HT = hypertension; POPA = popliteal artery; SFA = superficial femoral artery; TPT = tibioperoneal trunk.
*Laterality indicated in parentheses: L = left; R = right.

Imaging Protocol

All studies were performed on a 128-slice CT scanner (Revolution GSI; GE Healthcare, Chicago, Illinois) at room temperature. Patients were examined in the supine position, and the angiography scan was obtained in the craniocaudal direction. The positions of both feet were stabilized with adhesive tape during the examination. CT angiography was performed with a standard protocol from the diaphragm to the feet after injection of 110 mL of iodinated nonionic contrast medium (Ultravist 370, iodine at 370 mg/mL; Bayer Schering, Leverkusen, Germany) followed by 50 mL of saline solution at a flow rate of 4 mL/s.

Patients also underwent foot perfusion examinations before and within the first week after endovascular treatment. The acquisition scanning length was 14 cm, enabling imaging of the entire foot and ankle. A shuttle mode technique was employed with the following parameters: 0.625-mm × 64-mm collimation (coverage, 40 mm); 0.4-second gantry rotation time; pitch, 1.375; 1.25-mm reconstruction interval thickness; number of passes, 28; time per pass, 1.7 s; 80-kVp tube voltage; reference tube current, 220 mA; and total acquisition time, 47.7 seconds. Images were obtained after injection of 40 mL of iodinated nonionic contrast medium followed by 30 mL of saline solution at a flow rate of 4 mL/s. Scan delay was individualized for each patient by using the manufacturer's proprietary bolus-tracking software (SmartPrep; GE Healthcare) to capture 100 HU in the ascending thoracic aorta to assess the arrival of contrast medium in the examined area.

The dose–length product of each CT perfusion examination was recorded. The mean dose–length product was used to estimate the mean effective dose by using a conversion coefficient of 0.0002 $mSv \cdot mGy^{-1} \cdot cm^{-1}$ as previously proposed (10). All images were transferred to a dedicated workstation for further analysis.

Image Analysis

CT perfusion images were transferred to a dedicated workstation (AW server 3.2; GE Medical Systems, Chicago, Illinois) and analyzed by using commercial CT software (CT-Perfusion-4D; GE Medical Systems). CT-Perfusion-4D uses 2 computational algorithms: deconvolution and standard algorithm. CT perfusion maps of various hemodynamic parameters such as blood volume (BV), BF, and permeability surface (PS) were created (Fig 1) via a deconvolution algorithm based on the convolution model. Deconvolution analysis uses arterial and tissue time–concentration curves to compute impulse residue function for the tissue. The advantage of this algorithm is that it corrects time delay in contrast kinetics, taking into account the actual injection rate of contrast medium, and offers a more accurate estimation of impulse residue function. In the present study, the time–attenuation curve of the input artery was obtained by placing a region of interest (ROI) on the posterior tibial artery of the affected limb. If this artery was occluded or highly calcified, the ROI was placed in the anterior tibial artery or peroneal artery at the ankle level. Subsequently, multiple ROIs of the same size were placed around the entire foot on the dermis and muscle tissues on the dorsal and plantar aspects of the foot and the heel in the same region in the pre- and postprocedural examinations. Changes in relative perfusion parameter measurements

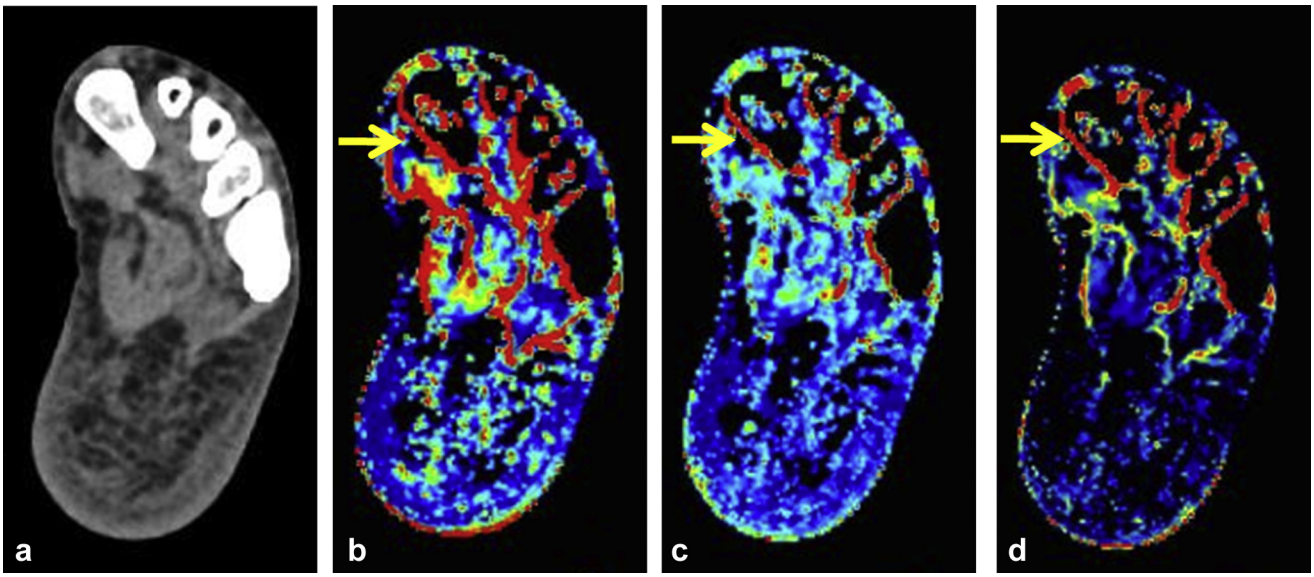

Figure 1. Axial CT image of the left foot **(a)** and axial perfusion maps of the left foot for the hemodynamic parameters PS **(b)**, BV **(c)**, and BF **(d)**. Note the red pseudohyperperfusing lines along the margins of bones, which are typical signs of motion artifact on a perfusion map (arrows, **b–d**).

before and after endovascular treatment were calculated. Studies from 6 patients were examined by a second observer to determine interobserver reproducibility.

Statistical Analysis

Statistical analysis was performed with MedCalc software (Medcalc, Mariakerke, Belgium). Wilcoxon signed-rank tests were used to compare pre- and postprocedural perfusion parameters, ie, BV, BF, and PS. The increase in ABI was also tested with a Wilcoxon signed-rank test. A Mann–Whitney test was employed to compare the percentage changes in perfusion parameters between dermis and muscle tissue regions, as defined as the percentage change of parameter values between pre- and post-PTA CT foot perfusion studies. It was also used to compare perfusion parameters values between patients with clinical improvement and no amputation after PTA and patients who finally underwent amputation. Correlation between perfusion parameter increases and ABI increase was evaluated with a Spearman rank correlation coefficient because the distribution of data was not normal, as shown by a Kolmogorov–Smirnov test. Receiver operating characteristic (ROC) analysis was performed to evaluate the potential of each perfusion parameter to differentiate patients with clinical improvement and no amputation and patients with poor clinical improvement who underwent an amputation after PTA. Interobserver agreement was measured with an intraclass correlation coefficient (ICC). Amputation-free survival was evaluated with Kaplan–Meier statistics. Amputation-free survival is a composite metric that incorporates the hard endpoints of mortality and major amputation. Toe and distal foot amputations were considered minor amputations. A P value $< .05$ was required to consider a test's results statistically significant.

RESULTS

Procedural Details and Clinical Outcome

Distribution of atherosclerotic lesions as determined by diagnostic CT angiography involved stenoses $> 50\%$ or occlusions in the common iliac artery (n = 5), external iliac artery (n = 6), superficial femoral artery (n = 8), and popliteal artery (n = 7), taking into consideration that some patients had more than 1 arterial lesion. Morphologic classification of target lesions was performed according to the TASC II classification system and resulted in 1 TASC class A lesion, 8 TASC class B lesions, 2 TASC class C lesions, and 2 TASC class D lesions. Technical success was achieved in all patients (13 of 13) included in the final analysis. There were no major complications after endovascular treatment aside from 1 femoral artery pseudoaneurysm treated with US-guided compression and thrombin injection (11). PTA was successfully performed in all patients, and provisional placement of self-expanding nitinol stents (Luminexx [Bard, Covington, Georgia]; Protege Everflex [Covidien, Dublin, Ireland]) was performed in 7 patients. Three patients underwent additional PTA with the use of drug-eluting balloons (Lutonix; Bard). After successful revascularization, the mean ABI increased from 0.36 ± 0.16 to 0.75 ± 0.22 ($P = .0002$; **Table 1**). The patients were followed up with clinical examination and color Duplex US for a mean of 9.1 months (range, 6–15 mo). During follow-up, 3 patients died as a result of non–procedure-related causes (colon cancer, myocardial infarction, and pulmonary embolism). Moreover, clinical status improved greatly ($\geq +3$ Rutherford categories) in 8 patients and moderately ($+2$ Rutherford categories) in 2 patients at 6 mo after PTA; these patients did not ultimately undergo amputation (group A). However, 3 patients showed no clinical improvement ($< +1$ Rutherford categories) after PTA

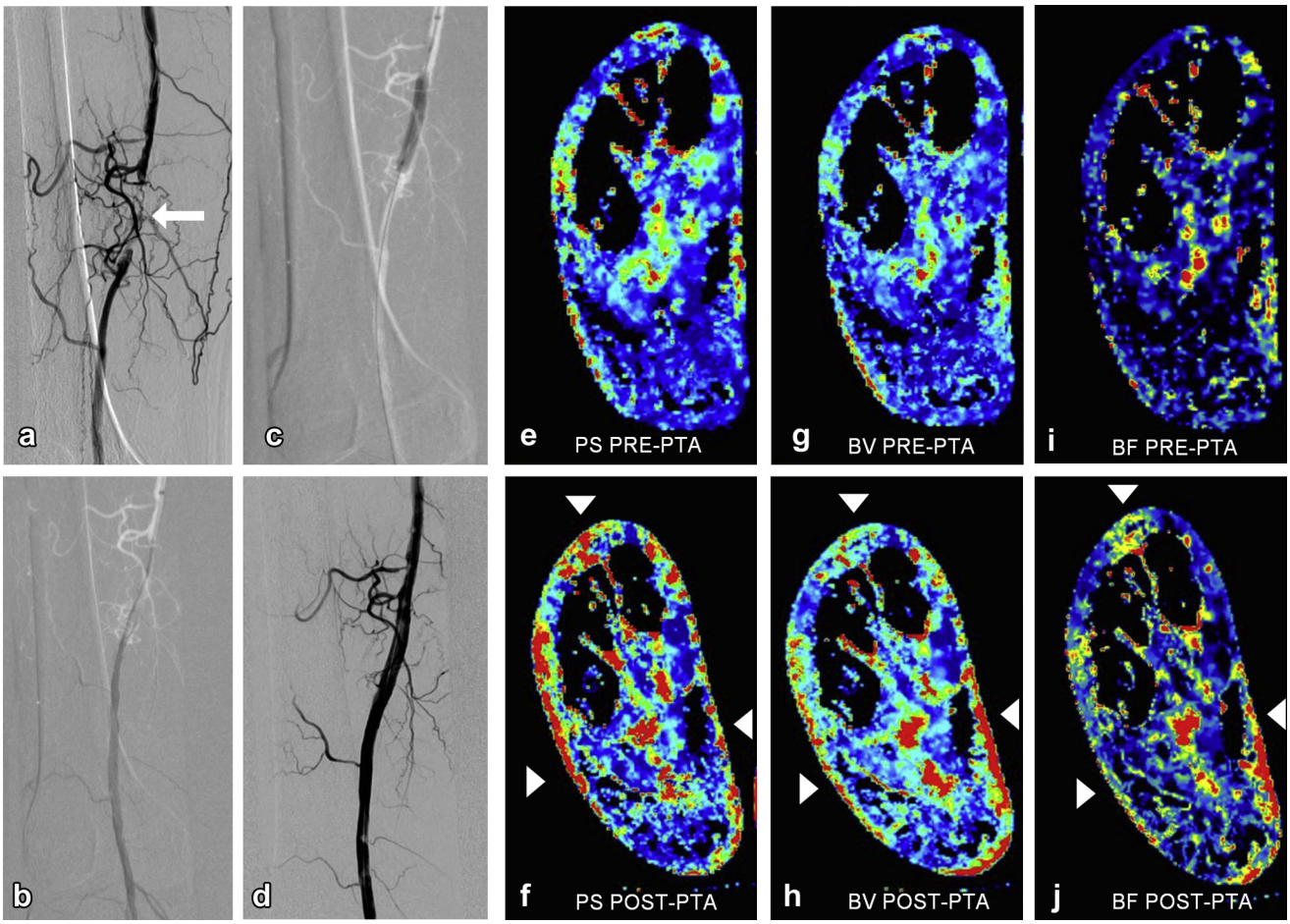

Figure 2. Images from an 84-year-old man with CLI of the right lower extremity. **(a)** DSA shows total occlusion of right distal superficial femoral artery (arrow). **(b)** Via a percutaneous ipsilateral approach from the right common femoral artery, the occlusion was traversed with a hydrophilic guide wire. **(c)** The patient underwent PTA with the use of a PTA balloon catheter and a drug-eluting balloon to prevent restenosis. **(d)** Final DSA shows significant flow restoration without complications. Axial perfusion maps of the foot demonstrate significant increases in PS **(e,f)**, BV **(g,h)**, and BF **(i,j)** after PTA, especially in the peripheral dermal layer (arrowheads, **f**, **h**, and **j**).

Table 2. Results of CT Foot Perfusion Examinations in the Study Population

Pt. No.	BV (mL/100 g)		BF (mL/100 g/min)		PS (mL/min/100 g)	
	Before PTA	After PTA	Before PTA	After PTA	Before PTA	After PTA
1	0.55	6.61	8.72	36.42	1.11	12.89
2	1.43	5.08	10.95	27.03	1.50	10.15
3	1.40	3.85	15.19	22.26	3.19	5.57
4	1.21	3.35	18.49	31.27	2.49	7.38
5	1.59	3.64	18.87	28.05	6.19	16.15
6	2.62	6.70	21.95	36.80	4.14	8.20
7	0.84	7.31	12.80	43.94	1.27	7.07
8	3.47	4.24	26.94	33.33	7.63	11.62
9	1.22	4.13	14.00	42.66	1.26	6.49
10	1.43	3.89	20.15	31.52	2.70	6.22
11	1.46	3.17	16.74	25.45	2.48	4.02
12	0.58	2.12	12.19	25.67	2.76	3.65
13	2.35	4.48	14.59	24.97	3.57	13.26
Median	1.43	4.13	15.19	31.27	2.70	7.38
Mean ± SD	1.55 ± 0.83	4.51 ± 1.53	16.28 ± 4.97	31.49 ± 6.86	3.1 ± 1.95	8.67 ± 3.85

BV = blood volume; BF = blood flow; PS = permeability surface; PTA = percutaneous transluminal angioplasty; SD = standard deviation.

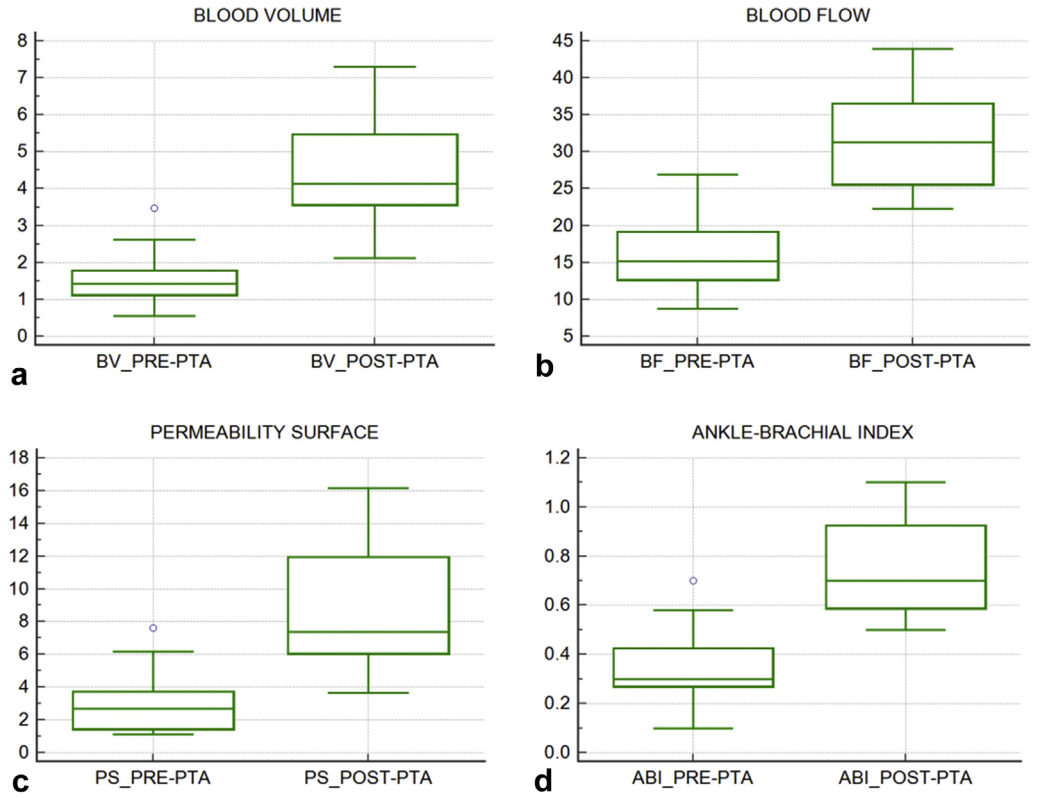

Figure 3. Box-and-whisker plots depict the median values and quartile ranges of the perfusion parameters BV **(a)**, BF **(b)**, and PS **(c)**, as well as ABI measurements **(d)**, before and after PTA. The boxes stretch from the 25th percentile at the lower edge to the 75th percentile at the upper edge. The median value is depicted as a line across the box. Outliers are depicted as lines at the outer areas of the box plots.

(group B), of whom 2 underwent minor amputation (toe, transmetatarsal) and 1 underwent major (above-knee) amputation as a result of extensive gangrene and tissue necrosis. The major and minor amputations took place during the first year after the procedure. The 6- and 12-month amputation-free survival rates, estimated by Kaplan–Meier analysis, were 100% and 62.5%, respectively.

Perfusion Evaluation

Successful revascularization led to a significant change in perfusion parameters (Fig 2). Qualitative changes in perfusion parameter maps were found in all patients postprocedurally (Table 2). After PTA, mean BV increased from 1.55 mL/100 g ± 0.83 to 4.51 mL/100 g ± 1.53 ($P = .0002$), BF increased from 16.28 mL/100 g/min ± 4.97 to 31.49 mL/100 g/min ± 6.86 ($P = .0002$), and PS increased from 3.1 mL/min/100 g ± 1.95 to 8.67 mL/min/100 g ± 3.85 ($P = .0002$; Fig 3). Perfusion parameter increases were greater in dermis than in muscle tissue regions ($P = .0016$ for BV increase, $P = .0333$ for BF increase, and $P = .0027$ for PS increase; Table 3). There was no significant correlation between perfusion parameter increases and ABI increase (Fig 4) per Spearman ρ test ($r = 0.0413$, $P = .8935$ for BV; $r = 0.215$, $P = .4814$ for BF; and $r = 0.462$, $P = .1118$ for PS). On the contrary, patients who exhibited significant clinical improvement and did not undergo amputation during follow-up (group A) had higher post-PTA perfusion values than patients who underwent an amputation (group B; $P = .028$ for BV, $P = .028$ for BF, and $P = .0112$ for PS). A nonsignificant difference in pre-PTA perfusion values was observed between these groups ($P = .499$ for BV, $P = .6121$ for BF, and $P = .8658$ for PS). Moreover,

Table 3. Comparison of CT Foot Perfusion Parameter Values and Mean Percent Increase of These Parameters between Dermis and Muscle Tissue Regions

Location/Timing	BV	BF	PS
Dermis			
Before PTA	1.5 ± 0.86	17.39 ± 7.12	2.62 ± 1.49
After PTA	5.44 ± 1.55	37.37 ± 9.61	10.88 ± 5.85
Increase (%)	345.24	139.14	395.45
Muscle tissue			
Before PTA	1.65 ± 0.88	14.85 ± 5.53	3.49 ± 2.25
After PTA	2.73 ± 0.83	22.84 ± 2.88	5.7 ± 2.32
Increase (%)	114.03	73.59	130.31
P Value*	.0016	.0333	.0027

Note–Values presented as mean ± standard deviation unless specified otherwise.
PTA = percutaneous transluminal angioplasty; BV = blood volume; BF = blood flow; PS = permeability surface; SD = standard deviation.
*Mann–Whitney test of perfusion parameter percentage change between dermis and muscle tissue regions.

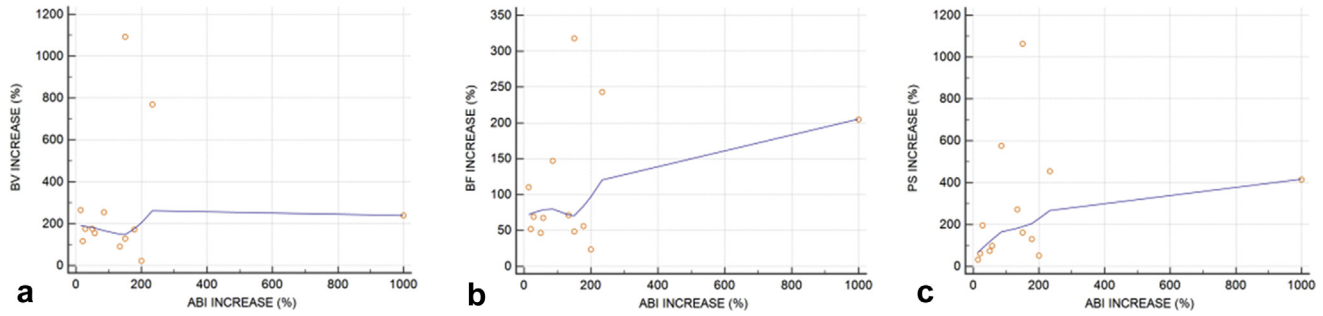

Figure 4. Correlation analyses between increase in ABI and increase in the perfusion parameters BV **(a)**, BF **(b)**, and PS **(c)**. The correlation analysis graphs demonstrate no significant correlation between these parameters.

only PS increase was significantly greater in group A than in group B ($P = .028$; Table 4).

ROC analysis results are presented in Table 5, and ROC curves are displayed in Figure 5. All perfusion parameters were found to have high sensitivity and specificity to predict poor clinical improvement and the occurrence of amputation after PTA ($P < .0001$). However, the small number of patients in the study is inadequate to support the reported cutoff values. All measurements demonstrated very good interobserver reproducibility, and ICCs were 0.91 (95% confidence interval [CI], 0.64–0.97) for BV, 0.94 (95% CI, 0.83–0.98) for BF, and 0.95 (95% CI, 0.86–0.98) for PS.

CT foot perfusion analysis was not feasible in 5 examinations (13.9% of total CT foot perfusion examinations) as a result of (i) diffuse calcification or total occlusion of the lower-limb arteries and inability to place the arterial ROI and (ii) motion artifacts that compromised image evaluation in the preprocedural (n = 4) or postprocedural (n = 1) CT foot perfusion evaluation. Additionally, 1 patient died of a myocardial infarction before postprocedural examination. The mean dose–length product of CT foot perfusion evaluation was 1,430.4 mGy·cm, and the mean effective dose was 0.29 mSv.

Table 4. Comparison of CT Foot Perfusion Parameters

Interval/Parameter	Group A	Group B	*P* Value
Before PTA			
BV	1.67 ± 0.89	1.15 ± 0.49	.4990
BF	16.75 ± 5.54	14.71 ± 2.31	.6121
PS	3.19 ± 2.24	2.81 ± 0.36	.8658
After PTA			
BV	4.94 ± 1.42	3.05 ± 0.87	.0280
BF	33.6 ± 6.37	24.46 ± 1.91	.0280
PS	9.94 ± 3.41	4.41 ± 1.02	.0112
Increase (%)			
BV	310.32 ± 342.95	185.88 ± 74.71	1
BF	124.93 ± 98.93	69.74 ± 35.55	.3105
PS	342.08 ± 305.92	56.31 ± 21.86	.0280

Note–Values presented as mean ± standard deviation where applicable. Group A comprises patients with clinical improvement and no amputation after PTA; group B comprises patients with poor response to PTA who underwent an amputation.
BF = blood flow; BV = blood volume; PS = permeability surface; PTA = percutaneous transluminal angioplasty; SD = standard deviation.

DISCUSSION

The technologic advancements in CT systems and the availability of dedicated CT perfusion software have created the opportunity for clinical and research investigations such as the present study. CT is used in clinical practice for a wide range of applications, but it can also provide qualitative and quantitative evaluation of tissue perfusion. The CT perfusion technique is clinically useful for diagnosis of acute cerebral ischemia (12), for diagnosis and evaluation of the response to treatment in patients with liver neoplasia (13), and for detection of hemodynamically significant coronary stenosis in patients with coronary artery disease (14). It can also be used to detect prostatic carcinoma (15), as perfusion parameters were shown to be higher for tumor compared with normal prostate tissue, or to evaluate the risk for abdominal artery aneurysm rupture (16). Other applications include the detection of active lymphoma and the assessment of different types of tumors (brain, lung, rectal, pancreatic) and prediction of their response to treatment (17). Moreover, CT perfusion has been used to monitor response to bevacizumab and radiation therapy in patients with soft-tissue sarcomas (18). The use of this imaging technique in the study of PAD or CLI is not widespread because imaging methods such as color duplex US, CT angiography, or MR angiography are capable of depicting stenoses and/or occlusions of peripheral arteries, and, in conjunction with clinical examination, are decisive in the evaluation of PAD and selection of appropriate treatment (1,2).

Dynamic volume CT can provide quantitative and qualitative information on perfusion status of the limb. Barfett et al (7) used an en bloc volumetric CT perfusion technique in the foot to differentiate between mild and major vascular impairment in healthy volunteers. A study by Iezzi et al (8) evaluated CT perfusion parameter changes after endovascular treatment in 10 patients with PAD. They deduced that foot CT perfusion examination is feasible and reproducible

Table 5. ROC Analysis of Post-PTA Perfusion Parameters Regarding the Ability to Predict Poor Response to Revascularization and the Occurrence of Amputation after PTA

Parameter	AUC	*P* Value	Sensitivity (%)	Specificity (%)	Cutoff Value
BV	0.933	< .0001	100	80	≤3.85
BF	0.933	< .0001	100	90	≤25.67
PS	1	< .0001	100	100	≤5.57

AUC = area under the curve; BF = blood flow; BV = blood volume; PS = permeability surface; PTA = percutaneous transluminal angioplasty; ROC = receiver operating characteristic.

and that PTA can induce slight changes in perfusion parameters. Recently, Hur et al (9) demonstrated the ability of CT perfusion technique to measure BF of the foot in animals and humans. The authors concluded that successful revascularization leads to significant increase of BF, especially in the dermal layer (9).

The present study demonstrates statistically significant changes in perfusion parameters in patients with CLI after successful revascularization. Compared with other studies, all patients had CLI and all but 1 were allocated to Rutherford class 5 or 6. As a result of the severe limb ischemia in the study population, successful PTA may have led to improvement in the macro- and microvascular states of the foot, which subsequently affected perfusion parameters.

In the present study, there was no significant correlation between ABI and increases in perfusion parameter measurements. Perfusion parameters are influenced by macrovascular and microvascular functions of the foot, as opposed to ABI, which reflects the macrovascular status of the limb. Moreover, the perfusion parameter changes were greater in the dermal layer than in the muscle tissues, which has been reported in only 1 previous study of which we are aware (9). Finally, patients with clinical improvement who did not undergo an amputation presented higher post-PTA perfusion parameter values than patients with poor response who underwent an amputation after PTA. As a result, CT foot perfusion may have a prognostic role in the evaluation of outcomes in patients with CLI and the prediction of amputation after PTA, but the small number of patients is inadequate to substantiate this hypothesis.

Radiation exposure should be always investigated in the evaluation of the diagnostic value of a CT examination. The mean effective dose from CT foot perfusion analysis was estimated to be minor in the present study (0.29 mSv), and the diagnostic benefit of this examination therefore outweighs any theoretic radiogenic risk associated with the examination. Nonetheless, efforts should be focused on further reduction of radiation exposure based on the "as low as reasonably achievable" principle of radiation protection.

The present study has several limitations. CT foot perfusion was not feasible in cases of diffuse calcification or absolute occlusion of the lower-limb arteries because of an inability to set an arterial ROI. Motion artifact is another significant reason for compromised image evaluation and false results. Five patients were excluded from this study because of these limitations on preprocedural (n = 4) or postprocedural (n = 1) CT foot perfusion examination, representing 13.9% of total CT foot perfusion examinations (5 of 36). Because this is a prospective study, it is not possible to foresee the outcomes of the patients. Three patients were treated with surgical revascularization such as axillofemoral bypass (n = 2) and femoropopliteal bypass (n = 1). Finally, 1 patient died of a myocardial infarction before postprocedural examination. All these patients (n = 9) were excluded from the study. Another limitation is the absence of correlation between CT foot perfusion parameters and measurements from other modalities such as $TcPO_2$, contrast-enhanced US, or MR imaging, which could be a promising area for future research.

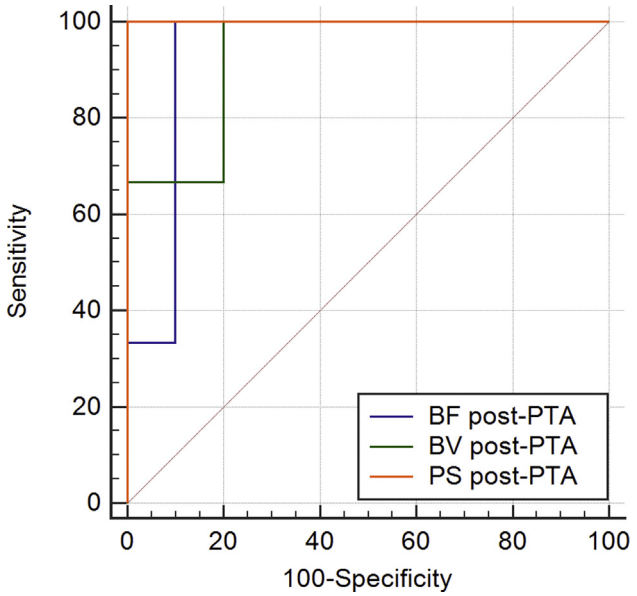

Figure 5. ROC curves for post-PTA perfusion parameters (BV, BF, and PS) regarding the ability to predict the occurrence of amputation after PTA.

In conclusion, CT foot perfusion is a reproducible technique that can be a useful tool for estimation of PTA outcome in patients with CLI. The information provided by this examination may aid the reliable prediction of poor response to revascularization or an imminent amputation in patients with CLI. Further research efforts, including not only CT but also MR perfusion and nuclear spectroscopy techniques, should be invested into this clinically important field to identify the most reliable study of the microvascular state of the foot.

ACKNOWLEDGMENTS

The authors thank all of the radiologic technologists who took part in this study, especially Nikolaos Kosidekakis for his specific effort in standardization of the CT foot perfusion protocol.

REFERENCES

1. Norgren L, Hiatt WR, Dormandy JA, et al. Inter-Society Consensus for the Management of Peripheral Arterial Disease (TASC II). Eu J Vasc Endovasc Surg 2007; 33(suppl 1):S1–S75.
2. Abdulhannan P, Russell DA, Homer-Vanniasinkam S. Peripheral arterial disease: a literature review. Br Med Bull 2012; 104:21–39.
3. Dhanoa D, Baerlocher MO, Benko AJ, et al. Position statement on noninvasive imaging of peripheral arterial disease by the Society of Interventional Radiology and the Canadian Interventional Radiology Association. J Vasc Interv Radiol 2016; 27:947–951.
4. Bajwa A, Wesolowski R, Patel A, et al. Assessment of tissue perfusion in the lower limb: current methods and techniques under development. Circ Cardiovasc Imaging 2014; 7:836–843.
5. Lindner JR, Womack L, Barrett EJ, et al. Limb stress-rest perfusion imaging with contrast ultrasound for the assessment of peripheral arterial disease severity. JACC Cardiovasc Imaging 2008; 1: 343–350.
6. Ouwendijk R, de Vries M, Pattynama PM, et al. Imaging peripheral arterial disease: a randomized controlled trial comparing contrast-enhanced MR angiography and multi-detector row CT angiography. Radiology 2005; 236:1094–1103.
7. Barfett J, Velauthapillai N, Kloeters C, Mikulis DJ, Jaskolka JD. An en bloc approach to CT perfusion for the evaluation of limb ischemia. Int J Cardiovasc Imaging 2012; 28:2073–2083.
8. Iezzi R, Santoro M, Dattesi R, et al. Foot CT perfusion in patients with peripheral arterial occlusive disease (PAOD): a feasibility study. Eur J Radiol 2013; 82:e455–e464.
9. Hur S, Jae HJ, Jang Y, et al. Quantitative assessment of foot blood flow by using dynamic volume perfusion CT technique: a feasibility study. Radiology 2016; 279:195–206.
10. Saltybaeva N, Jafari ME, Hupfer M, Kalender WA. Estimates of effective dose for CT scans of the lower extremities. Radiology 2014; 273:153–159.
11. Kontopodis N, Tsetis D, Tavlas E, Dedes A, Ioannou CV. Ultrasound guided compression versus ultrasound guided thrombin injection for the treatment of post-catheterization femoral pseudoaneurysms: systematic review and meta-analysis of comparative studies. Eur J Vasc Endovasc Surg 2016; 51:815–823.
12. Konstas AA, Wintermark M, Lev MH. CT perfusion imaging in acute stroke. Neuroimaging Clin N Am 2011; 21:215–238.
13. Kim SH, Kamaya A, Willmann JK. CT perfusion of the liver: principles and applications in oncology. Radiology 2014; 272:322–344.
14. Yang DH, Kim YH. CT myocardial perfusion imaging: current status and future perspectives. Int J Cardiovasc Imaging 2017; 33:1009–1020.
15. Luczynska E, Blecharz P, Dyczek S, et al. Perfusion CT is a valuable diagnostic method for prostate cancer: a prospective study of 94 patients. Ecancermedicalscience 2014; 8:476.
16. Kontopodis N, Galanakis N, Tsetis D, Ioannou CV. Perfusion computed tomography imaging of abdominal aortic aneurysms may be of value for patient specific rupture risk estimation. Med Hypotheses 2017; 101:6–10.
17. Kambadakone AR, Sahani DV. Body perfusion CT: technique, clinical applications, and advances. Radiol Clin N Am 2009; 47:161–178.
18. Kambadakone A, Yoon SS, Kim TM, et al. CT perfusion as an imaging biomarker in monitoring response to neoadjuvant bevacizumab and radiation in soft-tissue sarcomas: comparison with tumor morphology, circulating and tumor biomarkers, and gene expression. AJR Am J Roentgenol 2015; 204:W11–W18.

European Journal of Radiology 129 (2020) 109081

Contents lists available at ScienceDirect

European Journal of Radiology

journal homepage: www.elsevier.com/locate/ejrad

The role of dynamic contrast-enhanced MRI in evaluation of percutaneous transluminal angioplasty outcome in patients with critical limb ischemia

Nikolaos Galanakis[a], Thomas G Maris[b], Nikolaos Kontopodis[c], Christos V. Ioannou[c], Konstantinos Tsetis[a], Apostolos Karantanas[a], Dimitrios Tsetis[a,*]

[a] Department of Medical Imaging, University Hospital Heraklion, University of Crete Medical School, Voutes, 71110 Heraklion, Greece
[b] Department of Medical Physics, University Hospital Heraklion, University of Crete Medical School, Voutes, 71110 Heraklion, Greece
[c] Vascular Surgery Unit, Department of Cardiothoracic and Vascular Surgery, University Hospital Heraklion, University of Crete Medical School, Voutes, 71110 Heraklion, Greece

ARTICLE INFO

Keywords:
Dynamic contrast-enhanced MR
Quantitative imaging
MR perfusion
Peripheral arterial disease
Critical limb ischemia
Percutaneous transluminal angioplasty

ABSTRACT

Purpose: Imaging modalities such as CTA and MRA provide significant information about the distribution of macrovascular lesions of the limbs in patients with peripheral arterial disease but not for the local microvascular perfusion of the feet. The purpose of this study is to evaluate foot perfusion in patients with critical limb ischemia (CLI) and estimate percutaneous transluminal angioplasty (PTA) results, using dynamic contrast-enhanced magnetic resonance imaging (DCE-MRI).

Methods: Ten patients (6 male, median age 68 years) with CLI were examined. All patients underwent DCE-MRI of the lower limb before and within first month after PTA. Perfusion parameters such as blood flow (BF), Ktrans, Kep were analyzed and applied for statistical comparisons. The studies were also examined by a second observer to determine inter-observer reproducibility.

Results: Revascularization was technically successful in all patients and mean ankle brachial index (ABI) increased from 0.37 ± 0.18 to 0.76 ± 0.23, $p < 0.05$. After PTA, mean BF increased from 6.232 ± 2.867–9.867 ± 2.965 mL/min/100 g, K^{trans} increased from 0.060 ± 0.022 to 0.107 ± 0.041 min^{-1} and K_{ep} increased from 0.103 ± 0.024 to 0.148 ± 0.024 min^{-1}, $p < 0.05$. All measurements demonstrated very good inter-observer reliability with an ICC > 0.85 for all perfusion parameters.

Conclusions: DCE-MRI is a safe and reproducible modality for the diagnosis of foot hypo-perfusion. It seems also to be a promising tool for evaluation of PTA outcome, as significant restitution of perfusion parameters was observed after successful revascularization.

1. Introduction

Peripheral arterial disease (PAD) characterizes the impairment of blood flow to the extremities as a result of stenoses and/or occlusions of the lower limb arteries [1]. The major risk factors for PAD include increased age, cigarette smoking, diabetes mellitus, hyperlipidemia and hypertension [2]. Clinical presentation of PAD is varied and may appear as asymptomatic arterial disease with abnormal noninvasive test results, symptomatic disease presenting as classic or atypical intermittent claudication, or critical limb ischemia (CLI). CLI is defined as a recurring ischemic rest pain requiring analgesia for > 2 weeks or ulceration or gangrene of foot or toes with ankle systolic pressure < 50 mmHg or toe systolic pressure < 30 mmHg [3].

The goals of treatment for patients with claudication are to relieve their exertional symptoms, improve their walking capacity and reduce overall risk of cardiovascular mortality with risk-factor modification and pharmaceutical therapies [4]. Revascularization is indicated for severe claudication which has a negative impact on the quality of life, for rest pain and tissue loss. Revascularization strategies include endovascular (mainly percutaneous transluminal angioplasty (PTA) with/without stent deployment) or surgical procedures (endarterectomy, bypass using autologous vein or synthetic conduits) [5]. The choice between an endovascular or surgery first approach is guided by the TASC II classification of disease [3].

Abbreviations: PAD, peripheral arterial disease; CLI, critical limb ischemia; PTA, percutaneous transluminal angioplasty; ABI, ankle-brachial index; CDUS, color duplex ultrasound; CTA, computed tomography angiography; MRA, magnetic resonance angiography; DSA, digital subtraction angiography; DCE-MRI, dynamic contrast-enhanced magnetic resonance imaging; BF, blood flow; EES, extravascular extracellular space; ICC, interclass correlation coefficient

* Corresponding author.
E-mail address: tsetisd@uoc.gr (D. Tsetis).

https://doi.org/10.1016/j.ejrad.2020.109081
Received 12 March 2020; Received in revised form 7 May 2020; Accepted 18 May 2020

Evaluation of PAD includes clinical history, physical examination, measurement of ankle-brachial index (ABI) [1] and imaging studies such as color duplex ultrasound (CDUS), computed tomography angiography (CTA), magnetic resonance angiography (MRA) and digital subtraction angiography (DSA) [6]. These imaging modalities can depict the distribution of macrovascular lesions (stenoses, occlusions) of the lower extremities arteries but they do not specify the local microvascular perfusion status of the limbs. Moreover they cannot estimate the therapeutic results of endovascular or surgical procedures regarding the improvement in tissue perfusion.

The purpose of this study is to evaluate foot hypoperfusion in patients with CLI using dynamic contrast-enhanced magnetic resonance imaging (DCE-MRI) examination and estimate perfusion parameters changes before and after successful PTA.

2. Materials and methods

2.1. Study design

The aim of this prospective single-center study is to investigate the role of DCE-MRI in the evaluation of foot perfusion in patients with CLI. The study included patients with CLI (Rutherford categories 4–6) with either rest pain or minor/major tissue loss and anatomic distribution of atherosclerotic lesions which should make them suitable for endovascular treatment. Initially, patients underwent CDUS and diagnostic CTA in order to determine anatomic distribution of atherosclerotic lesions. In general, a primary endovascular approach was preferred whenever possible, even in selected cases with TASC C and D lesions which were judged as poor surgical candidates.

Patients with acute limb ischemia or less advanced PAD (Rutherford categories 1–3) as well those who underwent surgical or conservative treatment were excluded. The exclusion criteria included also all common contraindications to MRI such as ferromagnetic implants, pacemakers and severe claustrophobia and contraindications for gadolinium contrast medium injection such as previous severe allergic/anaphylactoid reaction, severe renal disease (eGFR < 30 mL/min/1.73 m^2) or acutely deteriorating renal function and pregnancy.

Selective patients that fulfilled these criteria were subjected to DCE-MRI of the affected foot. The patients also underwent a second DCE-MRI examination within 1 st month after endovascular treatment. All patients were followed-up with clinical examination at 1, 3, 6 and 12 months and color Doppler ultrasound combined with clinical examination on an annual basis.

The study was conducted according to the principles of the Declaration of Helsinki and in accord with the applicable national guidelines, regulations and acts. The study was approved by the local ethic committee and all patients signed informed consent prior to examination.

2.2. Imaging protocol

Studies were performed on a 1.5 T clinical MR Scanner (Vision/Sonata Hybrid system, Siemens, Erlangen, Germany) enforced with a powerful 3 T equivalent gradient system (Gradient strength : 45 m T/m, Gradient Slew rate : 200 m T/m/ms). A standard quadrature RF bird cage body coil was used for signal excitation and a two channel array Head Coil was used for signal detection.

Conventional and quantitative MR imaging protocols include:

The conventional qualitative imaging protocol consisted of a T1 weighted 3D GRE VIBE (Volume Interpolated Breath hold Examination) sequence (TR/TE/FA: 9.5 ms/3.4 ms/15°) and a T2/T1 weighted 3D GRE CISS (Constructive Interference in Steady State) sequence (TR/TE/FA: 9.3 ms/4.2 ms/70°), obtained both in sagittal planes at the area of lower limb. Forty (40) consecutive slices of 2 mm slice thickness and in-plane spatial resolution (pixel size) of 0.49 mm^2 (FOV = 250 × 250 mm, Matrix size = 512 × 512 interpolated) were obtained utilizing either T1 or T2/T1 weighted sequences. Pixel bandwidth was 130 Hz/pxl in both T1 and T2/T1 weighted sequences. Acquisition times were approximately 2.5 min for both sequences.

The quantitative DCE-MRI protocol of the lower limb was performed utilizing firstly a PD to T1 weighted 3D GRE VIBE sequence (TR/TE: 7.8 ms/2.7 ms) in the sagittal plane with variable flip angles (FA = 5°, 10°, 15°, 20°, 25°, 30°) for the initial calculation of the parametric T1 maps. Twenty six (26) consecutive slices of 3 mm slice thickness and in-plane spatial resolution (pixel size) of 0.49 mm^2 (FOV = 250 × 250 mm, Matrix size = 512 × 512 interpolated) were obtained. Pixel bandwidth was 150 Hz/pxl. The acquisition time was 21 s for each flip angle. Each flip angle was obtained separately and therefore, the sequence was repeated 6 times. The total acquisition time for all the set of flip angles was approximately 2 min. The final outcome of this sequence is the production of 26 consecutive slices depicting the calculated T1 parametric maps with the same anatomical characteristics (slice thickness, pixel size) of the base aforementioned sequence. These maps serve as the basis of the calculation of $T1_0$ in DCE-MRI perfusion imaging [7].

The actual T1 weighted DCE perfusion MR imaging of the lower limb was performed utilizing a T1 weighted 3D GRE VIBE sequence (TR/TE/FA: 9.5 ms/3.4 ms/15°) in sagittal plane. Twenty six (26) consecutive slices of 3 mm slice thickness and in-plane spatial resolution (pixel size) of 0.49 mm^2 (FOV = 250 × 250 mm, Matrix size = 512 × 512 interpolated) were obtained. Pixel bandwidth was 150 Hz/pxl. The acquisition time was 15 s. The sequence was repeated 40 times. The first 3 repetitions were used for the calculation of the baseline signal. Consequently, during the rest 37 repetitions of the aforementioned sequence, an intravenous continual injection of paramagnetic contrast medium [(Magnevist, Gadopentetate Dimeglumine, Bayer Healthcare, Bayer, 0.2 mL/kg, (0.1 mmol/kg)] was administered for approximately one minute. The mean dose of paramagnetic contrast medium delivered during the examination was 16.5 mL (range 14 − 20 ml). The total acquisition time for the 40 repetitions was approximately 10 min.

All images were transformed to a separate dedicated workstation for further analysis.

2.3. Image analysis

MR images were transferred and analyzed with a commercially available software (nordicICE v4.0, NNL, Bergen, Norway). DCE-analysis was performed utilizing an extended Tofts model (3-parameter fitting). Initially, T1 parametric maps were calculated using a 3D spoiled gradient echo sequence (3D GRE VIBE) with variable flip angles, as previously discussed. Fast T1 calculations using variable flip angles is based on the method proposed by Fram EK et al. [8]. This method is incorporated as a standard T1 measurement procedure on the (nordicICE) platform. T1 parametric maps are used for the calculation of the base $T1_0$ maps of the anatomic regions (slices) prior to perfusion analyses.

Quantitative perfusion maps based on pharmacokinetic parameters such us blood flow (BF), K^{trans} and K_{ep} were created from parametric data fitted to the extended Tofts model utilizing a population-based arterial input function [7]. K^{trans} express the volume transfer coefficient between blood plasma and extravascular extracellular space (EES), K_{ep} the exchange rate constant between EES and blood plasma (backflux exchange rate) and finally BF express flow of blood per unit mass of tissue [9]. K^{trans} and K_{ep} are expressed in min^{-1} and BF in ml/min/100 g of tissue. Subsequently, multiple ROIs were placed around the entire foot, on the dermis and muscles tissues in the pre- and post-procedure examination and the change in the relative perfusion parameters was calculated. Analysis and evaluation of DCE-MRI was performed by two blinded radiologists to determine inter-observer reliability.

2.4. Statistical analysis

Statistical analysis was performed with MedCalc (version Medcalc Software, Mariakerke, Belgium). Wilcoxon signed rank tests were used to compare perfusion parameters such as BF K^{trans} and K_{ep} before and after endovascular treatment. The relative change in ABI was also tested with Wilcoxon signed rank test. Correlation between perfusion parameters and ABI was evaluated with Pearson's correlation coefficient and normal distribution of data was tested with Kolmogorov–Smirnov test. Amputation-free survival was calculated using Kaplan–Meier method. Interobserver agreement was assessed using the interclass correlation coefficient (ICC). A p-value < 0.05 was considered as statistically significant.

3. Results

3.1. Study population

Between March 2015 and April 2019, 16 selective patients enrolled in the study. Technical success was achieved in 13/16 patients. Three cases with multilevel occlusive disease (TASC D), who underwent surgical revascularization after failed endovascular revascularization, were excluded from subsequent analysis. Moreover, there was one patient who died before post-procedural examination due to ischemic stroke and one patient who underwent amputation due to extensive ulcers and osteomyelitis before post-procedural examination. DCE analysis was not feasible in one case due to motion artifacts which compromised image evaluation. Totally, 10 patients (6 male, 4 female) with a median age of 68 years (range 58–79 years) were included in the final analysis. Patient's main risk factors were hypertension (n = 8), hyperlipidemia (n = 10), diabetes mellitus (n = 8), smoking (n = 9) and coronary artery disease (n = 5). According to Rutherford classification of PAD, two patients were allocated to class 4, six patients to class 5 and two patients to class 6 PAD. The study population's baseline characteristics are summarized in Table 1.

3.2. Procedural details – clinical outcome

Patients presented hemodynamically significant stenoses or occlusions in common iliac artery (n = 4), external iliac artery (n = 5), superficial femoral artery (n = 7), popliteal artery (n = 4) and below the knee arteries (n = 4) taking into consideration that some patients had more than one arterial lesion. The majority of patients had multilevel arterial disease but we only refer the targeted vessels for endovascular recanalization. Technical success was achieved in all patients included in final analysis, without major complications. PTA was successfully performed in all patients, drug coated balloons (Lutonix, Bard) were used in two patients and provisional stenting using self- expanding nitinol stents (Luminexx, Bard), (Protege Everflex, Covidien) was performed in seven patients (Table 2). There was significant hemodynamic improvement in all patients and mean ABI increased from 0.37 ± 0.18 to 0.76 ± 0.23 after revascularization ($p < 0.05$). All patients received the optimal medical treatment for hypertension, hyperlipidemia and diabetes mellitus. After PTA they received single or dual antiplatelet therapy as it is displayed in Table 2. The patients were followed-up with clinical examination and color Duplex ultrasonography for a mean duration period of 24 months (range 6–48). No recurrent hemodynamically significant stenoses were found at the site of the intervention during US examination, except patient No5 who underwent a second PTA with successful restoration of flow. During follow up one patient died due to acute myocardial infarction, one patient underwent major (above-knee) amputation due to extensive tissue necrosis and there were also two patients who underwent minor (toe) amputations (Table 2). The 12-month amputation-free survival rate, estimated by Kaplan-Meier analysis, was 80%.

Table 1
Clinical data of study population.

Pt No	Sex	Age	Risk Factors	Rutherford Classification
1	M	76	HT, HL, SM	5
2	M	75	DM, HL, SM,CAD	5
3	M	66	DM, HT, HL,SM, CAD	5
4	M	68	DM, HT, HL,SM, CAD	4
5	F	68	DM, HT, HL,SM	6
6	F	66	DM, HT, HL,SM, CAD	4
7	F	79	DM, HT, HL,SM	5
8	M	58	DM, HT, HL,SM, CAD	5
9	M	64	DM, HL	6
10	F	72	HT, HL, SM	5

Abbreviations: M = Male, F = Female, HT = Hypertension, DM = Diabetes Mellitus, HL = Hyperlipidemia, SM = Smoking, CAD = Coronary artery disease.

3.3. Perfusion evaluation

Successful revascularization led to a significant change in perfusion parameters (Fig1). After PTA, mean BF increased from 6.232 ± 2.867–9.867 ± 2.965 mL/min/100 g, K^{trans} increased from 0.060 ± 0.022 to 0.107 ± 0.041 min^{-1} and K_{ep} increased from 0.103 ± 0.024 to 0.148 ± 0.024 min^{-1}, $p < 0.05$. (Table 3, Fig. 2). There was no significant correlation between perfusion parameters and ABI, as it was tested with Pearson's correlation coefficient ($r = 0.37$, $p = 0.106$ for K^{trans}, $r = 0.39$, $p = 0.085$ for K_{ep} and $r = 0.41$, $p = 0.074$ for BF), (Fig3). The studies were also analyzed by a second observer to determine inter-observer reliability. All perfusion parameter measurements presented very good inter-observer reliability with an ICC greater than 0.85 for all perfusion parameters and specifically 0.92 (95% CI 0.82 − 0.97) for K^{trans}, 0.87 (95% CI 0.7 − 0.95) for K_{ep}, and 0.89 (95% CI 0.73 − 0.95) for BF.

4. Discussion

Non conventional imaging techniques such as MR diffusion weighted imaging (DWI) and MR perfusion weighted imaging (PWI) are well validated techniques for the diagnosis and the selection of appropriate therapeutic treatment for various diseases, especially as regards the study of brain parenchyma [10] and myocardium [11]. Apart from MR perfusion techniques, CT can provide qualitative and quantitative evaluation of tissue perfusion. However, these techniques are rarely used in clinical practice for the evaluation of PAD because imaging methods such as CDUS, CTA or MRA can highlight stenoses or occlusions of peripheral arteries and combined with clinical examination are used for the diagnosis and the selection of treatment in patients with PAD [1,3,5].

DCE-MRI with intravenous Gadolinium administration enables perfusion measurement of skeletal muscles. It can be used to differentiate benign from malignant tumors and estimate the treatment response after chemotherapy. Moreover, DCE-MRI is useful for the evaluation of inflammatory diseases such as Charcot foot or vascular abnormalities [12]. Isbell et al., developed a DCE-MRI technique to measure skeletal muscle perfusion in patients with moderate PAD. According to their findings peak-exercise measurement of limb perfusion with DCE-MRI distinguishes patients with PAD from controls [13]. Another study of Thompson et al. measured the regional distribution of skeletal muscle blood flow during postischemic reactive hyperemia using DCE-MRI. They used an occlusive thigh cuff which delivers a step-input of contrast concentration (onset of reactive hyperemia), when it released [14]. Non Gd-based techniques for muscle perfusion, like arterial spin labeling (ASL) and blood oxygenation level-dependent (BOLD) allow quantification of the skeletal muscle blood flow in patients with PAD. West et al. used ASL technique in order to measure blood flow in healthy volunteers and patients with PAD. The study showed statistically significant differences in peak exercise calf

Table 2
Procedural and Follow-up details.

Pt No	Lesion location	Endovascular procedure	Medical therapy after PTA	ABI pre-PTA	ABI post-PTA	Follow-up Rutherford classification (ABI) or event		
						1 month	6 month	1 year
1	(R) CIA,EIA	PTA Stenting	Clopidogrel	(0.25)	(0.6)	Minor (toe) amputation (0.6)	3 (0.5)	3 (0.5)
2	(L) SFA, POPA, TPT, PA	PTA	Aspirin + Clopidogrel	(0.33)	(0.55)	(0.5)	Death(AMI)	–
3	(R) SFA	DCB PTA	Aspirin + Clopidogrel	(0.55)	(0.73)	(0.7)	2 (0.7)	2 (0.8)
4	(R) SFA, POPA	PTAStenting	Aspirin + Clopidogrel	(0.53)	(0.9)	(0.9)	1 (0.9)	2 (0.8)
5	(R) CIA, EIA, CFA	PTA Stenting	Clopidogrel	(0.2)	(0.4)	Minor (toe) amputation (0.5)	5 (0.4)	5 (0.3)
6	(L) EIA, SFA	PTAStenting	Aspirin + Clopidogrel	(0.64)	(1.1)	(1)	2 (0.9)	2 (0.9)
7	(L) CIA, EIA, SFA, POPA	PTA Stenting	Aspirin + Clopidogrel	(0.1)	(1.1)	(1.1)	1 (1)	1 (0.9)
8	(R) SFA, POPA, PTA, ATA	PTA Stenting	Aspirin + Clopidogrel	(0.2)	(0.7)	(0.7)	3 (0.7)	3 (0.6)
9	(L) SFA	DCB PTA	Aspirin + Clopidogrel	(0.4)	(0.8)	(0.7)	2 (0.6)	2 (0.6)
10	(R) CIA, EIA	PTA Stenting	Clopidogrel	(0.5)	(0.7)	(0.5)	Major amputation	–

Abbreviations: CIA = Common Iliac Artery, EIA = External Iliac Artery, CFA = Common Femoral Artery, SFA = Superficial Femoral Artery, POPA = Popliteal Artery, TPT = Tibioperoneal trunk, PA = Peroneal Artery, PTA = Posterior Tibial Artery, ATA = Anterior Tibial Artery, ABI = Anke-brachial index, PTA = Percutaneous transluminal angioplasty, DCB = Drug-coated balloon, AMI = Acute myocardial infarction, Event concerns death or amputation (minor/major).

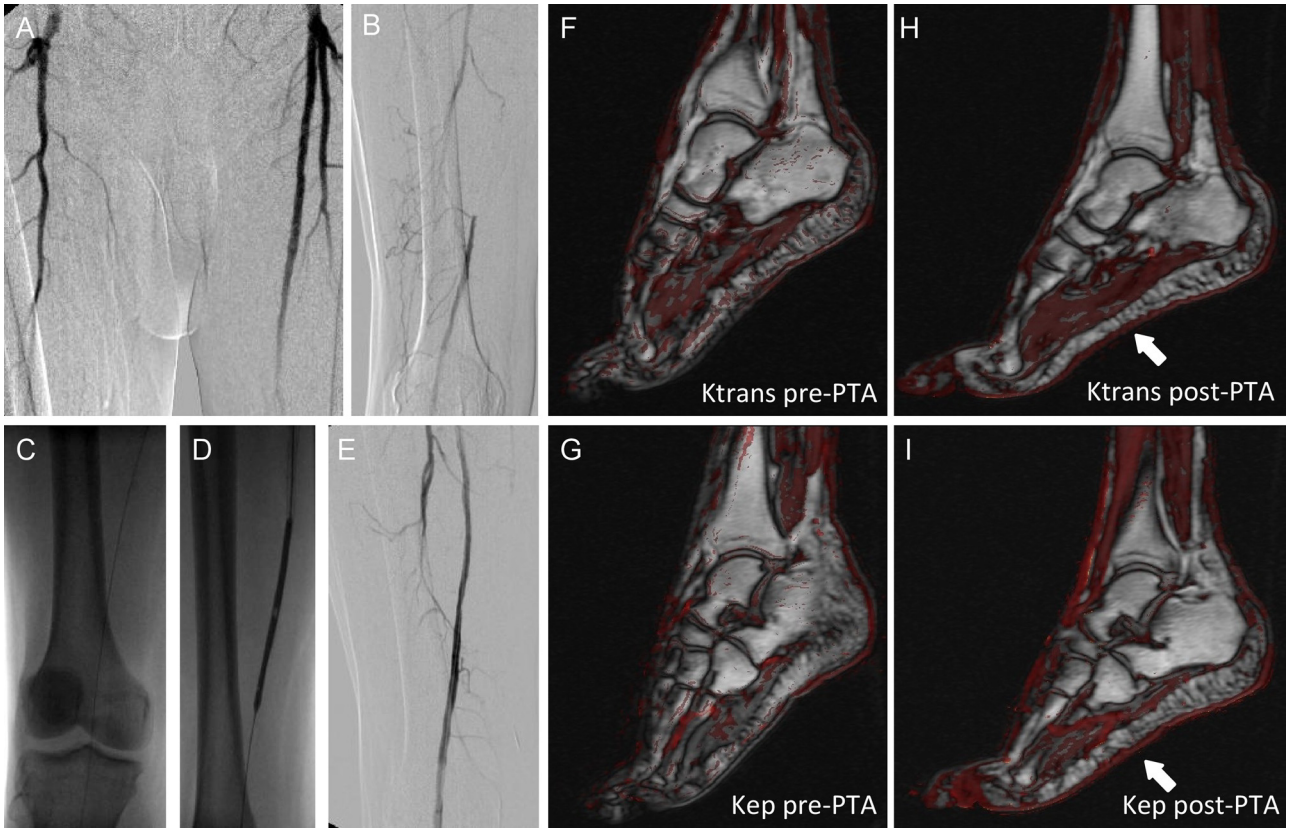

Fig. 1. A 68-year-old male patient with CLI of right lower extremity. DSA showed total occlusion of right SFA (A) and reconstruction of popliteal artery via collaterals (B). Through percutaneous approach from the left common femoral artery, the occlusion was traversed with a hydrophilic guide wire (C). The patient underwent successful PTA and stent placement (D) Final DSA showed significant flow restoration (E). Co-registration of anatomic sagittal T1w sequences combined with K^{trans} and K_{ep} parametric maps before (F,G) and after PTA (H,I) showed significant increase of perfusion parameters after revascularization, especially in the peripheral dermal layer (arrow).

perfusion between these groups [15]. Grözinger et al., evaluated muscle perfusion in 10 patients with PAD before and after PTA using MR-ASL perfusion measurements during reactive hyperemia. They concluded that ASL-MRI can detect changes in perfusion parameters after successful PTA [16]. A recent study also showed that ASL technique can be used to evaluate diabetic feet with ulcers and distinguish ischemic regions from normal perfused muscle tissue regions [17]. Ledermann et al., compared calf muscle perfusion in patients with PAD and healthy volunteers with BOLD-MRI. They demonstrated that statistical significant differences in perfusion parameters were found between the two groups [18]. Another study also evaluated the results of PTA in patients with PAD using BOLD-MRI. The authors indicated that successful revascularization leads to perfusion parameter's alterations, such as T2*max, time to peak and T2* end value [19]. Furthermore, a recent study showed that there is correlation between DWI and DCE-MRI perfusion parametric maps in patients with PAD after smoothing of

Table 3
Results of DCE-MRI examinations in the study population.

Pt No	Gd contrast medium dose (ml)	BF pre-PTA (ml/min/100 g)	BF post-PTA (ml/min/100 g)	K^{trans} (min^{-1})	K^{trans} (min^{-1})	K_{ep} (min^{-1})	K_{ep} (min^{-1})
1	16	7.234	10.673	0.050	0.055	0.103	0.184
2	15	6.164	10.282	0.035	0.115	0.053	0.133
3	20	6.991	9.255	0.058	0.065	0.129	0.142
4	18	12.682	14.527	0.109	0.182	0.125	0.149
5	15	3.909	8.373	0.080	0.163	0.128	0.151
6	14	3.218	7.727	0.055	0.095	0.093	0.120
7	15	5.182	9.627	0.042	0.077	0.084	0.105
8	18	8.309	14.182	0.075	0.097	0.099	0.175
9	20	5.645	9.693	0.043	0.094	0.092	0.164
10	14	2.982	4.327	0.052	0.131	0.124	0.158
Mean ± SD	16.5 ± 2.32	6.232 ± 2.867	9.867 ± 2.965	0.06 ± 0.022	0.107 ± 0.041	0.103 ± 0.024	0.148 ± 0.024

Abbreviations: Gd = Gadolinium, PTA = percutaneous transluminal angioplasty, BF = blood flow, SD = standard deviation.

the parametric maps using a Gaussian filter [20]. Dynamic CT can also provide information about perfusion status of the limb. Hur et al. used a CT perfusion technique in order to measure blood flow of the foot in animals and humans. They demonstrated that plantar dermis presented significant blood flow increase after revascularization [21]. Another study also showed that CT foot perfusion examination is a useful modality for estimation of PTA outcome in patients with CLI. After successful recanalization, a statistically significant increase in perfusion parameters was found. Moreover, patients with clinical improvement presented higher post-PTA perfusion parameter values compared to patients with poor response to PTA [22].

To our knowledge, this is the first study using a DCE-MRI technique in order to evaluate PTA outcome in patients with CLI. Our findings show that a statistically significant change in perfusion parameters is found after successful PTA in CLI patients. Compared to other studies (which also referred to different MRI techniques such as ASL or BOLD), all patients in this study presented with CLI (Rutherford 4–6 category). We suppose that successful PTA led to significant improvement in the macro- and microvascular status of the foot which improves also the perfusion parameters. We also noticed that there was no significant correlation between ABI and perfusion parameters as perfusion parameters are influenced not only by the macrovascular network of the foot (such as ABI) but also from the microvascular status of the limb.

Thirty years ago, Taylor and Palme introduced the angiosome theory in their anatomical study [23]. An angiosome is defined as a 3-dimensional block of tissue drained by specific vessels. Direct recanalization of the artery that supplies ischemic angiosome is associated with improved would healing and increased limb salvage in several studies [24–26]. On the other hand, not all lesions can be treated based on the angiosome model because of limitations such as

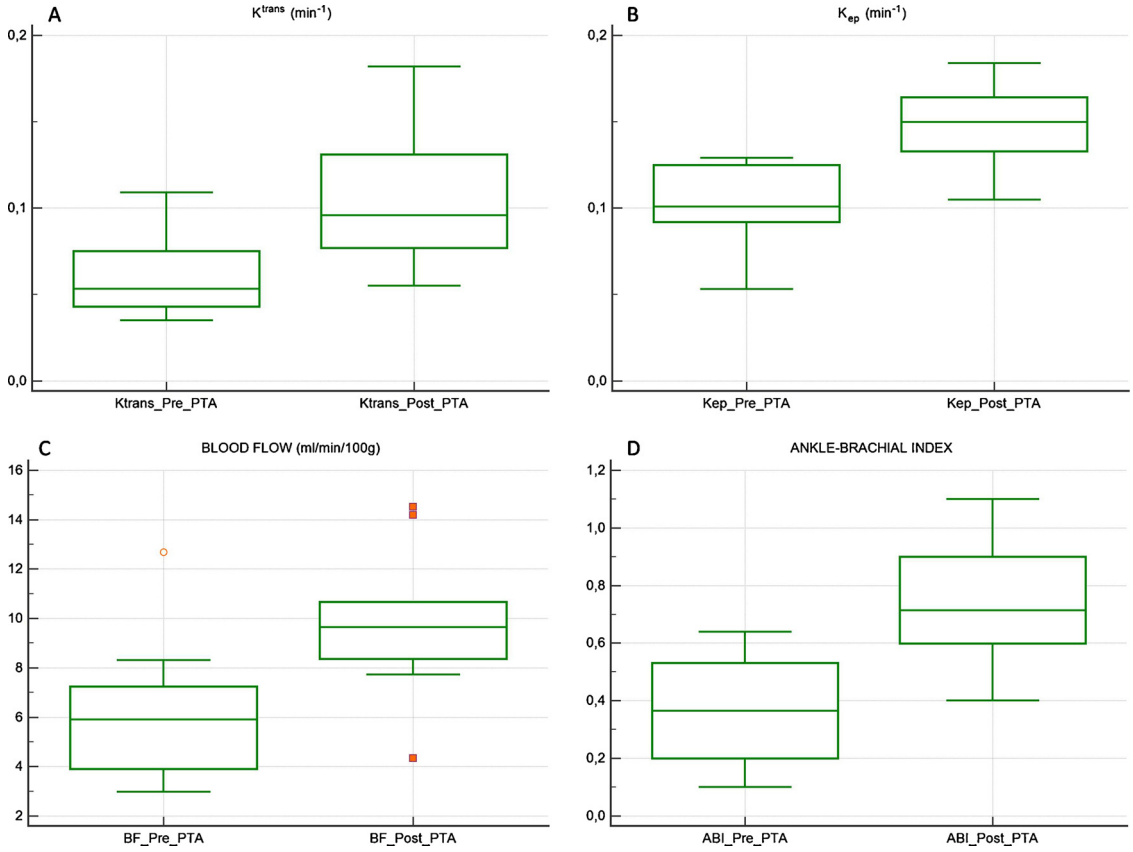

Fig. 2. Box-and-whisker plots depicting the median values and the quartile ranges of various perfusion parameters such as K^{trans} (A), K_{ep} (B) and Blood Flow (C), as well as the values of ankle-brachial index (D) before and after PTA. The boxes stretch from the 25th percentile at the lower edge up to the 75th percentile at the upper edge. The median value is depicted as a line across the box. Outliers are depicted as lines at the outer area of the box plot.

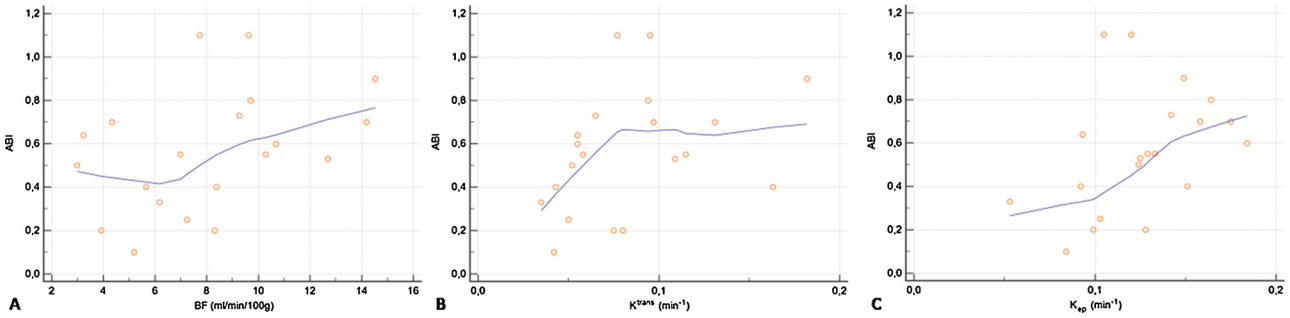

Fig. 3. Scatter plots showing the correlation between ABI and perfusion parameters such as BF (A), K^{trans} (B) and K_{ep} (C). The correlation analysis demonstrates no significant correlation between these parameters.

difficult access to the vessel or anatomical anomalies and this theory is also not applicable in by-pass surgery because the least affected artery is selected as the outflow vessel. As a result, there is great debate on targeting the procedure based on angiosomes and DCE-MRI may aid in quantifying and evaluating the angioplasty target area. The DCE-MRI perfusion maps can show the differences of the hemodynamic perfusion parameters in the affected angiosome after PTA which could be extensively useful to compare different endovascular therapeutic approaches (direct vs. indirect revascularization).

The current study has several limitations. DCE-MRI was not feasible in cases with severe motion artifact which compromised image evaluation. Moreover, this was a prospective study, so it was not possible to foresee the outcome of the patients. Three patients did not undergo successful endovascular recanalization and they were treated with surgical revascularization. Moreover, one patient died before post-procedural examination and one patient underwent amputation due to extensive ulcers before post-procedural examination too. These patients (n = 6) were excluded from the study. Furthermore, the post-procedural examinations were performed 1 month after PTA, so they did not describe the long-term changes in foot perfusion after PTA. Finally, the small number of patients is not adequate in order to correlate DCE-MRI results with the clinical improvement of patients.

5. Conclusion

In conclusion, DCE-MRI is a safe and reproducible technique which can be a useful modality for the evaluation of PTA outcome in patients with CLI. However, further investigations are warranted, including not only MRI but also CEUS, CT and nuclear spectroscopy techniques for the evaluation of foot perfusion and monitoring of endovascular treatment.

Funding

This research did not receive any specific grant from funding agencies in the public, commercial, or not-for-profit sectors.

CRediT authorship contribution statement

Nikolaos Galanakis: Conceptualization, Methodology, Formal analysis, Investigation, Data curation, Writing - original draft, Visualization. **Thomas G Maris:** Conceptualization, Software, Validation, Formal analysis, Visualization. **Nikolaos Kontopodis:** Validation, Resources, Data curation. **Christos V. Ioannou:** Conceptualization, Methodology, Writing - review & editing. **Konstantinos Tsetis:** Investigation, Resources. **Apostolos Karantanas:** Writing - review & editing, Supervision, Project administration. **Dimitrios Tsetis:** Conceptualization, Methodology, Writing - review & editing, Supervision, Project administration.

Declarations of Competing Interest

All authors of the submitted article entitled "The role of dynamic contrast-enhanced MRI in evaluation of percutaneous transluminal angioplasty outcome in patients with critical limb ischemia" declare that they have no conflicts of interest.

Acknowledgments

None.

References

[1] P. Abdulhannan, D.A. Russell, S. Homer-Vanniasinkam, Peripheral arterial disease: a literature review, Br. Med. Bull. 104 (2012) 21–39.
[2] J.W. Olin, C.J. White, E.J. Armstrong, D. Kadian-Dodov, W.R. Hiatt, Peripheral artery disease: evolving role of exercise, medical therapy, and endovascular options, J. Am. Coll. Cardiol. 67 (11) (2016) 1338–1357.
[3] L. Norgren, W.R. Hiatt, J.A. Dormandy, M.R. Nehler, K.A. Harris, F.G. Fowkes, T.I.W. Group, K. Bell, J. Caporusso, I. Durand-Zaleski, K. Komori, J. Lammer, C. Liapis, S. Novo, M. Razavi, J. Robbs, N. Schaper, H. Shigematsu, M. Sapoval, C. White, J. White, D. Clement, M. Creager, M. Jaff, E. Mohler 3rd, R.B. Rutherford, P. Sheehan, H. Sillesen, K. Rosenfield, Inter-society consensus for the management of peripheral arterial disease (TASC II), Eur. J. Vasc. Endovasc. Surg. 33 (Suppl 1) (2007) S1–75.
[4] W.R. Hiatt, Medical treatment of peripheral arterial disease and claudication, N. Engl. J. Med. 344 (21) (2001) 1608–1621.
[5] O. European Stroke, M. Tendera, V. Aboyans, M.L. Bartelink, I. Baumgartner, D. Clement, J.P. Collet, A. Cremonesi, M. De Carlo, R. Erbel, F.G. Fowkes, M. Heras, S. Kownator, E. Minar, J. Ostergren, D. Poldermans, V. Riambau, M. Roffi, J. Rother, H. Sievert, M. van Sambeek, T. Zeller, E.S.C.Cf.P. Guidelines, ESC guidelines on the diagnosis and treatment of peripheral artery diseases: document covering atherosclerotic disease of extracranial carotid and vertebral, mesenteric, renal, upper and lower extremity arteries: the Task Force on the Diagnosis and Treatment of Peripheral Artery Diseases of the European Society of Cardiology (ESC), Eur. Heart J. 32 (22) (2011) 2851–2906.
[6] A.W. Pollak, P.T. Norton, C.M. Kramer, Multimodality imaging of lower extremity peripheral arterial disease: current role and future directions, Circ. Cardiovasc. Imaging 5 (6) (2012) 797–807.
[7] P.S. Tofts, A.G. Kermode, Measurement of the blood-brain barrier permeability and leakage space using dynamic MR imaging. 1. Fundamental concepts, Magn. Reson. Med. 17 (2) (1991) 357–367.
[8] E.K. Fram, R.J. Herfkens, G.A. Johnson, G.H. Glover, J.P. Karis, A. Shimakawa, T.G. Perkins, N.J. Pelc, Rapid calculation of T1 using variable flip angle gradient refocused imaging, Magn. Reson. Imaging 5 (3) (1987) 201–208.
[9] G. Brix, W. Semmler, R. Port, L.R. Schad, G. Layer, W.J. Lorenz, Pharmacokinetic parameters in CNS Gd-DTPA enhanced MR imaging, J. Comput. Assist. Tomogr. 15 (4) (1991) 621–628.
[10] P. Vilela, H.A. Rowley, Brain ischemia: CT and MRI techniques in acute ischemic stroke, Eur. J. Radiol. 96 (2017) 162–172.
[11] C. Klassen, M. Nguyen, A. Siuciak, N.M. Wilke, Magnetic resonance first pass perfusion imaging for detecting coronary artery disease, Eur. J. Radiol. 57 (3) (2006) 412–416.
[12] P. Sujlana, J. Skrok, L.M. Fayad, Review of dynamic contrast-enhanced MRI: technical aspects and applications in the musculoskeletal system, Journal of magnetic resonance imaging: JMRI 47 (4) (2018) 875–890.
[13] D.C. Isbell, F.H. Epstein, X. Zhong, J.M. DiMaria, S.S. Berr, C.H. Meyer, W.J. Rogers, N.L. Harthun, K.D. Hagspiel, A. Weltman, C.M. Kramer, Calf muscle perfusion at peak exercise in peripheral arterial disease: measurement by first-pass contrast-enhanced magnetic resonance imaging, J. Magn. Reson. Imaging 25 (5) (2007) 1013–1020.
[14] R.B. Thompson, R.J. Aviles, A.Z. Faranesh, V.K. Raman, V. Wright, R.S. Balaban,

E.R. McVeigh, R.J. Lederman, Measurement of skeletal muscle perfusion during postischemic reactive hyperemia using contrast-enhanced MRI with a step-input function, Magn. Reson. Med. 54 (2) (2005) 289–298.
[15] A.W. Pollak, C.H. Meyer, F.H. Epstein, R.S. Jiji, J.R. Hunter, J.M. Dimaria, J.M. Christopher, C.M. Kramer, Arterial spin labeling MR imaging reproducibly measures peak-exercise calf muscle perfusion: a study in patients with peripheral arterial disease and healthy volunteers, JACC Cardiovasc. Imaging 5 (12) (2012) 1224–1230.
[16] G. Grozinger, R. Pohmann, F. Schick, U. Grosse, R. Syha, K. Brechtel, K. Rittig, P. Martirosian, Perfusion measurements of the calf in patients with peripheral arterial occlusive disease before and after percutaneous transluminal angioplasty using MR arterial spin labeling, J. Magn. Reson. Imaging 40 (4) (2014) 980–987.
[17] M. Edalati, M.K. Hastings, D. Muccigrosso, C.J. Sorensen, C. Hildebolt, M.A. Zayed, M.J. Mueller, J. Zheng, Intravenous contrast-free standardized exercise perfusion imaging in diabetic feet with ulcers, J. Magn. Reson. Imaging 50 (2) (2019) 474–480.
[18] H.P. Ledermann, A.C. Schulte, H.G. Heidecker, M. Aschwanden, K.A. Jager, K. Scheffler, W. Steinbrich, D. Bilecen, Blood oxygenation level-dependent magnetic resonance imaging of the skeletal muscle in patients with peripheral arterial occlusive disease, Circulation 113 (25) (2006) 2929–2935.
[19] R.W. Huegli, A.C. Schulte, M. Aschwanden, C. Thalhammer, S. Kos, A.L. Jacob, D. Bilecen, Effects of percutaneous transluminal angioplasty on muscle BOLD-MRI in patients with peripheral arterial occlusive disease: preliminary results, Eur. Radiol. 19 (2) (2009) 509–515.
[20] G.S. Ioannidis, K. Marias, N. Galanakis, K. Perisinakis, A. Hatzidakis, D. Tsetis, A. Karantanas, T.G. Maris, A correlative study between diffusion and perfusion MR imaging parameters on peripheral arterial disease data, Magn. Reson. Imaging 55 (2019) 26–35.
[21] S. Hur, H.J. Jae, Y. Jang, S.K. Min, S.I. Min, D.Y. Lee, S.G. Seo, H.C. Kim, J.W. Chung, K.G. Kim, E.A. Park, W. Lee, Quantitative assessment of foot blood flow by using dynamic volume perfusion CT technique: a feasibility study, Radiology 279 (1) (2016) 195–206.
[22] N. Galanakis, T.G. Maris, N. Kontopodis, C.V. Ioannou, E. Kehagias, N. Matthaiou, A.E. Papadakis, A. Hatzidakis, K. Perisinakis, D. Tsetis, CT foot perfusion examination for evaluation of percutaneous transluminal angioplasty outcome in patients with critical limb ischemia: a feasibility study, J. Vasc. Interv. Radiol. 30 (4) (2019) 560–568.
[23] G.I. Taylor, J.H. Palmer, The vascular territories (angiosomes) of the body: experimental study and clinical applications, Br. J. Plast. Surg. 40 (2) (1987) 113–141.
[24] V.A. Alexandrescu, G. Hubermont, Y. Philips, B. Guillaumie, C. Ngongang, P. Vandenbossche, K. Azdad, G. Ledent, J. Horion, Selective primary angioplasty following an angiosome model of reperfusion in the treatment of Wagner 1-4 diabetic foot lesions: practice in a multidisciplinary diabetic limb service, J. Endovasc. Ther. 15 (5) (2008) 580–593.
[25] K. Spillerova, N. Settembre, F. Biancari, A. Alback, M. Venermo, Angiosome targeted PTA is more important in endovascular revascularisation than in surgical revascularisation: analysis of 545 patients with ischaemic tissue lesions, Eur. J. Vasc. Endovasc. Surg. 53 (4) (2017) 567–575.
[26] H. Jongsma, J.A. Bekken, G.P. Akkersdijk, S.E. Hoeks, H.J. Verhagen, B. Fioole, Angiosome-directed revascularization in patients with critical limb ischemia, J. Vasc. Surg. 65 (4) (2017) 1208–1219 e1.

Magnetic Resonance Imaging 55 (2019) 26–35

Contents lists available at ScienceDirect

Magnetic Resonance Imaging

journal homepage: www.elsevier.com/locate/mri

A correlative study between diffusion and perfusion MR imaging parameters on peripheral arterial disease data

Georgios S. Ioannidis[a,d,*,1], Kostas Marias[a,e], Nikolaos Galanakis[b,d], Kostas Perisinakis[a,c], Adam Hatzidakis[b], Dimitrios Tsetis[b], Apostolos Karantanas[a,b], Thomas G. Maris[a,c]

[a] Foundation for Research and Technology - Hellas (FORTH), Institute of Computer Science (ICS), Computational Bio-Medicine Laboratory (CBML), Heraklion, Greece
[b] Department of Medical Imaging, University of Crete, Heraklion, Greece
[c] Department of Medical Physics, University of Crete, Heraklion, Greece
[d] Medical School, University of Crete, Heraklion, Greece
[e] Technological Educational Institute of Crete, Department of Informatics Engineering, Heraklion, Greece

ARTICLE INFO

Keywords:
Dynamic contrast enhanced MR imaging
Diffusion weighted imaging
Peripheral arterial disease
Intravoxel incoherent motion
Mutual information (MI)
Pearson's correlation coefficient

ABSTRACT

Purpose: The purpose of this study was to correlate diffusion and perfusion quantitative and semi-quantitative MR parameters, on patients with peripheral arterial disease. In addition, we investigated which perfusion model better describes the behavior of the dynamic contrast-enhanced (DCE) MR data signal on ischemic regions of the lower limb.

Methods: Linear and nonlinear least squares algorithms, were incorporated for the quantification of the parameters through a variety of widely used models, able to extract physiological information from each imaging technique. All numerical calculations were implemented in Python 3.5 and include the: Intra voxel incoherent motion for diffusion and Patlak's, Extended Toft's and Gamma Capillary Transit time (GCTT) models for perfusion MRI.

Results: Our initial voxel by voxel correlation analysis didn't show any significant correlation based on the Pearson's Correlation metric between diffusion and perfusion parameters. To account for the inherited noise from the raw data, a Gaussian filter was applied to the parametric maps in order for the data to be comparable. By repeating our analysis in the filtered image maps, a good correlation (> 0.5) of diffusion and perfusion parameters was achieved.

Conclusions: Perfusion and diffusion MRI quantitative and semi-quantitative parameters can be obtained through a variety of physiological-pharmacokinetic models. This paper compares most of the widely-known models and parameters in both techniques with data from patients with peripheral arterial disease. Initial analysis showed no correlation in the perfusion parametric maps of DWI and DCE MRI data but a good correlation was obtained after smoothing the parametric maps indicating that perfusion information could be obtained from diffusion MRI images in patients with peripheral arterial disease.

1. Introduction

Dynamic contrast enhanced magnetic resonance imaging (DCE-MRI) is one of the most commonly used imaging techniques for measuring perfusion in biological tissues. DCE-MRI is based on acquiring a series of T1-weighted (T1W) images through time before and after the injection of exogenous gadolinium based contrast agent (CA) [1]. This procedure produces signal intensity time curves that after a suitable mathematical process and a selection of a proper model may provide information on vascular permeability, tissue perfusion, and expansions of extravascular- extracellular spaces (EES) [2].

Diffusion Weighted Imaging (DWI) is a technique that exploits the mobility of water molecules (molecular diffusion or Brownian motion) to produce signal on an MR image without contrast administration. A significant parameter that quantifies the degree of diffusion weighting (DW) applied is the b-value (in s/mm^2) which is mainly related with the

* Corresponding author at: Computational Bio-Medicine laboratory, Foundation for Research and Technology – Hellas, 100 Nikolaou Plastira str., Vassilika Vouton, Heraklion, Crete GR 700 13, Greece.
E-mail address: geo3721@ics.forth.gr (G.S. Ioannidis).
URL: http://www.ics.forth.gr/cbml/ (G.S. Ioannidis).
[1] Postal address: P.O. Box 1385, Heraklion, Crete GR - 711 10, Greece.

https://doi.org/10.1016/j.mri.2018.08.006
Received 26 January 2018; Received in revised form 7 August 2018; Accepted 14 August 2018

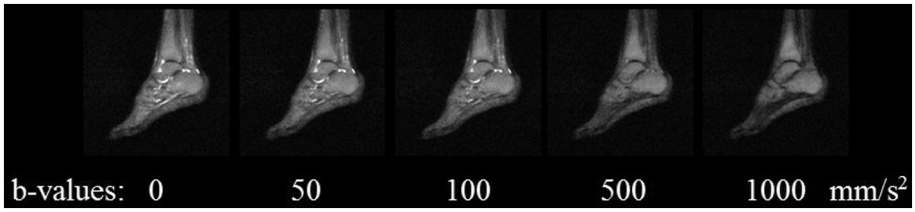

Fig. 1. DWI sequence of a central slice of the lower limb with 5 b values.

amplitude and time of the diffusion sensitizing gradients utilized on the MR scanner. The DW signal as a function of the b-value is considered to follow a mono-exponential decay providing the Apparent Diffusion Coefficient (ADC) (mm^2/s) [3]. In biological tissues, the mono-exponential model was not capable of analyzing the DW signal due to the presence of blood micro-circulation [4]. The micro-circulation of blood or micro-perfusion was considered to follow a Brownian motion model due to the random organization of the capillary network. Le Bihan et al. suggested the Intra-Voxel Incoherent Motion (IVIM) model in order to take into account both the real diffusion of water and the micro-circulation of blood inside a voxel [4].

Fitting the IVIM model to the DWI data, provides information not only about water diffusivity but also about soft tissue perfusion. This advantage of the diffusion IVIM model leads to the clinical question of the possible correlation between perfusion parameters deriving from DWI and DCE-MRI and whether the former can provide reliable, clinically-useful tissue perfusion information.

Several published works have shown the positive correlation of perfusion information between DCE-MRI and DWI in different regions and pathologies of the human body such as brain malignancies, [5,6] breast cancer [7] and head and neck squamous cell carcinoma [8]. These studies have in common the aggressiveness of each cancer type and consequently high vascularity and perfusion. On the contrary, the study of low tissue perfusion has not been extensively examined. To this end, we employ DCE-MRI and DWI techniques as a preliminary step for perfusion quantification on patients with peripheral arterial disease (PAD). The targeted impact of this work concerns the potential extraction of perfusion information from DWI-MRI avoiding CA administration especially in cases of clinical or other contraindications.

To address the above issues the aim of this paper is to qualitatively show the linear relationship between parametric maps originating from various known models obtained by DWI and DCE-MRI techniques with the application of a Gaussian filter. This comparative study was applied to patients with severe PAD before any kind of treatment.

PAD is an atherosclerotic process that causes stenosis or occlusion on lower extremity arteries. The major risk factors for PAD include older age, diabetes mellitus, hypertension, hyperlipidemia and smoking [9]. Patients with PAD may be asymptomatic or develop intermittent claudication. Ischemic rest pain, gangrene or ischemic ulcers may represent severe complications of PAD, leading to critical limb ischemia (CLI) [10]. Patients with CLI are at a higher amputation risk and require immediate revascularization by means of surgical or endovascular procedures [11].

2. Materials and methods

2.1. Patient population

During a 2 year-year study period (2015–2017), 13 patients (8 males, 5 females) with PAD underwent MR examination of lower limb. The median age was 68 years (range 56–78 years). All patients presented with CLI and according to Fontaine classification [12], 4 patients had stage III and 9 patients stage IV PAD. Exclusion criteria were all common contraindications to MRI, like pacemakers, ferromagnetic implants and claustrophobia and contraindications for administration of Gadolinium contrast medium such us renal insufficiency and allergy to gadolinium. The study was approved by the local ethic committee and all patients signed informed consent prior to examination.

2.2. MRI protocol

Each of 13 patients underwent MR examination on a 1.5 T clinical MR Scanner (Vision/Sonata Hybrid system, Siemens, Erlangen, Germany) enforced with powerful gradients (Strength: 45 mT/m, Slew rate: 200 mT/m/ms), equivalent with those gradients operating on 3 T systems.

The imaging protocol, apart from the conventional sequences, included DWI and DCE-MRI quantitative techniques. DW sagittal images of the lower limb were acquired utilizing a high resolution HASTE (Half-Fourier Acquisition Single-shot Turbo spin Echo) sequence with diffusion sensitizing gradients with b-values (b = 0, 50, 100, 150, 200, 500, 800, 1000 s/mm^2), number of slices = 13, echo time (TE) = 105 ms, repetition time (TR) = 2000 ms, matrix size = 384 × 384, field of view (FOV) = 250 × 250, slice thickness = 5 mm. Additionally, a reverse polarization gradient technique was applied by acquiring two sets of sagittal DW images, each time altering the polarization direction of the frequency encoding gradient A-P and P-A (Anterior-Posterior) [13]. This technique has been applied for the reduction of machine related geometrical distortions or apparent distortions in signal intensities. The final calculated image was the mathematical average of the two aforementioned DW sets. An example for five b-values of a central slice is shown in Fig. 1.

T1W DCE perfusion MR imaging of the lower limb was performed by utilizing a 3D VIBE (volume interpolated breath hold examination) sequence in the sagittal plane with variable flip angles (FA = 5°,10°,15°, 20°, 25°, 30°) for the initial calculation of the parametric T1 maps. Consequently, an intravenous continual injection of the paramagnetic CA (Magnevist, Gadopentetate Dimeglumine, Bayer Healthcare, Bayer, 0.1 mmol/kg) was administered for approximately 1 min. The aforementioned T1W DCE VIBE perfusion sequence was continuously repeated for 10min (20 s temporal resolution) after the intravenous injection of the CA with the following imaging parameters: number of slices = 26, FA = 15°, TE = 2.73 ms, TR = 7.8 ms, matrix size = 512 × 512, FOV = 250 × 250 and slice thickness = 3 mm.

2.3. DWI-MRI analysis

The quantification of both diffusion and perfusion parameters was implemented in our platform using python 3.5 [14]. More specifically, all parametric maps were obtained with the use of a trust region reflective algorithm [15], suitable for solving nonlinear bound-constrained minimization problems as defined in SciPy library [16] (scipy.optimize.least_squares).

According to the IVIM, the DWI signal as a function of the b-value is expressed in Eq. (A.1). S(b) is the measured signal intensity at the current b-value and $S(0)$ is the measured signal intensity without diffusion gradient attenuation factor (typically a T2 image), D is the diffusion coefficient, D^* is the pseudo-diffusion coefficient and f is the micro-perfusion fraction denoting the ratio of water flowing in capillaries to the total water contained in a voxel.

The quantification of the DW signal with the IVIM model is mainly succeeded by two different fitting methods. The first method is a direct

estimation of the IVIM parameters using the aforementioned nonlinear fitting algorithm with the following constraints for each parameter:

$$f \in (0,1),\ D \in (0,5) \times 10^{-3} mm^2/s,\quad D^* \in (10{,}200) \times 10^{-3} mm^2/s.$$

The second method is relied on the fact that for b-values $>$ 200 s/mm^2 the micro-perfusion effect is eliminated and does not contribute to the DW signal decay [17]. Thus, in the high b-value range (b $>$ 200 s/mm^2) the signal attenuation is considered to be of the form of Eq. (A.2) and D is estimated by using a linear fit to Eq. (A.2) after taking the logarithm of both sides (scipy.optimize.lsq_linear). Once D is known, parameters f and D* are estimated from Eq. (A.1) by using the nonlinear fitting algorithm with the same bound constraints as in the first method for all available b-values.

2.4. DCE-MRI analysis

The procedure for the quantification of the DCE-MRI signal has two important steps [18]. First, the concentration curve as a function of time of the CA is computed ($C_t(t)$) and then, after the choice of a suitable pharmacokinetic model, nonlinear fitting of the concentration curve is required in order to produce tissue perfusion parameters.

The linear relationship between the relaxation rates ($R_1 = 1/T_1$, $R_{10} = 1/T_{10}$) and the CA concentration (c) in the tissue is given by Eq. (A.3). T_{10} is the relaxation time of tissues before the injection of CA and T_1 after the injection of CA and $r_1 \approx 4.5\,s^{-1}\,mM^{-1}$ is the ratio of CA concentration to the increase in relaxation rate R_1 measured at 1.5 T.

The signal (S) of the variable flip angle (θ) sequence before the injection of the CA, is given by Eq. (A.4) [19] with TR = 7.8 ms from the imaging protocol. S_0 is the relaxed signal. Therefore, both S_0 and T_{10} were fitted to Eq. (A.4) with bound constraints $S_0 \in (1{,}10.000)$, $T_{10} \in (0,5)$ ms. Thus, for every voxel in time, the concentration curve was calculated from Eq. (A.3) after solving for T_1 on Eq. (A.4).

In order to provide information about tissue perfusion to patients with PAD a variety of pharmacokinetic models were used such as, the extended Tofts model (ETM) [20], the Patlak model (PM) [21], the steady state model (SSM) [22] and the Gamma capillary transit time model (GCTT) [23].

ETM is the most widely used model for the analysis of DCE MRI data [24] and describes a highly perfused tissue with the assumption of a bidirectional transfer of the CA between the blood plasma and the EES. Mathematically, the model is described by Eq. (A.5).

The symbol $\circledast$ represents the convolution operator, $K^{Trans}\ min^{-1}$ is the transfer constant from the blood plasma into the EES and $K_{ep} min^{-1}$ is the transfer constant from the EES back to the blood plasma while v_p stands for the plasma volume and $C_a(t)$ for the time concentration curve of a feeding artery, also known as the arterial input function (AIF). In our case, the AIF was the same for all perfusion models and selected carefully by clinicians from the posterior tibial artery. The selection of the AIF and the AIF curve over time is shown in Fig. 2.

A special case of the ETM when there is no transfer of CA from the EES back to blood plasma is the PM and it is given by Eq. (A.6). In addition, if it is assumed that there is no transfer of CA from the blood plasma into the EES, the SSM model is acquired, indicating that the concentration of the feeding artery and the tissue concentration are in a state of equilibrium. The one parameter SSM is presented by Eq. (A.7).

Except from its complex form, the GCTT model was included in this study since it is a more recently suggested physiological model unifying well-known models such as the Tofts Model [25],the ETM, the adiabatic tissue homogeneity (ATH) model [26] and the two compartment exchange (2CX) model [27]. The GCTT model is presented in Eq. (A.8). F $mL/mL/min^{-1}$is the blood flow or blood perfusion, $a^{-1} = t_c/\tau$ is the width of the distribution of the capillary transit times inside a voxel, $\gamma(a,z)$ is the gamma function, E is the extraction fraction of CA that is extracted into the EES during a single capillary transit.

Except from the previous models, two semi quantitative parameters were also calculated from the signal intensity curve over time $SI(t)$ such as the area under the curve (AUC) and the relative enhancement ratio (RER) Eqs. (A.9) and (A.10) respectively.

2.5. Statistical analysis

In this work, two statistical metrics were used, the adjusted R squared ($\overline{R}^2$) and the root mean squared error (RMSE), to determine the goodness of fit for every voxel. Assuming that the model function is $G(x,t)$ with parameters $x = \{x_1, x_2, \ldots, x_p\}$ and N data points d the RMSE formula is given by Eq. (A.11).

$\overline{R}^2$ is a generalized metric that is based on the R squared (R^2) and its value will always be less than or equal to that of $\overline{R}^2 \in [0,1]$. This metric was proposed to overcome the limitation of R^2 concerning that its value increases when more explanatory variables are added to the model. Therefore, it was considered to be more suitable for this study than R^2 since it captures the number of data points (N) as well as the number of the explanatory variables (p) of the model function Eq. (A.12).

2.6. Correlation analysis

Firstly, to examine the relation between DWI and DCE-MRI data for every individual patient, perfusion parametric maps were resized through cubic interpolation to the size of the diffusion parametric maps. Pearson's r correlation coefficient was then calculated taking into account the slices from perfusion and diffusion sequences with the same slice location dicom tag, while rejecting all voxels from tissues without significant blood supply (non-perfused) such as the osseous structures ($v_p = 0$). To ensure that after resizing, the parametric maps are accurately registered in space, we performed two tests as shown in Fig. 8. The color-coded fusion of a DW image on a perfusion T1W image is presented and a Canny edge detector ($\sigma = 0.5$) [28] highlighted the edges of DCE T1W image which are then superimposed on the corresponding DW image. Both tests clearly demonstrated accurate alignment in all DWI, DCE-MRI image pairs used in our analyses according to senior radiologists involved in the study.

The effects of noise, after the fitting process, led to parametric maps that exhibit large variations within voxels in small neighborhoods (Fig. 6). Thus, in order to examine the relationship between DCE and DWI parameters in a more effective and qualitative way, a 5×5 Gaussian filter ($\sigma = 0.9$) was applied on the derived parametric maps.

2.7. Mutual information analysis

Except from the Pearson's Correlation metric and the consideration of the images (parametric maps) as random variables, we also calculated the Mutual Information (MI) of the previously described diffusion and perfusion parameters with and without Gaussian filter. Mutual information metric arises from information theory and measures how much one random variable (an image in our case) tells us about another [29]. MI is an alternative perspective of checking the correlation between different imaging techniques that does not take into account only pixel values such as Pearson's correlation but also the entropy of the image pair.

Considering two discrete random variables X and Y of size N with their mass probability functions p(X), p(Y) and with their joint probability mass function p(x, y) it is possible to calculate their mutual information. On our case the random variables (X,Y) are (f,vp). Prior to the definition of the mutual information it is obligatory to define the entropy of a random variable X which is given by Eq. (A.13). Furthermore, the joint entropy H(X,Y) of a pair of discrete random variables (X,Y) with a probability mass function p(x,y) is given by Eq. (A.14). Having the formulae of the entropies above, the MI is calculated by Eq. (A.15) [30].

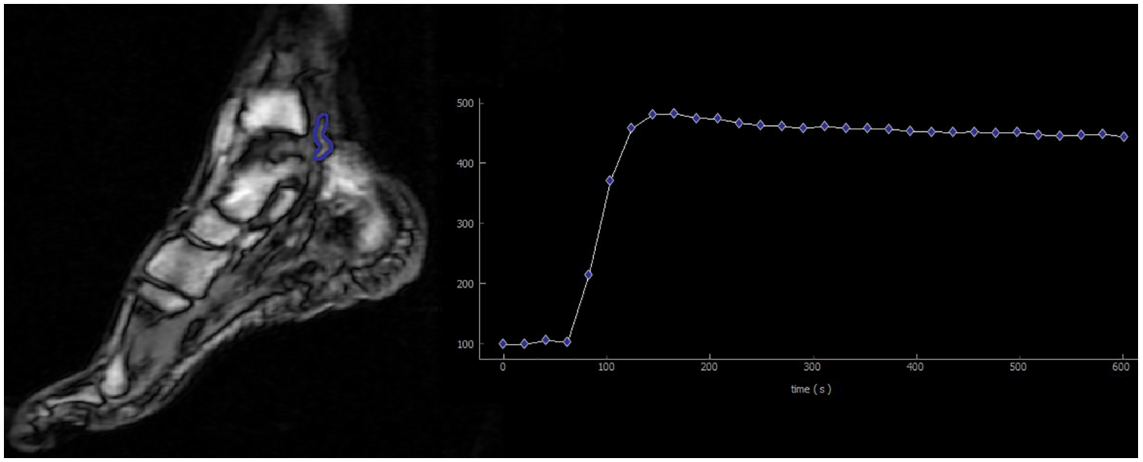

Fig. 2. The blue ROI of the AIF is shown on the T1W image of perfusion sequence (left) and its curve over time on the plot (right). (For interpretation of the references to color in this figure legend, the reader is referred to the web version of this article.)

2.8. Signal to noise ratio (SNR)

A significant factor about image quality is SNR. In our study, SNR was calculated by Eq. (A.16) in which, mean(SI_{ROI}) is the mean signal intensity from the selected region of interest (ROI) and std(BG_{ROI}) is the standard deviation of a background ROI which was meticulously taken outside of the depicted image volume avoiding any prominent artifact. Since the recorded signals from the BG_{ROI} follow a Rayleigh rather than a Gaussian distribution, the SNR value was multiplied by the correction factor 0.655 [31]. For every patient, SI_{ROI} was selected from the whole anatomical image of the central slice. The calculated SNR for DW images was graphically presented as a box and whisker plot for every b-value (Fig. 3). The calculated SNR for the variable flip angle Proton Density weighted (PDW) and T1W images is shown in Fig. 4. Finally, the calculated SNR for the perfusion weighted images was calculated for three time points, the one before the injection of the CA (Baseline), the time at the Maximum signal from the signal intensity curve (time to peak TTPK) and at the last time point of the perfusion sequence as is shown in Fig. 5. Every box and whisker plot contains the calculated SNR for every patient.

3. Results

3.1. DWI and DCE MRI fitting performance

Metrics from the statistical analysis, showed that regarding the DWI fitting, both the first and the second fitting method were quite accurate since RMSE and $\overline{R}^2$ were as expected at the desired levels, meaning low RMSE and high $\overline{R}^2$. More precisely, for the first fitting method, RMSE = 0.081 ± (0.048), $\overline{R}^2$ = 0.637 ± (0.292) and for the second method, RMSE = 0.085 ± (0.05), $\overline{R}^2$ = 0.627 ± (0.285). DCE MRI statistical metrics for each perfusion model are shown in Table 1. A graphical representation of each aforementioned model fit in a region of the peroneus brevis muscle for DWI and DCE-MRI is depicted in Fig. 9 and Fig. 10 respectively.

3.2. DWI and DCE MRI correlation

Pearson's correlation (r) coefficient was calculated for every perfusion and diffusion model-based parametric map. In Table 2, Pearson's correlation coefficient r, is presented between the parameter (f-IVIM) and the perfusion plasma volume parameters. A graphical illustration of the normalized parametric maps is depicted in Fig. 6. Analogously, r after the application of the Gaussian filter on the parametric maps is presented between (f-IVIM) and the perfusion parameters in Table 3

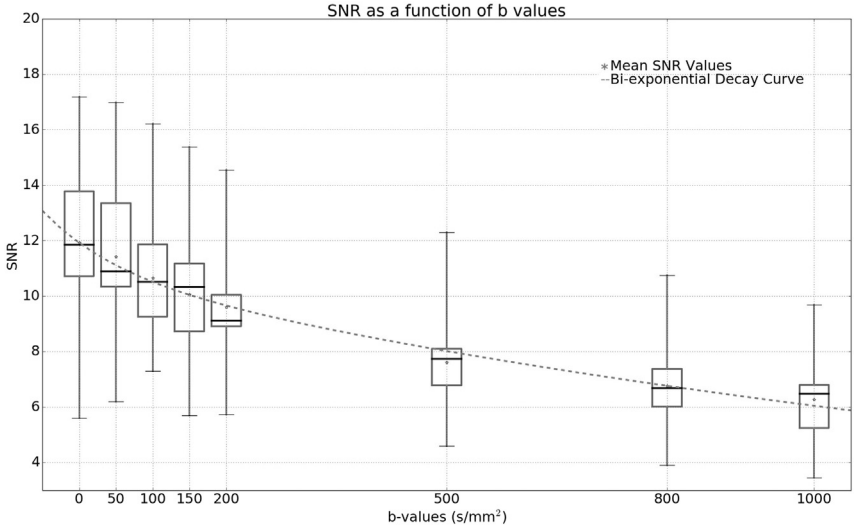

Fig. 3. SNR as a function of b-values for every patient. Star dots present the mean SNR value and the dotted line is the fitted IVIM function to the star dots.

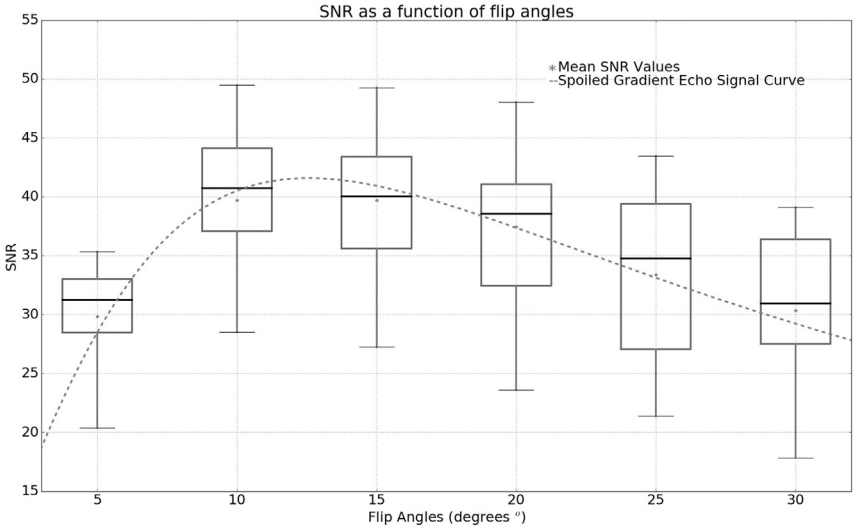

Fig. 4. SNR as a function of flip angles for every patient. Star dots present the mean SNR value and the dotted line is the fitted Eq. (A.4) to the star dots.

while the smoothed parametric maps are shown in Fig. 7. All p-values of the correlation analysis for both tables were lower than 0.05.

3.3. Mutual information analysis

As in the previous paragraph MI was calculated between f-IVIM (method 1) and the perfusion plasma volume parameters. The results for each model are depicted as boxplots before and after applying the Gaussian filter in Fig. 11.

4. Discussion and conclusions

The main goal of this study was to show the relationship between diffusion and perfusion related parameters. This constitutes a challenging goal since gadolinium based contrast agents are increasingly restricted due to effects on the human body according to EMA (European Medicines Agency) [32]. For this reason, the use of DWI taking advantage of its micro-perfusion instead of perfusion, is of outmost importance.

To the best of our knowledge, the majority of the published works on patients with PAD disease arterial spin labeling (ASL) and Blood oxygenation level-dependent (BOLD) MRI techniques are used [33–36]

Table 1
Perfusion statistical Metrics per model.

Fitting model	RMSE ± (std)	$\bar{R}^2$ ± (std)
SSM	0.033 ± (0.092)	0.126 ± (0.171)
PM	0.031 ± (0.091)	0.337 ± (0.316)
ETM	0.039 ± (0.101)	0.322 ± (0.321)
GCTT	0.029 ± (0.082)	0.143 ± (0.221)

Table 2
Pearson's Correlation coefficient r without Gaussian Filtering to the parametric maps.

Fitting model (parameter)	DWI-Method 1 (f)	DWI-Method 2 (f)
SSM (v_p)	0.082	0.086
PM (v_p)	0.073	0.071
ETM (v_p)	0.046	0.043
GCTT (E)	0.039	0.045
AUC	0.011	0.013
RER	−0.114	−0.107

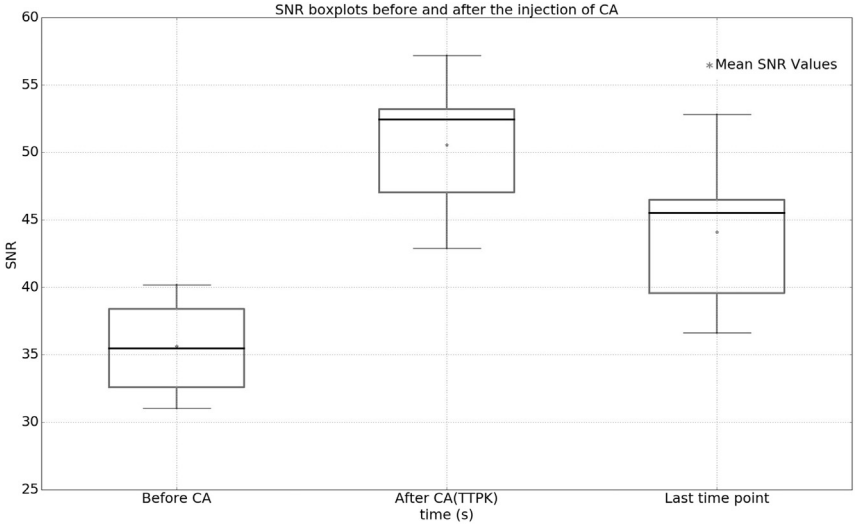

Fig. 5. SNR of the perfusion imaging sequence for three indicative time points (Baseline, TTPK, Last point of imaging sequence).

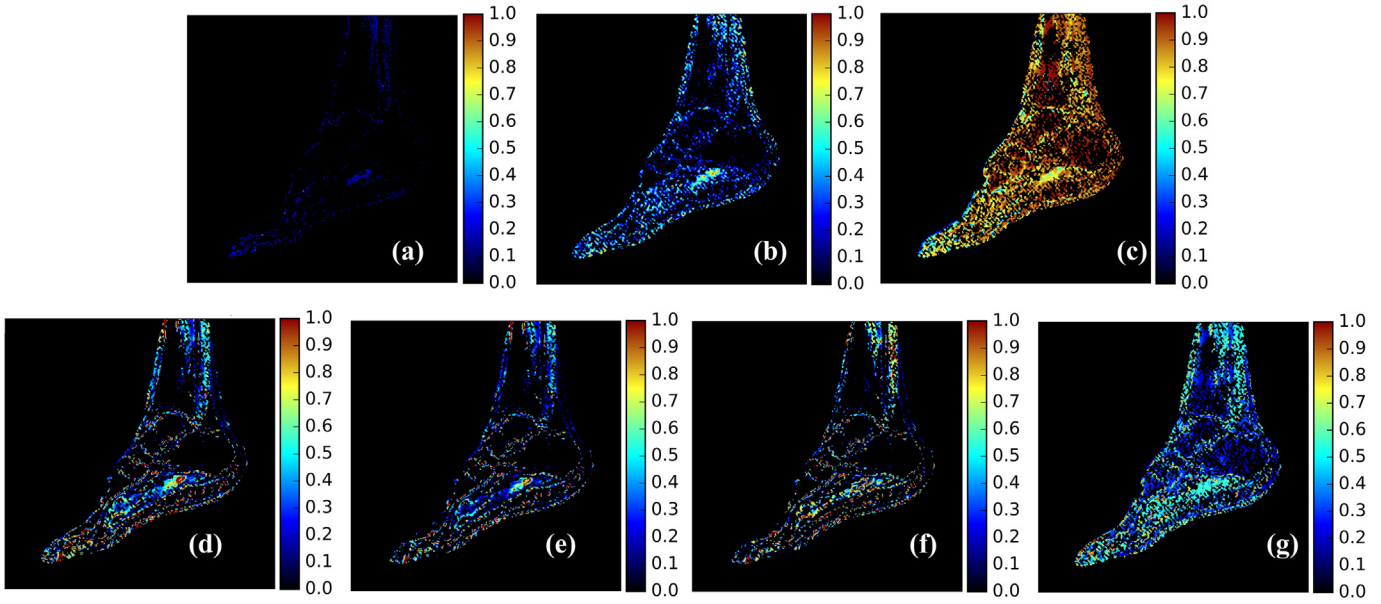

Fig. 6. Blood plasma volume related parametric maps. (b) f-IVIM, semi- quantitative: (a) RER and (c) AUC and (d)-(g) SSM (vp), PM (vp), ETM (vp), GCTT (E) respectively.

Table 3
Pearson's Correlation coefficient r with Gaussian Filtering to the parametric maps.

Fitting model (parameter)	DWI-Method 1 (f)	DWI-Method 2 (f)
SSM (v_p)	0.429	0.427
PM (v_p)	0.379	0.366
ETM (v_p)	0.406	0.397
GCTT (E)	**0.544**	**0.551**
AUC	0.254	0.252
RER	**0.592**	**0.601**

to quantify PAD disease. Moreover, DWI technique has not been used. Thus, a priori knowledge of quantitative results in PAD disease could not be possible to be compared with our results.

This paper examined the possible correlation between perfusion parameters derived from DWI and DCE-MRI and whether the former can provide robust and accurate information regarding perfusion of an individual anatomic region which in cases of PAD is clinically important.

To examine this possible correlation, we analyzed PAD data. The statistical metrics RMSE and $\overline{R}^2$ were used for both diffusion and perfusion models and were computed in all cases in order to enhance the reliability of the results. RMSE for diffusion fitting methods and perfusion models was (as expected) low and very similar (in order of magnitude) for all models due to the tolerance of the fitting algorithm (10^{-16}). Though, the dominant statistical metric that played a great role to our analysis was the strict metric $\overline{R}^2$ due to its ability to handle the number of data points and explanatory variables of each model.

Due to $\overline{R}^2$, it could be expected that the best and the most widely used model for perfusion imaging would be the extended Tofts model.

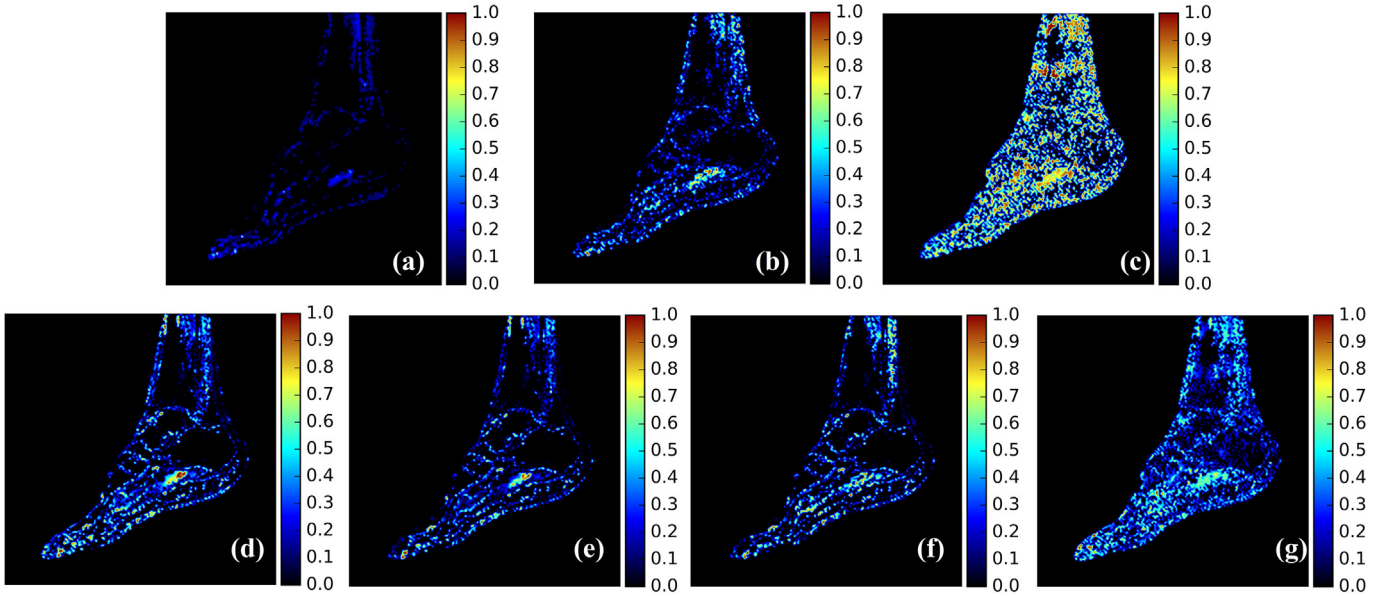

Fig. 7. Blood plasma volume related parametric maps after the application of a 5 × 5 Gaussian filter (σ = 0.9). (b) f-IVIM, semi- quantitative: (a) RER and (c) AUC and (d)-(g) SSM (vp), PM (vp), ETM (vp), GCTT (E) respectively.

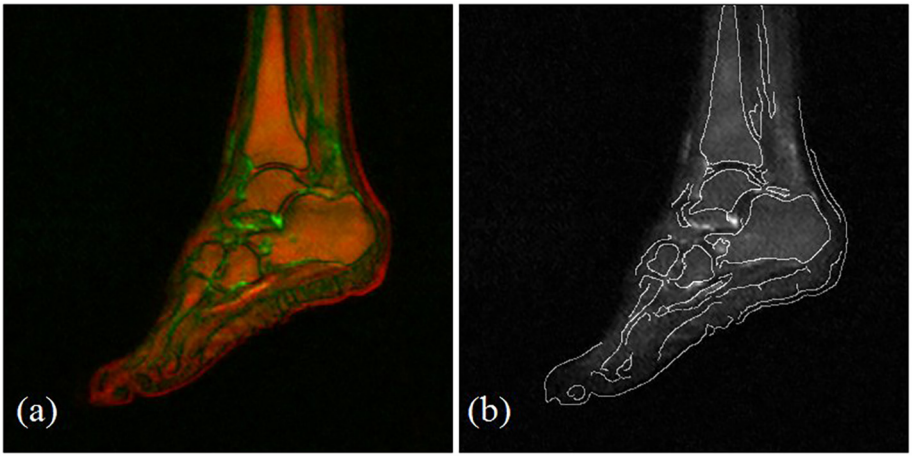

Fig. 8. (a) Color fusion of aligned DCE-MRI and DWI. Red color intensity indicates areas of high perfusion and green intensity represents high DWI signal. (b) T1W edges with Canny edge detector with σ = 0.5 superimposed on the DW corresponding image. (For interpretation of the references to color in this figure legend, the reader is referred to the web version of this article.)

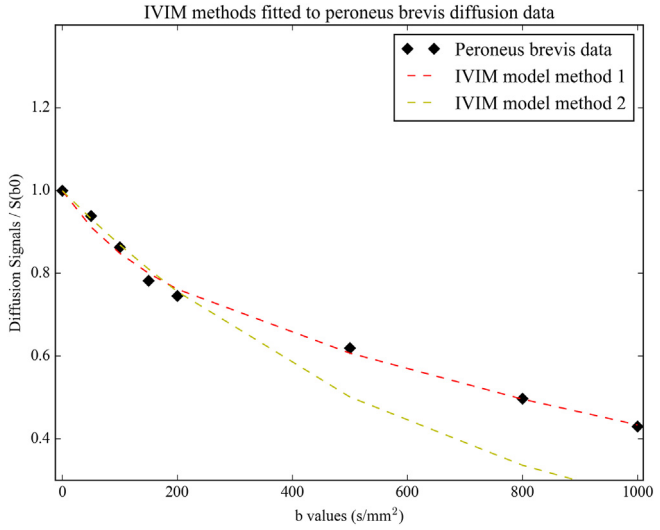

Fig. 9. IVIM model method 1 and 2 fitted to DWI data obtained from the peroneus brevis muscle.

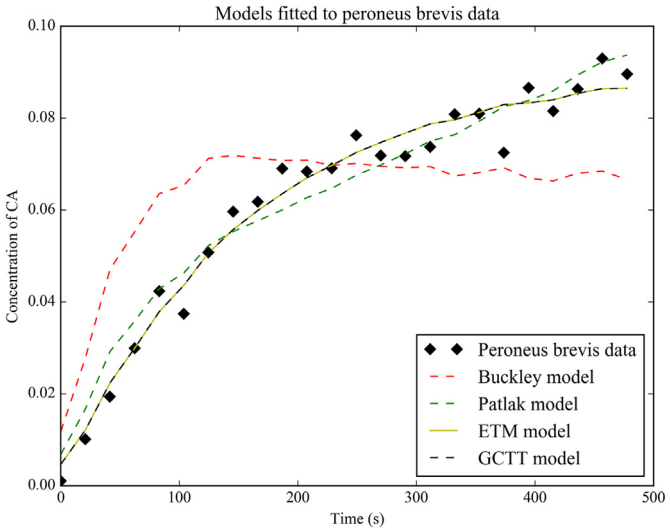

Fig. 10. Pharmacokinetic models fitted to DCE data derived from the peroneus brevis muscle.

On the contrary, Patlak's model achieved a little higher $\overline{R}^2$ than ETM (Table 1). This could be attributed to the PAD which causes stenosis or occlusion on lower extremity arteries. As mentioned earlier Patlak's model assumes no transfer of CA from the EES back to blood plasma, in contrast to ETM that assumes a bidirectional transfer of the CA between the blood plasma and the EES. Regarding to DWI, no significant differences on adjusted R2 values between IVIM fitting method 1 and method 2 were observed.

A variety of perfusion models quantitative and semi-quantitative and two diffusion analysis methods were used. The results of the standard fitting procedure (meaning no Gaussian filtering) showed no correlation at all because Pearson's r was close to zero. However, looking at the parametric maps, (Fig. 6) the visual inspection of the raw data confirmed the noise coming from the imaging process and led us to use the Gaussian filter for smoothing the parametric maps (Fig. 7) and removing the inherent noise. Subsequently, diffusion parameter f-IVIM on both diffusion methods was correlated well with GCTT-E ($r_{GCTT\ E-fmethod\ 1} = \mathbf{0.54}, r_{GCTT\ E-fmethod\ 2} = \mathbf{0.551}$) and with RER ($r_{RER-fmethod\ 1} = \mathbf{0.592}, r_{RER-fmethod\ 2} = \mathbf{0.601}$). These encouraging results point out the necessity for more thorough studies, possibly by utilizing MR scanners with higher field strengths and diffusion sensitizing gradients. Moreover, the use of HASTE or TSE sequences enforced with powerful fast switching diffusion sensitizing gradients and multiple b-values with higher ranges (> 2000) is an absolute necessity. The ultimate goal would be therefore, to reduce DCE-MR perfusion examinations by performing DWI micro-perfusion studies. This will eventually whittle the use intravenous injections of CA and increase the number of patient groups enrolling in such type of studies.

Furthermore, in all of our cases of the results from mutual information analysis (Fig. 11) we observed an increment in MI of image pairs greater than approximately 42% after the application of the Gaussian filter. This strongly indicates that Gaussian filtering significantly increases the similarity between DWI and DCE image pairs and explains the vast improvement in the perfusion correlation results.

Similar published works on different parts of the human body and diseases confirm our results and altogether add to the consistent correlation of DCE and DWI MRI perfusion maps. Kim et al. and Federau et al. on their research concerning quantitative parameters on brain malignancies report that f-IVIM and CBV from Dynamic Susceptibility Contrast MRI, were positively correlated with $r = 0.67$ and $r = 0.75$ respectively [5,6]. Furthermore, Suo et al. on their semi-quantitative perfusion DCE analysis on breast cancer with a 3 T MR scanner and by filtering the DCE data with a Gaussian filter, achieved a correlation between (f-IVIM) values and RER with $r = 0.55$ and (f-IVIM) values and AUC with $r = 0.56$ [7]. We appraise that possible reasons these two studies achieved better correlations than ours and Suo's et al., might be: the absence of macroscopic motion artifacts of the patient, the presence

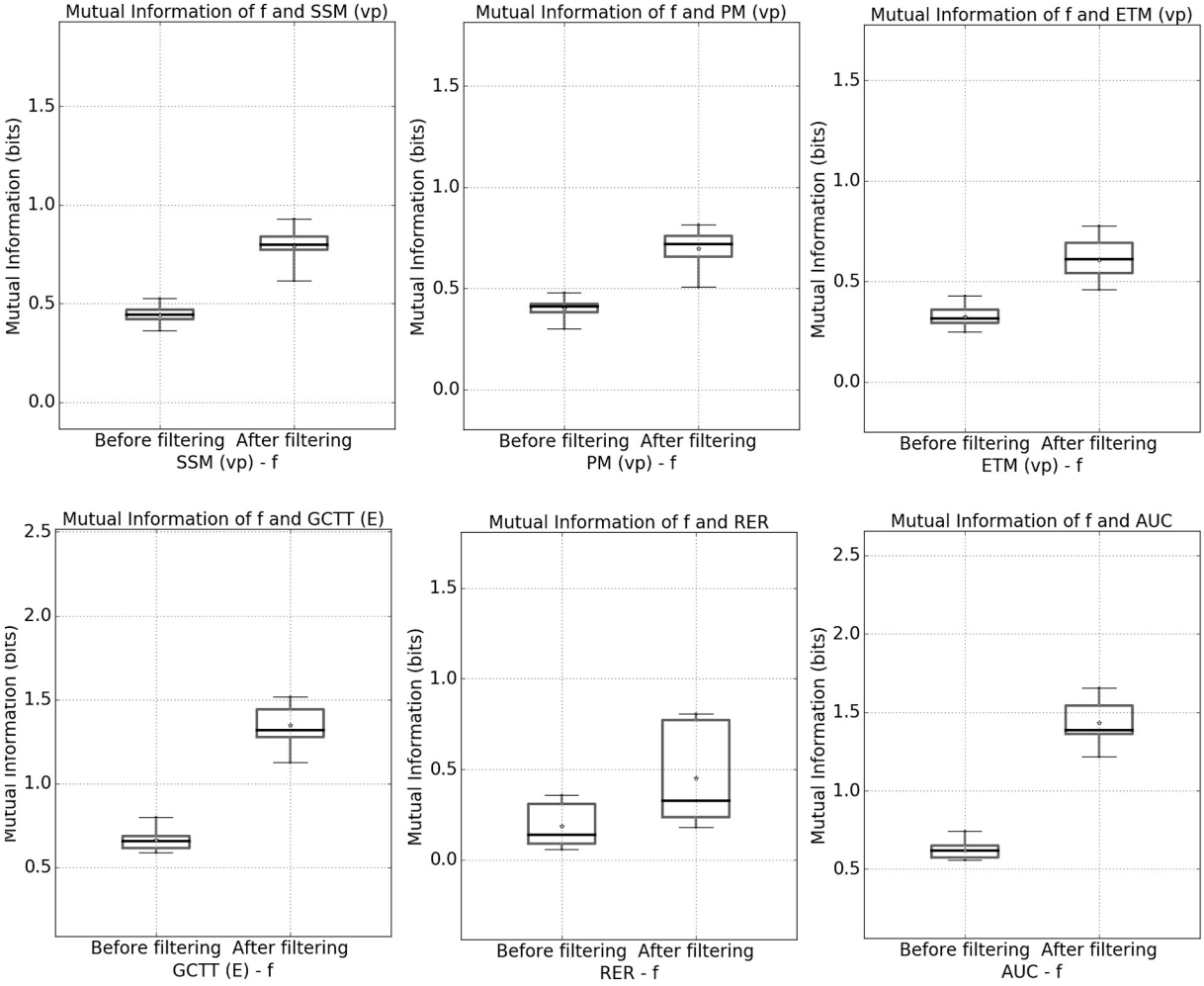

Fig. 11. Mutual information between f-IVIM method 1 and SSM (vp), PM (vp), ETM (vp), GCTT (E), RER, AUC before and after Gaussian filtering.

of anatomical barriers (membranes) in the brain that direct the anisotropic water diffusion and the reduced tissue perfusion due to PAD in our patients. In addition, another reason for the better correlation of Federau et al. could be attributed to their DWI experimental protocol consisting of 16 b-values ranging from 0 to 900 s/mm^2 that makes the diffusion measurement more precise.

The purpose of the clinical study in which this work is based, was to evaluate the perfusion of soft tissues in the foot of PAD patients. Thus, the relatively slow injection rate was chosen for two reasons. Firstly, muscles are normally characterized by slow perfusion rate which can be easily quantified using a slow injection rate. Secondly, the “bolus” injection technique induces susceptibility artifacts from the presence of highly concentrated contrast agent which in turn can be downgraded with the slow rate non-bolus administration. The low temporal resolution was chosen in order to compensate for the spatial covering of the imaging volume which has been previously reported in [37]. In fact, the total volume coverage was 26 space filling slices of 3 mm slice thickness. The selected volume coverage was considered adequate for the depiction of lower limb arteries and veins that might be related to blood supply to the ischemic regions of interest.

At this stage it is important to highlight the limitations of this study. The first limitation is that due to the clinical imaging protocol a good spatial resolution was chosen at the expense of a compromised SNR (matrix size 384 × 384) at the DW images. Additionally, in order to estimate the Pearson's correlation coefficient (r) through voxel by voxel analysis we had to resize the perfusion maps to match the size of the diffusion maps and this may have had a negative impact on the results. Regarding our dataset, it is noteworthy that it is limited to a relatively small subset of patients ($N = 13$) which means that further studies based on larger cohorts will be necessary for increasing the statistical significance of our results. Furthermore, the patients of the study presented with critical limb ischemia and some motion artifacts were observed especially in the perfusion imaging sequence (30 min approximately). To account for this, an idea for future work is to also use image registration which is hard due to the non-rigid nature of the transformation which might be affecting the results.

In conclusion, in this study we assessed different DWI and DCE-MRI analysis methods on data obtained from patients with PAD. According to $\overline{R}^2$ criterion we found that the best DWI fitting method was the direct estimation of the IVIM parameters (first method) and the most accurate perfusion model for this disease was the Patlak's model. Initially, IVIM parameters did not correlate with any of the perfusion parameters (quantitative and semi-quantitative) but, after the application of Gaussian filtering, a positive correlation between the extraction fraction E (GCTT) and RER with the micro-perfusion fraction (IVIM) with both of the DWI fitting methods rGCTTE − fmethod = 0.54, rGCTTE − fmethod = 0.551, rRER − fmethod = 0.592, rRER − fmethod = 0.601was obtained. Our results indicate that diffusion IVIM analysis could provide reliable information about tissue micro-perfusion and can be easily incorporated as a part of a conventional imaging clinical MRI protocol.

Acknowledgements

This work was supported by the General Secretariat for Research and Technology (GSRT) and the Hellenic Foundation for Research and Innovation (HFRI).

Appendix A. Formulae and equations

$$S(b)/S(0) = (1-f)e^{-bD} + fe^{-bD^*} \tag{A.1}$$

$$S(b)/S(0) = e^{-bD} \tag{A.2}$$

$$\frac{1}{T_1} = \frac{1}{T_{10}} + r_1 c \tag{A.3}$$

$$\frac{S}{S_0} = \frac{(1-e^{-TR/T_1})sin\theta}{1-e^{-TR/T_1}cos\theta} \tag{A.4}$$

$$C_t(t) = K^{trans} e^{-K_{ep}t} \circledast C_a(t) + v_p C_a(t) \tag{A.5}$$

$$C_t(t) = K^{trans} \int_0^t C_a(\tau)d\tau + v_p C_a(t) \tag{A.6}$$

$$C_t(t) = v_p C_a(t) \tag{A.7}$$

$$C_t(t) = F\left[\gamma\left(\frac{1}{a^{-1}}, \frac{t}{\tau}\right) + \frac{Ee^{-K_{ep}t}}{(1-K_{ep}\tau)^{1/a-1}}\left[1-\gamma\left(\frac{1}{a^{-1}}, \left(\frac{1}{\tau}-K_{ep}\right)t\right)\right]\right] \circledast C_a(t) \tag{A.8}$$

$$AUC = \int_0^t SI(\tau)d\tau \tag{A.9}$$

$$RER = \frac{SI_{post} - SI_{pre}}{SI_{pre}} \tag{A.10}$$

$$RMSE = \sqrt{\sum_{i=1}^{N} \frac{(G(x,t_i) - d_i)^2}{N}} \tag{A.11}$$

$$\overline{R}^2 = 1 - (1-R^2)\frac{N-1}{N-p-1} \tag{A.12}$$

$$H(X) = -\sum_{x \in X} p(x)\log(p(x)) \tag{A.13}$$

$$H(X,Y) = -\sum_{x \in X}\sum_{y \in Y} p(x,y)\ \log(p(x,y)) \tag{A.14}$$

$$\mathrm{MI}(\mathrm{X},\mathrm{Y}) = \mathrm{H}(\mathrm{X}) + H(Y) - H(X,Y) \tag{A.15}$$

$$\mathrm{SNR} = \frac{\mathrm{mean}(\mathrm{SI_{ROI}})}{\mathrm{std}(\mathrm{BG_{ROI}})} \times 0.655 \tag{A.16}$$

References

[1] Choyke PL, Dwyer AJ, Knopp MV. Functional tumor imaging with dynamic contrast-enhanced magnetic resonance imaging. J Magn Reson Imaging 2003;17:509–20. https://doi.org/10.1002/jmri.10304.
[2] Essig M, Shiroishi MS, Nguyen TB, Saake M, Provenzale JM, Enterline D, et al. Perfusion MRI: the five most frequently asked technical questions. 2013. https://doi.org/10.2214/AJR.12.9543.
[3] Hagmann P, Jonasson L, Maeder P, Thiran J, Wedeen VJ, Meuli R. Central nervous system: state of the art understanding diffusion MR imaging techniques: from scalar imaging to diffusion. Radiographics 2006:205–24.
[4] Le Bihan Denis, Eric Breton DL. Seperation of diffusion and perfusion in intravoxel incoherent motion MR imaging. Radiology 1988;168:497–505.
[5] Kim HS, Suh CH, Kim N, Choi C-G, Kim SJ. Histogram analysis of intravoxel incoherent motion for differentiating recurrent tumor from treatment effect in patients with glioblastoma: initial clinical experience. AJNR Am J Neuroradiol 2014;35:490–7. https://doi.org/10.3174/ajnr.A3719.
[6] Federau C, O'Brien K, Meuli R, Hagmann P, Maeder P. Measuring brain perfusion with intravoxel incoherent motion (IVIM): initial clinical experience. J Magn Reson Imaging 2014;39:624–32. https://doi.org/10.1002/jmri.24195.
[7] Suo S, Lin N, Wang H, Zhang L, Wang R, Zhang S, et al. Intravoxel incoherent motion diffusion-weighted MR imaging of breast cancer at 3.0 tesla: comparison of different curve-fitting methods. J Magn Reson Imaging 2015;42:362–70. https://doi.org/10.1002/jmri.24799.
[8] Fujima N, Yoshida D, Sakashita T, Homma A, Tsukahara A, Tha KK, et al. Intravoxel incoherent motion diffusion-weighted imaging in head and neck squamous cell carcinoma: assessment of perfusion-related parameters compared to dynamic contrast-enhanced MRI. Magn Reson Imaging 2014;32:1206–13. https://doi.org/10.1016/J.MRI.2014.08.009.
[9] Wood AJJ, Hiatt WR. Medical treatment of peripheral arterial disease and claudication. N Engl J Med 2001;344:1608–21. https://doi.org/10.1056/NEJM200105243442108.
[10] Peach G, Griffin M, Jones KG, Thompson MM, Hinchliffe RJ. Diagnosis and management of peripheral arterial disease. BMJ 2012;345.
[11] Norgren L, Hiatt WR, Dormandy JA, Nehler MR, Harris KA, Fowkes FGR, et al. Inter-society consensus for the management of peripheral arterial disease (TASC II). J Vasc Surg 2007;45:S5–67. https://doi.org/10.1016/j.jvs.2006.12.037.
[12] Fontaine R, Kim M, Kieny R. Surgical treatment of peripheral circulation disorders. Helv Chir Acta 1954;21:499–533.
[13] Chang H, Fitzpatrick JM. A technique for accurate magnetic resonance imaging in the presence of field inhomogeneities. IEEE Trans Med Imaging 1992;11:319–29. https://doi.org/10.1109/42.158935.
[14] Welcome to Python.org n.d. https://www.python.org/(accessed December 6, 2017).
[15] Branch MA, Coleman TF, Li Y. A subspace, interior, and conjugate gradient method for large-scale bound-constrained minimization problems. SIAM J Sci Comput 1999;21:1–23. https://doi.org/10.1137/S1064827595289108.
[16] Peterson Pearu, TB Eric Jones. SciPy: open source scientific tools for Python. http://www.scipy.org/; 2001.

[17] Hu Y-C, Yan L-F, Wu L, Du P, Chen B-Y, Wang L, et al. Intravoxel incoherent motion diffusion-weighted MR imaging of gliomas: efficacy in preoperative grading. Sci Rep 2014;4:7208. https://doi.org/10.1038/srep07208.
[18] Tofts PS, Kermode AG. Measurement of the blood-brain barrier permeability and leakage space using dynamic MR imaging. 1. Fundamental concepts. Magn Reson Med 1991;17:357–67.
[19] Dathe H, Helms G. Exact algebraization of the signal equation of spoiled gradient echo MRI. Phys Med Biol 2010;55:4231–45. https://doi.org/10.1088/0031-9155/55/15/003.
[20] Tofts PS, Brix G, Buckley DL, Evelhoch JL, Henderson E, Knopp MV, et al. Estimating kinetic parameters from dynamic contrast-enhanced T(1)-weighted MRI of a diffusable tracer: standardized quantities and symbols. J Magn Reson Imaging 1999;10:223–32.
[21] Patlak CS, Blasberg RG, Fenstermacher JD. Graphical evaluation of blood-to-brain transfer constants from multiple-time uptake data. J Cereb Blood Flow Metab 1983;3:1–7. https://doi.org/10.1038/jcbfm.1983.1.
[22] Sourbron SP, Buckley DL. Classic models for dynamic contrast-enhanced MRI. NMR Biomed 2013;26:1004–27. https://doi.org/10.1002/nbm.2940.
[23] Schabel MC. A unified impulse response model for DCE-MRI. Magn Reson Med 2012;68:1632–46. https://doi.org/10.1002/mrm.24162.
[24] Sourbron SP, Buckley DL. On the scope and interpretation of the Tofts models for DCE-MRI. Magn Reson Med 2011;66:735–45. https://doi.org/10.1002/mrm.22861.
[25] Tofts PS. Modeling tracer kinetics in dynamic Gd-DTPA MR imaging. J Magn Reson Imaging 1997;7:91–101.
[26] St Lawrence KS, Lee T-Y. An adiabatic approximation to the tissue homogeneity model for water exchange in the brain: I. Theoretical derivation. J Cereb Blood Flow Metab n.d.;18:1365–77.
[27] Brix G, Salehi Ravesh M, Zwick S, Griebel J, Delorme S, Brix G. On impulse response functions computed from dynamic contrast-enhanced image data by algebraic deconvolution and compartmental modeling. Phys Med 2012;28:119–28. https://doi.org/10.1016/j.ejmp.2011.03.004.
[28] Canny J. A computational approach to edge detection. IEEE Trans Pattern Anal Mach Intell 1986;PAMI-8:679–98. https://doi.org/10.1109/TPAMI.1986.4767851.
[29] Pluim JPW, Maintz JBA, Viergever MA. Mutual-information-based registration of medical images: a survey. IEEE Trans Med Imaging 2003;22:986–1004. https://doi.org/10.1109/TMI.2003.815867.
[30] Cover TM, Thomas JA. Elements of information theory. Wiley-Interscience; 2006.
[31] Henkelman RM. Measurement of signal intensities in the presence of noise in MR images. Med Phys 1985;12:232–3. https://doi.org/10.1118/1.595711.
[32] European Medicines Agency - Human medicines - gadolinium-containing contrast agents n.d. http://www.ema.europa.eu/ema/index.jsp?curl=pages/medicines/human/referrals/Gadolinium-containing_contrast_agents/human_referral_prac_000056.jsp&mid=WC0b01ac05805c516f (accessed December 6, 2017).
[33] Pollak AW, Meyer CH, Epstein FH, Jiji RS, Hunter JR, Dimaria JM, et al. Arterial spin labeling MR imaging reproducibly measures peak-exercise calf muscle perfusion: a study in patients with peripheral arterial disease and healthy volunteers. JACC Cardiovasc Imaging 2012;5:1224–30. https://doi.org/10.1016/j.jcmg.2012.03.022.
[34] Huegli RW, Schulte A-C, Aschwanden M, Thalhammer C, Kos S, Jacob AL, et al. Effects of percutaneous transluminal angioplasty on muscle BOLD-MRI in patients with peripheral arterial occlusive disease: preliminary results. Eur Radiol 2009;19:509–15. https://doi.org/10.1007/s00330-008-1168-6.
[35] Grözinger G, Pohmann R, Schick F, Grosse U, Syha R, Brechtel K, et al. Perfusion measurements of the calf in patients with peripheral arterial occlusive disease before and after percutaneous transluminal angioplasty using Mr arterial spin labeling. J Magn Reson Imaging 2014;40:980–7. https://doi.org/10.1002/jmri.24463.
[36] Jiji RS, Pollak AW, Epstein FH, Antkowiak PF, Meyer CH, Weltman AL, et al. Reproducibility of rest and exercise stress contrast-enhanced calf perfusion magnetic resonance imaging in peripheral arterial disease. J Cardiovasc Magn Reson 2013;15:14. https://doi.org/10.1186/1532-429X-15-14.
[37] Mostardi PM, Haider CR, Glockner JF, Young PM, Riederer SJ. High spatial and temporal resolution imaging of the arterial vasculature of the lower extremity with contrast enhanced MR angiography. Clin Anat 2011;24:478–88. https://doi.org/10.1002/ca.21124.